



Efficient removal of tannins from anaerobically-treated palm oil mill effluent using protein-tannin complexation in conjunction with electrocoagulation

Peerawat Khongkliang^{a,i}, Maneerat Khemkhao^{b,c}, Sithipong Mahathanabodee^d, Sompong O-Thong^e, Abudukeremu Kadier^{f,g}, Chantaraporn Phalakornkule^{a,h,i,*}

^a The Joint Graduate School of Energy and Environment, King Mongkut's University of Technology Thonburi, Bangkok, 10140, Thailand

^b Rattanakosin College for Sustainable Energy and Environment, Rajamangala University of Technology Rattanakosin, Nakhon Pathom, 73170, Thailand

^c Microbial Informatics and Industrial Product of Microbe Research Center, King Mongkut's University of Technology North Bangkok, Bangkok, 10800, Thailand

^d Department of Production Engineering, Faculty of Engineering, King Mongkut's University of Technology North Bangkok, Bangkok, 10800, Thailand

^e International College, Thaksin University, Songkhla, 90000, Thailand

^f Laboratory of Environmental Science and Technology, The Xinjiang Technical Institute of Physics and Chemistry, Key Laboratory of Functional Materials and Devices for Special Environments, Chinese Academy of Sciences (CAS), Urumqi, 830011, Xinjiang, China

^g Center of Materials Science and Optoelectronics Engineering, University of Chinese Academy of Sciences, Beijing, 100049, China

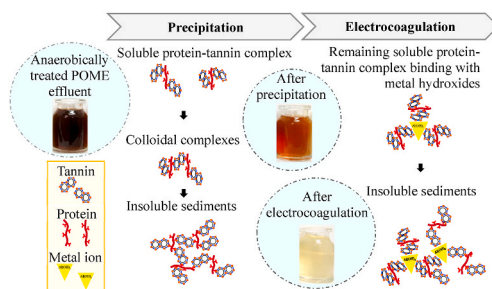
^h Department of Chemical Engineering, Faculty of Engineering, King Mongkut's University of Technology North Bangkok, Bangkok, 10800, Thailand

ⁱ Research Center for Circular Products and Energy, King Mongkut's University of Technology North Bangkok, Bangkok, 10800, Thailand

HIGHLIGHTS

- Addition of pig blood protein caused the formation of protein-tannin complexes.
- Insoluble protein-tannin complexes could be removed by precipitation.
- Electrocoagulation further removed soluble protein-tannin complexes.
- The overall tannin removal from anaerobically treated POME was 93%.
- Important parameters were protein-tannin ratios, protein type, and aqueous pH.

GRAPHICAL ABSTRACT



ARTICLE INFO

Handling Editor: A ADALBERTO NOYOLA

Keywords:

Covered lagoon effluent
Pig blood protein
Protein-tannin complex
Precipitation
Electrocoagulation

ABSTRACT

Despite the significant removal of chemical oxygen demand (COD) by anaerobic digestion, anaerobically-treated palm oil mill effluent (POME) still contains tannins and other phenolic compounds, resulting in residual COD and a brownish color. In this study, we investigated the removal of tannins from anaerobically treated POME using protein-tannin complexation in conjunction with electrocoagulation. The amino acid composition of the protein, aqueous pH, and protein: tannin ratios were found to be important parameters affecting the tannin removal efficiency. Pig blood protein was superior to casein protein in removing tannins, possibly because it had aspartic acid as the major amino acid component. At an optimal condition with a pig blood protein: tannin ratio of 0.33

* Corresponding author. Department of Chemical Engineering, Faculty of Engineering, King Mongkut's University of Technology North Bangkok, Bangkok 10800, Thailand.

E-mail addresses: cphalak21@gmail.com, chantaraporn.p@eng.kmutnb.ac.th (C. Phalakornkule).

<https://doi.org/10.1016/j.chemosphere.2023.138086>

Received 26 November 2022; Received in revised form 9 January 2023; Accepted 5 February 2023

Available online 6 February 2023

0045-6535/© 2023 Elsevier Ltd. All rights reserved.

(w/w), a current density of 30 mA/cm², pH 5, and an electrolysis time of 10 min, the removals of tannins, COD, and color were 93%, 96%, and 97%, respectively.

1. Introduction

The palm oil industry is economically important in several Southeast Asian countries. However, palm oil production inevitably generates large amounts of heavily polluted wastewater known as palm oil mill effluent (POME). POME is typically treated using anaerobic digestion, which results in a COD removal efficiency as high as 90% and residual COD content of approximately 6960 mg/L (Seengenyong et al., 2019; Khemkhao et al., 2016, 2022). However, the treated POME still contains a variety of compounds in relatively small quantities, such as fatty acids, humic acids, lipids, melanoidins, tannins, and phenolic compounds (Dexter et al., 2016). All of these compounds resulted in residual COD and a brownish color of the treated POME. The color intensity of the treated POME could be as high as 6400–19,600 Pt–Co owing to the presence of tannins and other phenolic compounds, as well as the repolymerization of coloring compounds (Rakamthong and Prasertsan, 2011; Jalani et al., 2016). These residual compounds can also be toxic to aquatic life (Zahrim, 2014) and should be removed before discharging the effluent into the environment. The removal of these residual compounds is an important step in making water recycling more feasible during the palm oil milling process (Kamyab et al., 2018; Ujang et al., 2021).

Tannins have been recognized for their ability to interact with proteins and form protein-tannin complexes (Banch et al., 2019). The formation of protein-tannin complexes can lead to the precipitation of tannins and proteins, which depends on the chemical structures of proteins and tannins, protein charge, protein isoelectric point (pI), and their concentrations, as well as on environmental conditions, such as pH and ionic strength (Oh and Hoff, 1987; Adamczyk et al., 2012; Banch et al., 2019; Soares et al., 2020). In addition, the composition and temperature of the aqueous system can affect the formation of protein-tannin complexes (Soares et al., 2020). Over the past few years, several studies have demonstrated the use of tannins for the removal of various proteins from beverages (Jordão et al., 2005; Jones-Moore et al., 2022) and animal food (Dentinho and Bessa, 2016). Compared with the precipitates from coagulation with inorganic salts, the precipitated protein-tannin complexes have relatively low volumes (Maeng et al., 2017). In addition, the precipitation of protein-tannin complexes is considered more eco-friendly than inorganic coagulation because no salt is added to the aqueous system; thus, there is no significant increase in water conductivity or change in water pH (Al-Amshawee et al., 2020). For example, dos Santos et al. (2018) used a modified Tanfloc SL®, a tannin-based agent, with an applied concentration of 640 mg/L for treating cassava processing wastewater and showed the removal of color and turbidity of the wastewater by more than 52%. Additionally, Dashti et al. (2022) reported the removal of color and COD from POME by 54% and 44%, respectively, using 2 g/L chickpea powder protein. Based on these studies, the formation and precipitation of protein-tannin complexes is a potential method for removing color and COD from POME. However, the removal efficiency of this method alone is still low, possibly because some soluble compounds remain in POME. Therefore, other methods, such as coagulation and electrocoagulation, which can be operated in series or in combination with precipitation, are required to improve the tannin removal efficiency.

In the past few decades, electrocoagulation has been demonstrated to be an effective method for treating POME (Mohamad et al., 2022; Nasrullah et al., 2022), tannery wastewater (Maisuria et al., 2022), and other wastewater containing phenolic compounds (Reilly et al., 2019; Oktawan et al., 2021; Gasmi et al., 2022). In the electrocoagulation process, an electrical current is applied to anodic electrodes, that is, aluminum, iron, or their alloys, which are immersed in wastewater. The

anodes are oxidized to release free metallic ions (Al³⁺, Fe²⁺ or Fe³⁺), which then combine with the hydroxyl ions released at the cathode to form metal hydroxides, polyhydroxides, and polyhydroxy metallic compounds (Phalakornkule et al., 2010c; Hakizimana et al., 2017). The efficiency of the removal of tannins and other phenolic compounds was as high as 80% using electrocoagulation with current densities ranging 3–75 mA/cm² and electrolysis times ranging 5–60 min (Adhoum and Monser, 2004; Ugurlu et al., 2008; Fajardo et al., 2015; Maisuria et al., 2022). Despite the relatively high tannin removal efficiency, electrocoagulation requires high applied current densities and long electrolysis times, resulting in high material cost and energy consumption (Rana and Saini, 2022). Electrocoagulation requires high applied current densities and long electrolysis times, possibly owing to the low solubility of tannins and other phenolic compounds.

Most previous studies reported treatment systems consisting of electrocoagulation as a pretreatment step followed by a biological treatment step (Al-Qodah et al., 2019), whereas this study presents a combined treatment process consisting of biological treatment, chemical coagulation, and finally electrocoagulation. Because the formation of protein-tannin complexes can reduce the solubility of tannins, we investigated the removal of tannins from POME using protein-tannin complexation in conjunction with electrocoagulation. POME-treated effluent with relatively low COD but high color intensity was collected from the discharge of an anaerobic-covered lagoon of a biogas plant. The precipitation of tannins in the POME-treated effluent was first performed by adding pig blood and casein proteins, followed by electrocoagulation of the remaining soluble protein-tannin complexes. The effects of protein type (pig blood and casein proteins), aqueous pH, and protein: tannin ratio on the tannin removal efficiency were investigated. In addition, the operating parameters of the electrocoagulation system (current density, inter-electrode distance, and electrolysis time) were optimized to minimize the energy consumption of the electrocoagulation process. Finally, the characteristics of the flocs from electrocoagulation with and without the protein-tannin complex formation step were compared.

2. Materials and methods

2.1. Materials

The effluent samples were collected from the discharge of an anaerobic lagoon at a palm oil factory (Suksomboon Vegetable Oil Co., Ltd., Chonburi, Thailand). These samples are referred to as “the covered lagoon effluent” and were stored at 4 °C before use. Table 1 shows the properties of the covered lagoon effluent, with a tannin concentration of 545 ± 13 mg/L. Pig blood was collected from a slaughterhouse and was stored at 4 °C before use. Commercial casein (tryptone type-I) was purchased from HiMedia Laboratories (India). Stock solutions of pig blood and casein were prepared with a fixed protein concentration of 11,000 ± 230 mg/L. Aluminum chloride (AlCl₃·6H₂O, AR.grade) and ferric chloride (FeCl₃·6H₂O, AR.grade) were purchased from KemAus (Australia) and Qrec (New Zealand), respectively.

2.2. Precipitation experiments

The precipitation of tannins in the covered lagoon effluent using proteins was investigated in the batch mode. The covered lagoon effluent was added to a 500-mL beaker with a working volume of 300 mL. Pig blood and casein proteins were added to the covered lagoon effluent in separate beakers in protein to tannin ratios of 0.20, 0.22, 0.25, 0.28, 0.33, 0.40, 0.50, 0.67, 0.80, and 1.0 (w/w). Depending on

Table 1

Characteristics of anaerobically-treated palm oil mill effluent from a palm oil factory and after treatment with precipitation and electrocoagulation.

Parameter	Unit	Anaerobically-treated POME	After precipitation and electrocoagulation	
			Without protein	With protein
Temperature	°C	28 ± 1	–	–
pH	–	8.0 ± 0.5	6.08 ± 0.04	5.63 ± 0.14
Color	Pt–Co	22,217 ± 325	4667 ± 142	743 ± 25
Total hardness	mg-CaCO ₃ /L	2200 ± 200	1733 ± 76	1433 ± 38
COD	mg/L	6146 ± 152	952 ± 72	248 ± 62
TS	g/L	16.05 ± 0.04	13.26 ± 0.48	13.03 ± 0.40
VS	g/L	5.15 ± 0.01	4.68 ± 0.35	3.54 ± 0.06
Ash	g/L	10.89 ± 0.04	8.57 ± 0.13	9.49 ± 0.43
TSS	g/L	2.3 ± 0.2	1.65 ± 0.14	1.80 ± 0.20
TDS	mg/L	364 ± 0.6	357 ± 1	371 ± 7
Turbidity	NTU	267 ± 0.4	147 ± 12	16 ± 3
Al ³⁺	mg/L	–	0.80 ± 0.05	0.75 ± 0.01
Tannins	mg/L	545 ± 13	158 ± 3	36 ± 2
Conductivity	µS/cm	605 ± 3	786 ± 8	832 ± 1

the trial, the pH of the mixture was adjusted to the desired value (in a pH range of 2–9) with solutions of 3 M HCl or 3 M NaOH. The mixture was stirred at 150 rpm for 3 min and then allowed to stand for 30 min prior to centrifugation for 1 min at 3300 g. The supernatant was collected for measurement of residual tannins. Each experiment was performed in triplicate.

2.3. Electrocoagulation

The electrocoagulation of the supernatant after precipitation with proteins was investigated in batch mode. After precipitation, the supernatant was added to a 300 mL beaker with a working volume of 200 mL. A pair of anodic and cathodic electrodes was immersed in the test solution. Two types of electrodes were employed, iron (Fe) and aluminum (Al), each with an immersed (active) surface area of 100 cm² (5 cm × 10 cm) and inter-electrode distances, depending on the trial, of 6, 8, 10, or 15 mm. The electrodes were connected to a direct current (DC) power supply (Matsui Denki, Japan) with a maximum voltage of 15 V and a maximum current of 30 A. Output voltages were monitored using a digital multimeter (Toolwiz XL830L, USA).

Before each experiment, the electrodes were cleaned with tap water, dipped in a 20% v/v HCl solution for at least 15 min, and rinsed several times with deionized water. The electrocoagulation was performed at three different current densities (20, 30, and 40 mA/cm²) and six different electrolysis times (5, 10, 15, 20, 25, and 30 min). After a certain electrolysis time, the mixture was allowed to stand for 15 min, and the supernatant and flocs were collected for the analysis of residual tannin and floc characteristics, respectively.

2.4. Coagulation

Chemical coagulation of the supernatant after precipitation with the proteins was performed in batch mode in a 300 mL beaker with a working volume of 200 mL. AlCl₃ and FeCl₃ were separately added to the test solution at concentrations of 84–503 mg/L Al and 260–1563 mg/L Fe. The dosages of AlCl₃ and FeCl₃ yielded equal amounts of Al³⁺ and Fe³⁺ in the electrocoagulation experiments, with an electrolysis time between 5 and 30 min and a current density of 30 mA/cm². Depending on the trial, the aqueous pH was adjusted to the desired value (in a pH

range of 2–9) with solutions of 3 M HCl or 3 M NaOH. The mixture was stirred at 150 rpm for 3 min and 60 rpm for 5 min and then allowed to stand for 15 min. The supernatant was collected for the analysis of residual tannins.

2.5. Analytical methods

2.5.1. Analysis of water compositions and properties

Aqueous pH and conductivity and total dissolved solids (TDS) were measured using a pH meter (Horiba PH2000, Japan) and conductivity meter (Mettler Toledo LE703, USA), respectively. Tannin content, total hardness as CaCO₃, and chemical oxygen demand (COD) were measured using closed reflux titrimetric methods according to the standard methods of the American Public Health Association (APHA et al., 2012). The color of the water samples was measured using a colorimeter (Thermo Fisher Scientific Orion AQ3700, USA). Total suspended solids (TSS), total solids (TS), and volatile solids (VS) were analyzed according to the standard methods of the American Public Health Association (APHA et al., 2012). Turbidity was measured using a turbidimeter (Hach 2100AN, USA).

2.5.2. Chemical analysis

The functional groups of the tannins were determined using Fourier-transform infrared spectroscopy (FTIR; PerkinElmer Spectrum, USA) with wavenumbers between 400 and 4000 cm⁻¹. Amino acids in the pig blood and casein were extracted using 10% trichloroacetic acid and analyzed using an amino acid analyzer (Hitachi L-8900, USA).

2.5.3. Floc characteristics

The morphology of the dried flocs was investigated using a scanning electron microscope equipped with an energy-dispersive X-ray spectrometer (SEM-EDS; JEOL JSM-IT300, Oxford X-Max 20, UK). The fresh sludge was investigated using a light microscope (Olympus DSX1000 digital microscope, Japan).

2.6. Calculation and statistical analysis

The removal efficiency was calculated as the percentage removal for each parameter, (B₀–B)/B₀, where B₀ and B are the concentrations of tannins, color, and COD in the wastewater before and after treatment, respectively.

The amounts of aluminum and iron ions released owing to the electrolytic oxidation of the anodes were estimated using Faraday's law as follows:

$$w = \left(\frac{ItM_{Al/Fe}}{ZF} \right) \quad (1)$$

where w is the amount of aluminum or iron dissolved (g), I = current (A), t = electrolysis time (s), $M_{Al/Fe}$ = molecular weight of Al (26.98 g/mol) or Fe (55.85 g/mol), Z = number of electrons involved in the redox reaction, and F = Faraday's constant (96,500 C/mol of electrons).

3. Results and discussion

3.1. Comparative removal of tannins using pig blood and casein proteins

Fig. 1 compares the effectiveness of pig blood and casein proteins in removing tannins from covered lagoon effluents. The investigation was performed with varying protein: tannin ratios between 0.20 and 1.00 (g/g) at an initial pH of 5. When using the pig blood protein, the tannin removal was highest at approximately 62–64% with protein: tannin ratios between 0.20 and 0.33 (Fig. 1a). When increasing the tannin: protein ratios further from 0.40 to 0.67 and 0.80, the tannin removal decreased from 59% to 47% and 12%, respectively. Similarly, Adamczyk et al. (2012) reported that the addition of bovine serum albumin protein

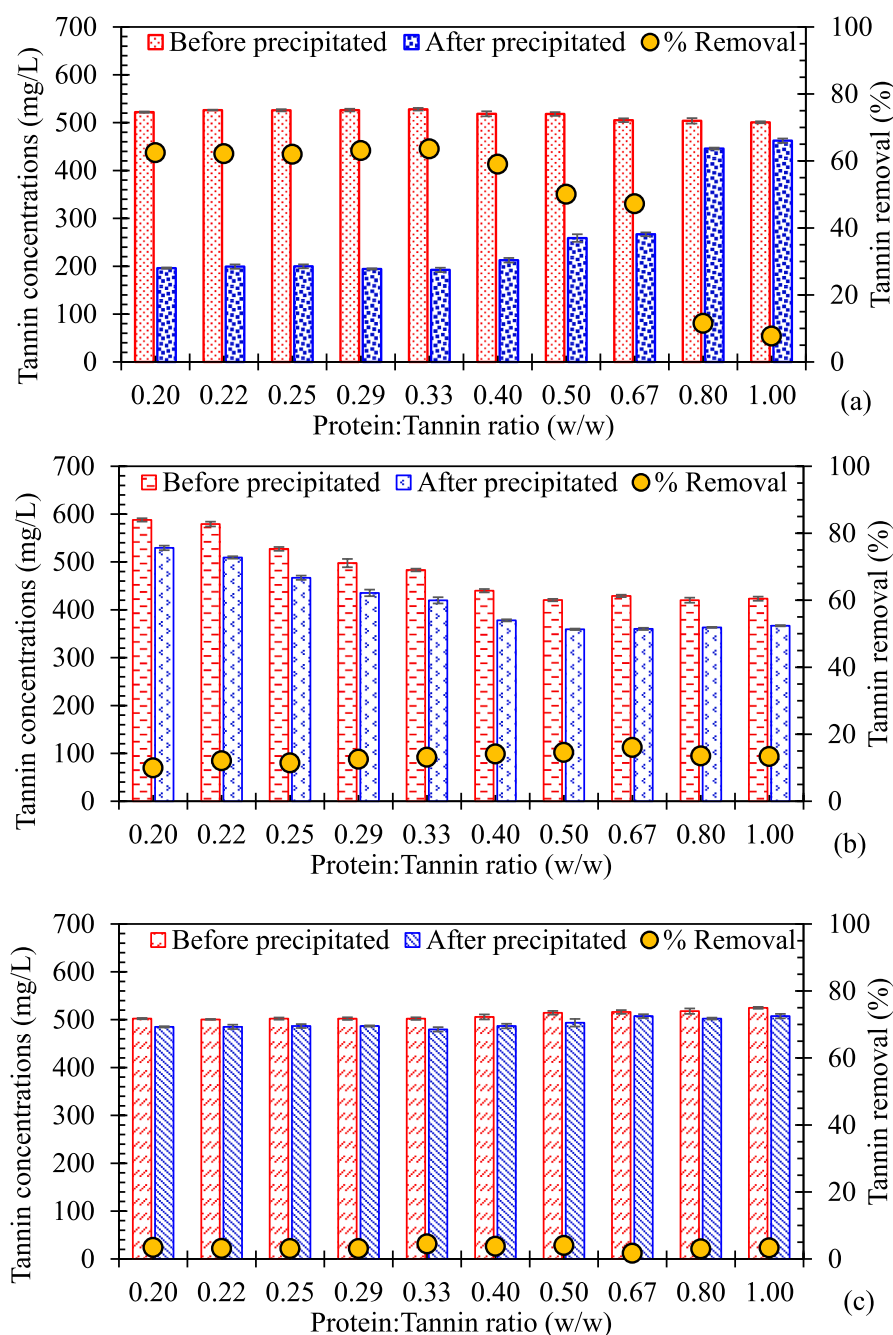


Fig. 1. Effects of protein: tannin ratios on residual tannin concentrations and percentage tannin removal by precipitation: (a) pig blood protein addition, (b) casein protein addition, and (c) without protein addition.

at a protein: tannin ratio of 0.43 could remove up to 80% of tannins from aqueous solutions. However, the tannin removal decreased significantly from 80% at a protein: tannin ratio of 0.43 to 40% at a protein: tannin ratio of 2.16.

The tannin removal was much lower when using the casein protein, ranging between 10 and 16% (Fig. 1b). The tannin removal by the addition of casein protein was only slightly higher than that of 3–4% in the control sample without protein addition (Fig. 1c). The results suggest that the type of proteins (pig blood and casein proteins) and protein: tannin ratios had a profound effect on the removal efficiency of tannins. This is because the removal of tannins is caused by the formation of protein-tannin complexes, which can be easily precipitated from aqueous solutions (Adamczyk et al., 2012; Mezzomo et al., 2015). The

formation of protein-tannin complexes depends on the interactions between the functional groups of tannins and proteins (Adamczyk et al., 2017), which in turn depends on the pH of the aqueous phase. Therefore, the pH of the wastewater should have a large influence on the effectiveness of removing tannins from pig blood and casein proteins. In addition, the formation of protein-tannin complexes depends on the protein: tannin ratio. For example, when the concentration of protein is too high compared to the concentration of tannins, the tannin molecules might dissociate from the protein-tannin complex and redissolve (Brooks et al., 2008). As observed in this study, when the protein: tannin ratio was higher than the optimal value, tannin removal was reduced.

3.2. Effect of pH on precipitation of protein-tannin complexes

Fig. 2 shows tannin removal as a function of initial pH values between 2 and 9 using pig blood and casein proteins. When using pig blood protein at a protein: tannin ratio of 0.33 (g/g), the increase in pH from 2 to 4 caused the tannin removal to increase from 50% to 72% (Fig. 2a). However, when the pH was increased from 5 to 8 and 9, the tannin removal decreased from 63% to 26% and 8%, respectively. Similarly, Kosińska et al. (2011) reported that a pH range of approximately 3-5 was optimal for removing tannins using bovine serum albumin and gelatin proteins, whereas pH 6-8 caused a sharp decrease in tannin removal. In addition, Adamczyk et al. (2012) and Engström et al. (2016) reported that pH 4.7 was optimal for tannin removal via the formation of tannin-protein complexes because of the relatively strong interaction

between tannins and protein at this pH under low ionic strength conditions. Likewise, Osawa and Walsh (1993) reported that an increase in pH above 6.5 facilitated the dissociation of protein-tannin complexes, whereas a pH of 8.6 caused the hydrolysis of Gallo tannin.

When using casein protein at a protein: tannin ratio of 0.67 (g/g), the tannin removal ranged between 18 and 25% at a pH range of approximately 2-5 (Fig. 2b). When the pH was increased to 6-9, the tannin removal decreased to 6-12%. The tannin removal by the addition of casein protein was only slightly higher than that of 1-10% in the control sample without protein addition (Fig. 2c). An explanation for these results is that the interactions between tannins and protein are pH-dependent (Oh and Hoff, 1987) because the two proteins have different amino acid compositions, and each amino acid in the proteins has a different isoelectric point and pKa value.

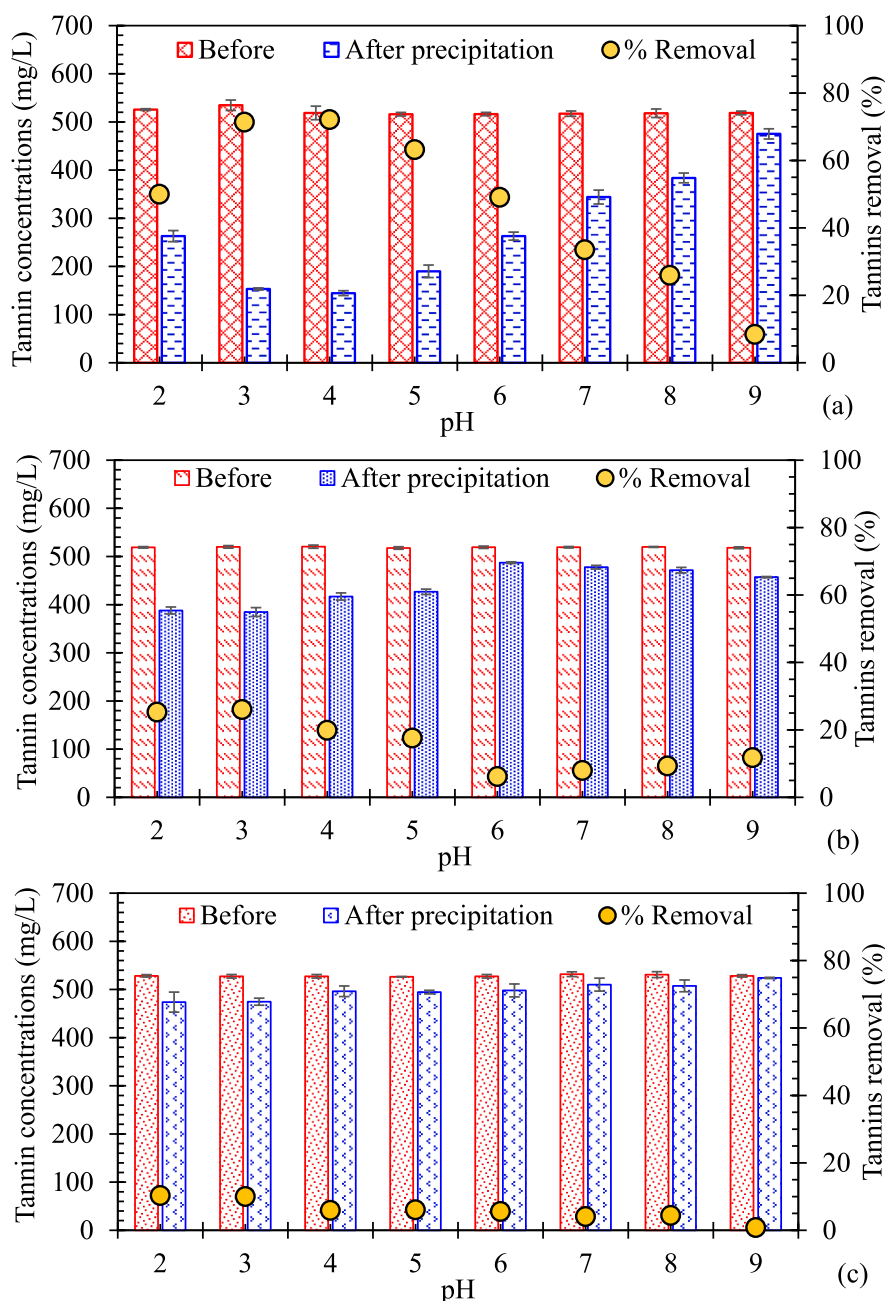


Fig. 2. Effects of pH on residual tannin concentrations and percentage tannin removal by precipitation at a protein: tannin ratio of 0.33 g/g: (a) pig blood protein addition, (b) casein protein addition, and (c) without protein addition.

3.3. Removal of soluble protein-tannin complexes using electrocoagulation

After separating the insoluble protein-tannin complexes by centrifugation, the suspension was subjected to electrocoagulation to remove the remaining tannins in the form of a soluble protein-tannin complex. Fig. 3 shows the removal efficiency of tannins using electrocoagulation with Al and Fe electrodes at an initial pH between 2 and 9, an electrolysis time of 30 min, and a current density of 20 mA/cm². When using the Al electrode, the tannin removal increased from 75% to 89% with an increase in the aqueous pH from 2 to 5, however, it then decreased from 86% to 50% with a further increase in the pH from 6 to 9 (Fig. 3a). The tannin removal was significantly higher for the system with the addition

of protein than those without the addition of protein (56–75%) (Fig. 3c).

The addition of protein helped increase tannin removal because the efficiency of electrocoagulation in removing soluble components depends on the solubility of the target molecules (Ardhan et al., 2021). Once the blood protein was added to the system, the solubility of tannins was reduced owing to the formation of protein-tannin complexes. Aqueous pH has a clear effect on the efficiency of electrocoagulation because the formation and stability of metal hydroxide species and their interactions with both dissolved and suspended matter are pH-dependent (Ali and Yaakob, 2012). Hassoune et al. (2017) reported that electrocoagulation with Al electrodes at a pH of 3–6 could remove hydrolyzable tannins from aqueous solutions with an efficiency of 90–95%. Tchamango et al. (2021) reported that the forms of Al (such as

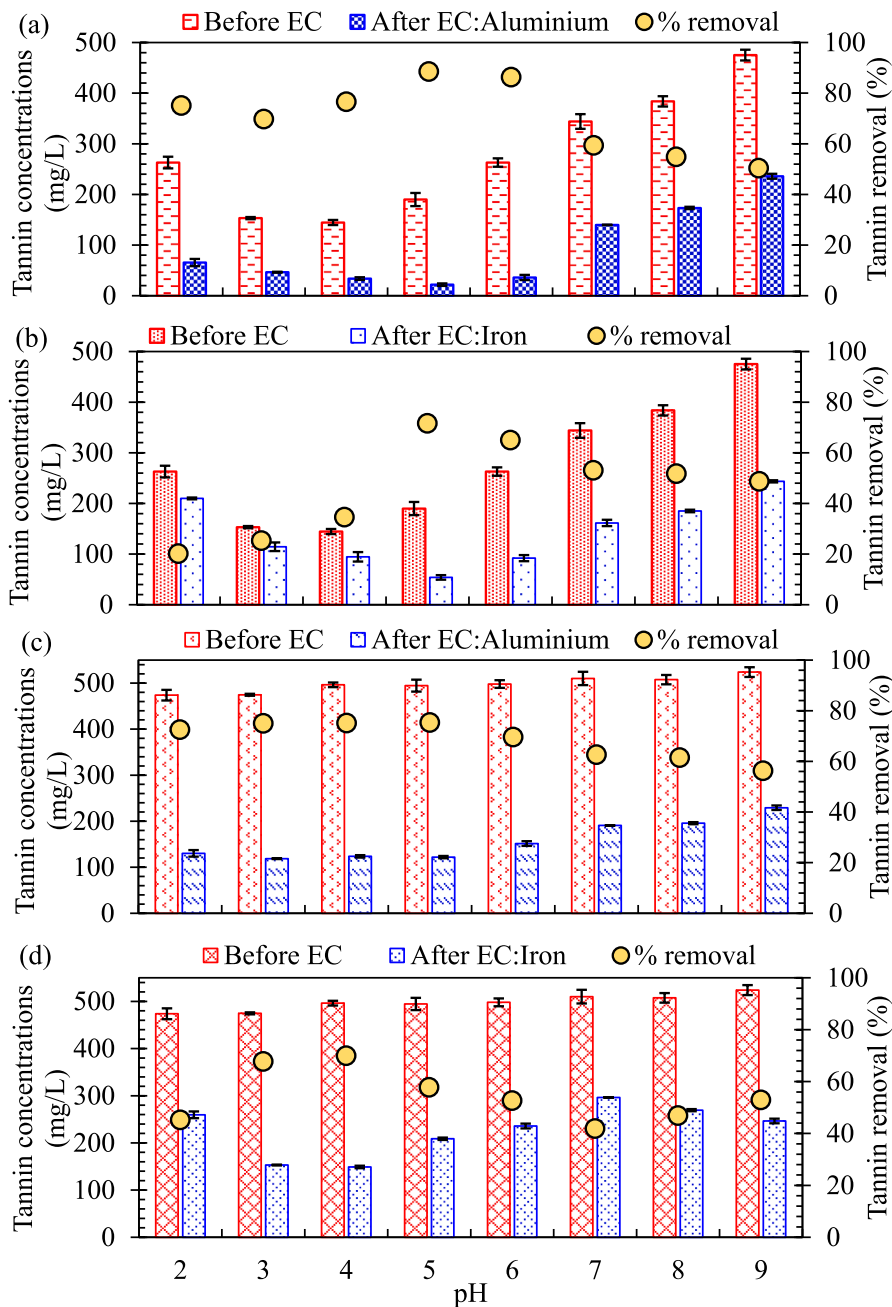
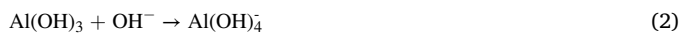


Fig. 3. Effects of pH on residual tannin concentrations and percentage tannin removal by electrocoagulation: (a) supernatant after precipitation treated with Al electrodes, (b) supernatant after precipitation treated with Fe electrodes, (c) anaerobically-treated POME treated with Al electrodes, and (d) anaerobically-treated POME treated with Fe electrodes.

aluminum hydroxide complexes) and the efficiency of the electrocoagulation process depend on the aqueous pH. For example, the removal efficiency increases with the formation of $\text{Al}(\text{OH})_3$ in an acidic medium in which the surface charges of colloidal particles are neutralized by cationic aluminum species. It should be mentioned that the presence of some compounds in the treated POME effluent could cause an early onset of electrode passivation. The operating pH of 5 offers the advantage of preventing the early onset of electrode passivation because the low pH environment inhibits the buildup of a surface layer (Ingels-son et al., 2020). In contrast, the removal efficiency decreased when the pH was increased above 7 because of the redissolution of $\text{Al}(\text{OH})_3$ in the presence of excess hydroxyl ions (OH^-) to form $\text{Al}(\text{OH})_4^-$ as shown in Eq. (2):



In general, the redissolution of $\text{Al}(\text{OH})_3$ has a negative effect on the efficiency of the electrocoagulation process (Kabdaşlı et al., 2012; Tchamango et al., 2021).

When using the Fe electrode, the tannin removal increased from 20% to 72% with an increase in the aqueous pH from 2 to 5 but then decreased from 65% to 48% with a further increase in the pH from 6 to 9 (Fig. 3b). The tannin removal was significantly higher for the system with the addition of protein than those without the addition of protein (42–70%) (Fig. 3d). Electrocoagulation with Al electrodes resulted in higher tannin removal than with Fe electrodes, possibly because the formation of protein–tannin complexes is favorable at an acidic pH, whereas the formation of iron hydroxide complexes is favorable at an alkaline pH (Mansouri et al., 2011). In addition, aluminum hydroxide complexes exist in various forms with more definite binding sites when compared to iron hydroxide complexes (Kabdaşlı et al., 2012; Tibebe et al., 2019).

3.4. Effects of current density and inter-electrode distance on the removal of soluble protein-tannin complexes by electrocoagulation

Fig. 4 illustrates the tannin removal efficiency and energy

consumption using electrocoagulation with Al electrodes, a current density between 20 and 40 mA/cm^2 , and a fixed inter-electrode distance of 15 mm. The tannin removal efficiency increased significantly when the current density was applied for 5 min but increased relatively slowly as the electrolysis time increased to 10 and 20 min. For the system with the addition of blood proteins, the tannin removal of approximately 81% was achieved with current densities of 30 and 40 mA/cm^2 and an electrolysis time of 10 min (Fig. 4a). Conversely, for the system without the addition of blood proteins, the significant removal of tannins was achieved with much longer electrolysis times, specifically, 78% with an electrolysis time of 30 min and a current density of 20 mA/cm^2 , 78% with an electrolysis time of 25 min and a current density of 30 mA/cm^2 , and 80% with an electrolysis time of 15 min and a current density of 40 mA/cm^2 . Owing to the shorter electrolysis time and lower current density, the system with the addition of blood proteins required significantly less energy to remove tannins. Fig. 4b shows the energy consumption as a function of the current density and electrolysis time. The energy consumption for the electrocoagulation process varied significantly between 2.9 and 75 kWh/m^3 , depending on the electrolysis time (5–30 min) and current density (20–40 mA/cm^2). For the system with the addition of blood proteins, a tannin removal of 81% was achieved with an electrolysis time of 10 min and a current density of 30 mA/cm^2 , consuming 12.5 kWh/m^3 . Without the addition of blood proteins, a tannin removal of 72% was achieved with an electrolysis time of 10 min and a current density of 40 mA/cm^2 , consuming 25 kWh/m^3 .

To reduce the energy input of the electrocoagulation treatment, the inter-electrode distances were reduced from 15 mm to 10, 8, and 6 mm. Fig. 5 shows the tannin removal efficiency and energy consumption of electrocoagulation with inter-electrode distances of 6, 8, and 10 mm at a current density of 30 mA/cm^2 . For the system with the addition of blood proteins, a decrease in the inter-electrode distance from 15 to 10 mm increased the tannin removal efficiency from 81% to 88%, whereas the energy consumption decreased significantly from 12.5 to 6.3 kWh/m^3 . As the inter-electrode distance decreased further to 8 and 6 mm, the tannin removal efficiency decreased to approximately 82%, with a slight decrease in the energy consumption to 5.5 kWh/m^3 . The tannin removal

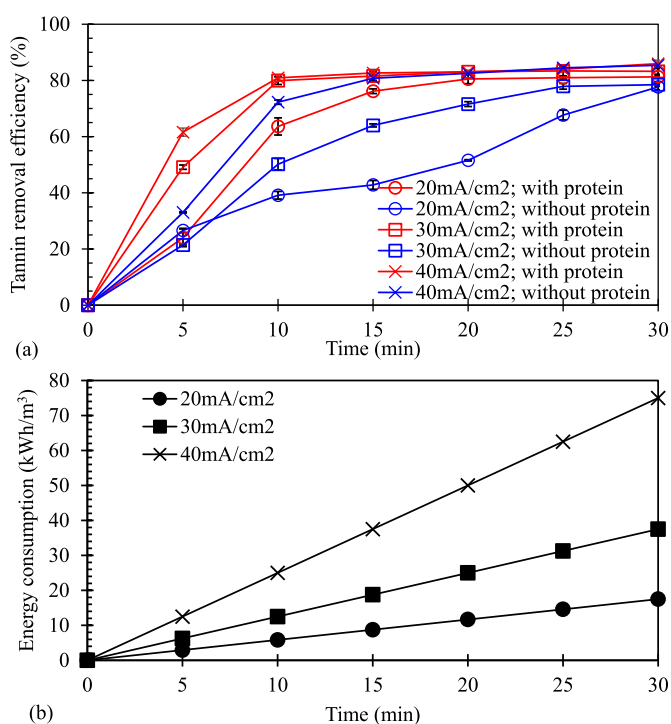


Fig. 4. Effects of current density and electrolysis time on the electrocoagulation removal of tannins: (a) tannin removal efficiency and (b) energy consumption.

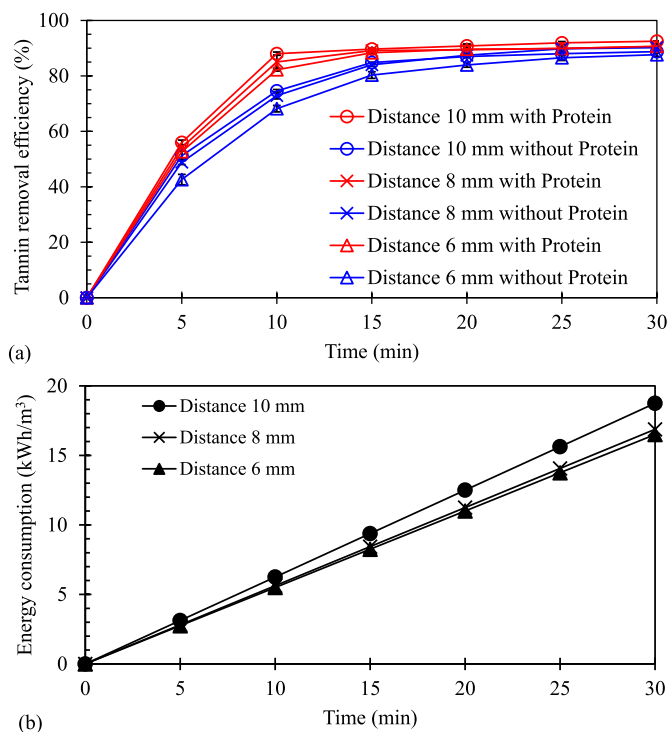


Fig. 5. Effects of the inter-electrode distance on the electrocoagulation removal of tannins: (a) tannin removal efficiency and (b) energy consumption.

efficiency could be further increased by increasing the electrolysis time to >10 min (Fig. 5a), but with higher energy consumption (Fig. 5b).

It has been reported that the inter-electrode distance influences the interaction of colloidal particles during electrocoagulation, floc formation, and their settling and flotation characteristics. Although electrical energy consumption decreases with decreasing inter-electrode distance, flocs created within a narrow inter-electrode distance of less than 10 mm possess poor settling characteristics (Shankar et al., 2014). Conversely, an inter-electrode distance of 10–12 mm is suitable for creating an electrostatic field in which ions can be easily transferred between the electrodes, stimulating aggregation of suspended particles to settleable flocs (Khandegar and Saroha, 2012). In contrast, floc formation becomes less effective when the inter-electrode distance is increased to >12 mm because the region with a low electric field becomes larger, causing the interaction between particles to become less important (Kumari and Naresh Kumar, 2020).

Table 1 shows the properties of the effluents after treatment by the precipitation and electrocoagulation processes using the optimum conditions of pH 5, a current density of 30 mA/cm², an inter-electrode distance of 10 mm, and an electrolysis time of 10 min. After tannin precipitation in series with electrocoagulation, the COD decreased from 6146 ± 152 for the covered lagoon effluent to 248 ± 62 mg/L (with added blood protein) and 952 ± 72 mg/L (without added blood protein). The covered lagoon effluent appeared dark brown in color (Fig. S1) with a color value of 22,217 ± 325 Pt-Co and tannin concentration of 545 ± 13 mg/L. After tannin removal without added protein, the sample appeared light brown (Fig. S1) with a color value of 4667 ± 142 Pt-Co and tannin concentration of 158 ± 3 mg/L, whereas that with the added protein appeared light yellow (Fig. S1) with a color value of 743 ± 62 Pt-Co and tannin concentration of 36 ± 2 mg/L.

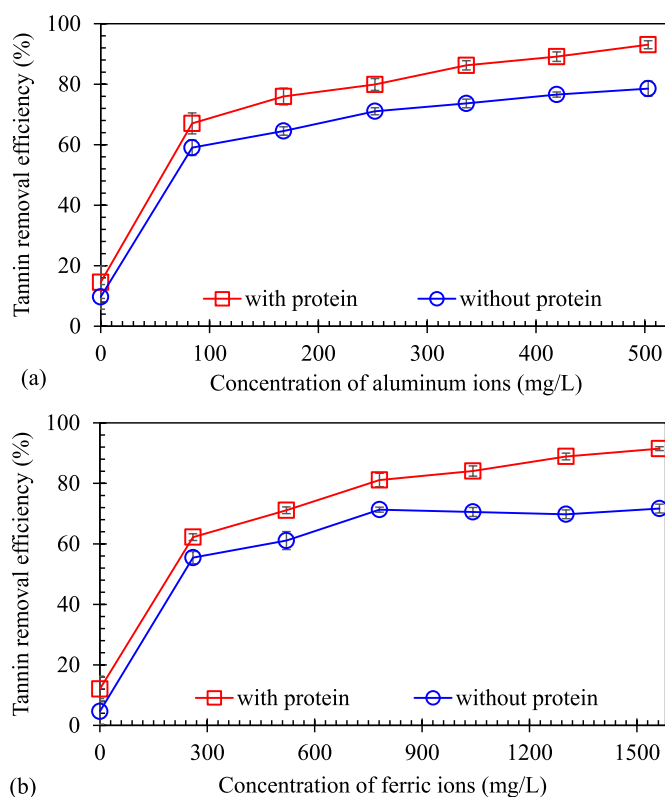


Fig. 6. Effects of coagulant dosages on the tannin removal efficiency at pH 5: (a) AlCl₃ and (b) FeCl₃.

3.5. Removal of soluble protein-tannin complexes using coagulation with AlCl₃ and FeCl₃

Fig. 6 shows the tannin removal efficiency using chemical coagulation with AlCl₃ and FeCl₃ at an initial pH of 5. The concentrations of Al³⁺ (0–503 mg/L) and Fe³⁺ (0–1563 mg/L) used in the coagulation experiments were in the same range as the amounts of Al³⁺ and Fe³⁺ released from the electrolytic oxidation of the anode electrode with electrolysis times between 5 and 30 min and a current density of 30 mA/cm². In addition, the Al³⁺ concentrations used in this study were in the same range as those previously reported for the treatment of paper and pulp mill effluents (Chaudhari et al., 2010; Gasmi et al., 2022). To ensure the effectiveness of the coagulation process, the concentrations of Al³⁺ and Fe³⁺ must be within the optimum range. Otherwise, the pH would decrease, causing the formation of other species with lower interspecies interactions than Al(OH)₃ such as Al(OH)₄⁻ and Al(OH)₂⁺, resulting in a decreased removal efficiency of the coagulation process (Nowacka et al., 2014; Gasmi et al., 2022). The results illustrated that the addition of blood proteins at a protein: tannin ratio of 0.33 (g/g) enhanced tannin removal by coagulation. With the addition of blood proteins, the tannin removal was 67% and 93% with Al³⁺ concentrations of 84 and 503 mg/L, respectively (Fig. 6a). Conversely, without protein addition, the tannin removal was relatively low, in the range of 59–79%, for all applied Al³⁺ concentrations (Fig. 6a).

Coagulation with FeCl₃ could also effectively remove tannins when used in a concentration range of 260–1563 mg/L Fe³⁺. The tannin removal ranged between 62 and 91% with the addition of blood protein and between 55 and 72% without protein (Fig. 6b). The pH is an important parameter that affects the efficiency of coagulation with FeCl₃. Abbas et al. (2021) found that coagulation with an Fe³⁺ concentration of 2000 mg/L at pH 4 was optimal for COD removal from dye wastewater of approximately 87%, whereas an increase in the Fe³⁺ concentration to 3000 mg/L caused the pH to decrease below 4, and the COD removal decreased to 72%.

In the coagulation of tannins using Al³⁺, the tannin molecule first interacts with Al³⁺ on the surface of Al(OH)₃ via anion exchange between the carboxylic group on the tannin and hydroxyl group on Al(OH)₃, followed by gradual adsorption of the rest of the tannin molecule onto the surface of Al(OH)₃ via van der Waals forces and H-bonding (An and Dultz, 2007; An and Dultz, 2007; acar and Şengil, 2003; Proença et al., 2022). In the coagulation of tannins using Fe³⁺, the hydroxyl group of catechol in tannin compounds interacts with Fe³⁺ to form quinones, which in turn self-polymerize to form brown-colored compounds. However, the oxidation of catechol by Fe³⁺ occurs relatively slowly, resulting in poor coagulation. (Bijlsma et al., 2020; Murugananthan et al., 2005; Nkhili et al., 2014).

When comparing the efficiencies of electrocoagulation with chemical coagulation in removing tannins, electrocoagulation using Al electrodes was found to be more effective than chemical coagulation with AlCl₃ and FeCl₃. With the addition of blood proteins, the removal efficiency of tannins by electrocoagulation was 88% at a current density of 30 mA/cm², an inter-electrode distance of 10 mm, and electrolysis time of 10 min. For the same amounts of Al³⁺ and Fe³⁺ ions, the chemical coagulation with 168 mg/L Al³⁺ and 521 mg/L Fe³⁺ removed 76% and 71% of the tannins, respectively. This can be explained by the fact that, in electrocoagulation, the released Al³⁺ and Al(OH)₂⁺ species at the anode combine with OH⁻ released at the cathode, leading to formation of metal hydroxides, and polyhydroxide and polyhydroxy metallic compounds (Phalakornkule et al., 2010a). These complex molecules have a relatively high affinity for dissolved solids (Ali and Yaakob, 2012). In addition, H₂ bubbles generated from water splitting at the cathode enhance floc flotation (Phalakornkule et al., 2010b; Hakizimana et al., 2017; Rakhmania et al., 2022).

3.6. Characteristics of tannin, pig blood, casein proteins, and protein-tannin complexes

Fig. S2 compares the FTIR spectra of tannins in the covered lagoon effluent and Gallo tannins in the range of 500–4000 cm^{-1} . The FTIR spectra of the tannins in the covered lagoon effluent were similar to those of Gallo tannins, suggesting that the tannin sample was Gallo tannins. Both FTIR spectra exhibited a broad peak centered at 3234 cm^{-1} , which can be assigned to hydroxyl groups (O–H) and aromatic C–H (Wahyono et al., 2019). The sharp peak around 2878–2800 cm^{-1} is attributed to the symmetric and antisymmetric C–H stretching vibrations of the CH_2 and CH_3 groups of aliphatic hydrocarbons (Subramonian et al., 2014; Wahyono et al., 2019). The peaks at 1651, 1558, and 1263 cm^{-1} are due to C=O stretching vibrations in primary, secondary, and tertiary amides, respectively (Fatombi et al., 2013). The peak at 1397 cm^{-1} was due to the C–OH stretch of phenols, whereas the peak at 1035 cm^{-1} was due to the C–H in-plane deformation of aromatic compounds (Jensen et al., 2008).

Table S1 shows the amino acid composition of the pig blood and casein. The major amino acids in the pig blood included aspartic acid ($297.5 \pm 77.3 \mu\text{mol/mL}$), leucine ($18.4 \pm 5.8 \mu\text{mol/mL}$), and tyrosine ($18.9 \pm 1.4 \mu\text{mol/mL}$), whereas the major amino acids in casein included lysine ($57.7 \pm 2.2 \mu\text{mol/mL}$), valine ($50.6 \pm 2.1 \mu\text{mol/mL}$), and arginine ($30.8 \pm 1.2 \mu\text{mol/mL}$). Because the experimental pH (pH 4) was lower than the $\text{pK}_{\text{a}2}$ of aspartic acid, the amine group of aspartic acid could accept a proton to become positively charged. The positive amino group can interact with the carboxyl group ($-\text{COO}^-$) on the phenolic rings of tannins via ionic bonds (Braghiroli et al., 2013; Ghahri et al., 2016). In addition, the H-acceptor of the carbonyl, amide, and amine groups of aspartic acid could interact with the hydroxyl group ($-\text{OH}$) on the phenol rings of tannins via a hydrogen bond to form protein–tannin complexes. After gradual coagulation, they become large enough to form insoluble precipitates, which then precipitate out of solution (Braghiroli et al., 2013; Ghahri et al., 2018, 2021).

Similarly, at the optimal pH for the removal of tannins by the addition of casein (pH 3), the amine groups of both lysine and valine are positively charged and can interact with the carboxyl group ($-\text{COO}^-$) on the phenolic rings of tannins via ionic bonds. In addition, the phenolic carboxyl group on tannins forms an ionic bond with the NH_3^+ side chain of the guanidyl group of arginine (Ghahri et al., 2016). The differences in the tannin removal efficiency between the addition of pig blood (72% at pH 4) and casein (26% at pH 3) could be due to the proportion of amino acids that can interact with tannins to form protein–tannin complexes. That is, the proportion of aspartic acid in pig blood was 5.2-, 5.9-, and 9.7 fold more than that of lysine, valine, and arginine in casein, respectively.

Fig. S3 shows the microscopic morphological characteristics of the flocs formed during electrocoagulation with a fixed current density of 30 mA/cm^2 , inter-electrode distance of 10 mm, and electrolysis time of 5–30 min. The flocs from the system with the addition of blood protein were the largest and densest at the optimum electrolysis time of 10 min, at which the tannin removal efficiency was the highest. However, when the electrolysis time was further increased from 10 min to 15, 20, and 25 min, the floc size decreased but remained dense. When the electrolysis time was further increased to 30 min, the flocs broke and became less dense. In contrast, flocs from the system without the addition of blood protein were smaller and less dense. The floc size gradually increased until the electrolysis time of 15 min but broke apart and became less dense when the electrolysis time was longer than 20 min.

Fig. S4 shows the SEM images and SEM-EDS spectra of the precipitates in the electrocoagulation system with (Fig. S4a) and without pig blood (Fig. S4b). The flocs consisted of small aggregates that were densely interconnected. The major elements in the flocs were C, O, Na, Mg, Al, Cl, and K (Figs. S4c and d). The identified C and O elements supported the presence of C- and O-containing functional groups, and therefore tannins and blood proteins, in the precipitates, whereas Al

originated from the released Al anodes. The composition of Al in the precipitates in the electrocoagulation system with pig blood (3.10%) was slightly lower than that without pig blood (4.33%).

4. Conclusion

In this study, protein–tannin complexation in conjunction with electrocoagulation was investigated to remove tannins from anaerobically-treated POME effluents. At an optimal condition with a pig blood protein: tannin ratio of 0.33 (w/w), a current density of 30 mA/cm^2 , pH 5, and an electrolysis time of 10 min, the removals of tannins, COD, and color were 93%, 96%, and 97%, respectively. Pig blood protein causes the formation and precipitation of insoluble protein–tannin complexes, whereas subsequent electrocoagulation causes the precipitation of soluble protein–tannin complexes. The addition of pig blood protein not only increased the tannin removal efficiency but also reduced the energy consumption of the process.

Credit author statement

Peerawat Khongkliang: Conceptualization, Methodology, Visualization, Writing – original draft. Maneerat Khemkhao: Investigation, Resources, Visualization. Sithipong Mahathanabodee: Investigation, Resources. Sompong O-Thong: Review & Editing, Abudukeremu Kadier: Review & Editing, Chantaporn Phalakornkule: Conceptualization, Methodology, Resources, Visualization, Writing – review & editing, Supervision.

Declaration of competing interest

The authors declare that they have no known competing financial interests or personal relationships that could have appeared to influence the work reported in this paper.

Data availability

Data will be made available on request.

Acknowledgments

The authors gratefully acknowledge the financial support provided by King Mongkut's University of Technology North Bangkok (Grant No. KMUTNB-BasicR-64-28-12 and KMUTNB-66-IP-03), and the National Research Council of Thailand. The authors gratefully acknowledge the postdoctoral grant to Peerawat Khongkliang from the Science and Technology Postgraduate Education and Research Development Office (PERDO) and the Joint Graduate School of Energy and Environment (JGSEE), King Mongkut's University of Technology Thonburi (Grant No. JGSEE/THESIS/343, and Bioeconomy_PI_2563_04).

Appendix A. Supplementary data

Supplementary data to this article can be found online at <https://doi.org/10.1016/j.chemosphere.2023.138086>.

References

- Abbas, M.J., Mohamed, R., Al-Sahari, M., Al-Gheethi, A., Daud, A.M.M., 2021. Optimizing FeCl_3 in coagulation-flocculation treatment of dye wastes. *Songklanakarinn J. Sci. Technol.* 43, 1094–1102. <https://doi.org/10.14456/sjst-psu.2021.144>.
- Adamczyk, B., Salminen, J.P., Smolander, A., Kitunen, V., 2012. Precipitation of proteins by tannins: effects of concentration, protein/tannin ratio and pH. *Int. J. Food Sci. Technol.* 47, 875–878. <https://doi.org/10.1111/j.1365-2621.2011.02911.x>.
- Adamczyk, B., Simon, J., Kitunen, V., Adamczyk, S., Smolander, A., 2017. Tannins and their complex interaction with different organic nitrogen compounds and enzymes: old paradigms versus recent advances. *Chemistry* 6, 610–614. <https://doi.org/10.1002/open.201700113>.

- Adhoum, N., Monser, L., 2004. Decolourization and removal of phenolic compounds from olive mill wastewater by electrocoagulation. *Chem. Eng. Process. Process Intensif.* 43, 1281–1287. <https://doi.org/10.1016/j.cep.2003.12.001>.
- Al-Amshawe, S.K., Yunus, M.Y., Azoddein, A.A., 2020. A review on hybrid processes for palm oil mill effluent: possible approaches. *IOP Conf. Ser. Mater. Sci. Eng.* 736 <https://doi.org/10.1088/1757-899X/736/2/022036>.
- Al-Qudah, Z., Al-Qudah, Y., Omar, W., 2019. On the performance of electrocoagulation-assisted biological treatment processes: a review on the state of the art. *Environ. Sci. Pollut. Res.* 26, 28689–28713. <https://doi.org/10.1007/s11356-019-06053-6>.
- Ali, E., Yaakob, Z., 2012. In: *Electrocoagulation for Treatment of Industrial Effluents and Hydrogen Production*. IntechOpen, London, 13. <https://www.intechopen.com/chapters/40138>.
- An, J.H., Dultz, S., 2007. Adsorption of tannic acid on chitosan-montmorillonite as a function of pH and surface charge properties. *Appl. Clay Sci.* 36, 256–264. <https://doi.org/10.1016/j.clay.2006.11.001>.
- APHA, AWWA, WEF, 2012. *Standard Methods for the Examination of Water and Wastewater, twenty-second ed.*
- Ardhan, N., Tongpadungrod, P., Phalakornkule, C., 2021. Effects of auxiliary chemicals and dye solubility on chemical oxygen demand reduction of dyes by electrocoagulation with Fe electrode. In: *Materials Today: Proceedings*. Elsevier, pp. 2529–2533. <https://doi.org/10.1016/j.matpr.2021.10.446>.
- Banch, T.J.H., Hanafiah, M.M., Alkarkhi, A.F.M., Abu Amr, S.S., 2019. Factorial design and optimization of landfill leachate treatment using tannin-based natural coagulant. *Polymers* 11, 1349. <https://doi.org/10.3390/polym11081349>.
- Bijlsma, J., de Bruijn, W.J.C., Hageman, J.A., Goos, P., Velikov, K.P., Vincken, J.P., 2020. Revealing the main factors and two-way interactions contributing to food discoloration caused by iron-catechol complexation. *Sci. Rep.* 10, 1–11. <https://doi.org/10.1038/s41598-020-65171-1>.
- Braghiroli, F., Fierro, V., Pizzi, A., Rode, K., Radke, W., Delmotte, L., Parmentier, J., Celzard, A., 2013. Reaction of condensed tannins with ammonia. *Ind. Crop. Prod.* 44, 330–335. <https://doi.org/10.1016/j.indcrop.2012.11.024>.
- Brooks, L., McCloskey, L., Mckesson, D., Sylvan, M., 2008. Adams-Harbertson protein precipitation-based wine tannin method found invalid. *J. AOAC Int.* 91, 1090–1094. <https://doi.org/10.1093/jaoac/91.5.1090>.
- Chaudhari, P.K., Majumdar, B., Choudhary, R., Yadav, D.K., Chand, S., 2010. Treatment of paper and pulp mill effluent by coagulation. *Environ. Technol.* 31, 357–363. <https://doi.org/10.1080/09593330903486665>.
- Dashti, A.F., Salman, N.A.S., Adnan, R., Zahed, M.A., 2022. Palm oil mill effluent treatment using combination of low cost chickpea coagulant and granular activated carbon: optimization via response surface methodology. *Groundw. Sustain. Dev.* 16 <https://doi.org/10.1016/j.gsd.2021.100709>.
- Dentinho, M., Bessa, R., 2016. Effect of tannin source and pH on stability of tannin-protein complexes. *Rev. Ciencias Agrar.* 39, 114–121. <https://doi.org/10.19084/rca15062>.
- Dexter, Z.D., Joseph, C.G., Zahrim, A.Y., 2016. A review on palm oil mill biogas plant wastewater treatment using coagulation-ozonation. *IOP Conf. Ser. Earth Environ. Sci.* 36 <https://doi.org/10.1088/1755-1315/36/1/012029>.
- dos Santos, J.D., Veit, M.T., Juchen, P.T., da Cunha Gonçalves, G., Palácio, S.M., Fagundes-Klen, M., 2018. Use of different coagulants for cassava processing wastewater treatment. *J. Environ. Chem. Eng.* 6, 1821–1827. <https://doi.org/10.1016/j.jece.2018.02.039>.
- Engström, M.T., Sun, X., Suber, M.P., Li, M., Salminen, J.P., Hagerman, A.E., 2016. The oxidative activity of ellagitannins dictates their tendency to form highly stabilized complexes with bovine serum albumin at increased pH. *J. Agric. Food Chem.* 64, 8994–9003. <https://doi.org/10.1021/acs.jafc.6b01571>.
- Fajardo, A.S., Rodrigues, R.F., Martins, R.C., Castro, L.M., Quinta-Ferreira, R.M., 2015. Phenolic wastewaters treatment by electrocoagulation process using Zn anode. *Chem. Eng. J.* 275, 331–341. <https://doi.org/10.1016/j.cej.2015.03.116>.
- Fatombi, J.K., Lartiges, B., Aminou, T., Barres, O., Caillet, C., 2013. A natural coagulant protein from copra (*Cocos nucifera*): isolation, characterization, and potential for water purification. *Sep. Purif. Technol.* 116, 35–40. <https://doi.org/10.1016/j.seppur.2013.05.015>.
- Gasmi, A., Ibrahim, S., Elboughdiri, N., Tekaya, M.A., Ghernaout, D., Hannachi, A., Mesloub, A., Ayadi, B., Kolsi, L., 2022. Comparative study of chemical coagulation and electrocoagulation for the treatment of real textile wastewater: optimization and operating cost estimation. *ACS Omega* 7, 22456–22476. <https://doi.org/10.1021/acsomega.2c01652>.
- Ghahri, S., Chen, X., Pizzi, A., Hajjassani, R., Papadopoulos, A.N., 2021. Natural tannins as new cross-linking materials for soy-based adhesives. *Polymers* 13, 1–15. <https://doi.org/10.3390/polym13040595>.
- Ghahri, S., Mohebbi, B., Pizzi, A., Mirshokraie, A., Mansouri, H.R., 2018. Improving water resistance of soy-based adhesive by vegetable tannin. *J. Polym. Environ.* 26, 1881–1890. <https://doi.org/10.1007/s10924-017-1090-6>.
- Ghahri, S., Pizzi, A., Mohebbi, B., Mirshokraie, A., Mansouri, H.R., 2016. Soy-based, tannin-modified plywood adhesives. *J. Adhes.* 94, 218–237. <https://doi.org/10.1080/00218464.2016.1258310>.
- Hakizimana, J.N., Gourich, B., Chafi, M., Stiriba, Y., Vial, C., Drogui, P., Naja, J., 2017. Electrocoagulation process in water treatment: a review of electrocoagulation modeling approaches. *Desalination* 404, 1–21. <https://doi.org/10.1016/j.desal.2016.10.011>.
- Hassoun, J., Tahiri, S., Aarfane, A., El krati, M., Salhi, A., Azzi, M., 2017. Removal of hydrolyzable and condensed tannins from aqueous solutions by electrocoagulation process. *J. Environ. Eng.* 143, 1–8. [https://doi.org/10.1061/\(asce\)jee.1943-7870.0001196](https://doi.org/10.1061/(asce)jee.1943-7870.0001196).
- Ingelsson, M., Yasri, N., Roberts, E.P.L., 2020. Electrode passivation, faradaic efficiency, and performance enhancement strategies in electrocoagulation—a review. *Water Res.* 187, 116433 <https://doi.org/10.1016/j.watres.2020.116433>.
- Jalani, N., Aziz, A., Wahab, N., Hassan, W.W., Zainal, N., 2016. Application of palm kernel shell activated carbon for the removal of pollutant and color in palm oil mill effluent treatment. *J. Earth, Environ. Heal. Sci.* 2, 15. <https://doi.org/10.4103/2423-7752.181802>.
- Jensen, J.S., Egebo, M., Meyer, A.S., 2008. Identification of spectral regions for the quantification of red wine tannins with fourier transform mid-infrared spectroscopy. *J. Agric. Food Chem.* 56, 3493–3499. <https://doi.org/10.1021/jf703573f>.
- Jones-Moore, H.R., Jelley, R.E., Marangon, M., Fedrizzi, B., 2022. The interactions of wine polysaccharides with aroma compounds, tannins, and proteins, and their importance to winemaking. *Food Hydrocolloids* 123, 107150. <https://doi.org/10.1016/j.foodhyd.2021.107150>.
- Jordão, A.M., Ricardo-da-Silva, J.M., Laureano, O., 2005. Extraction of some ellagic tannins and ellagic acid from oak wood chips (*quercus pyrenaica* L.) in model wine solutions: effect of time, pH, temperature and alcoholic content. *S. Afr. J. Enol. Vitic.* 26, 83–89. <https://doi.org/10.21548/26-2-2122>.
- Kabdashli, I., Arslan-Alaton, I., Ölmez-Hanci, T., Tüney, O., 2012. Electrocoagulation applications for industrial wastewaters: a critical review. *Environ. Technol. Rev.* 1, 2–45. <https://doi.org/10.1080/21622515.2012.715390>.
- Kamyab, H., Chelliapan, S., Din, M.F.M., Rezaia, S., Khademi, T., Kumar, A., 2018. Palm oil mill effluent as an environmental pollutant. In: *Palm Oil. InTech*, pp. 137–144. <https://doi.org/10.5772/intechopen.75811>.
- Khandegar, V., Saroha, A.K., 2012. Electrochemical treatment of distillery spent wash using aluminum and iron electrodes. *Chin. J. Chem. Eng.* 20, 439–443. [https://doi.org/10.1016/S1004-9541\(11\)60204-8](https://doi.org/10.1016/S1004-9541(11)60204-8).
- Khemkhao, M., Domrongpakkaphan, V., Phalakornkule, C., 2022. Process performance and microbial community variation in high-rate anaerobic continuous stirred tank reactor treating palm oil mill effluent at temperatures between 55 and 70 °C. *Water and Biomass Valorization* 13, 431–442. <https://doi.org/10.1007/s12649-021-01539-2>.
- Khemkhao, M., Techkarnjanaruk, S., Phalakornkule, C., 2016. Effect of chitosan on reactor performance and population of specific methanogens in a modified CSTR treating raw POME. *Biomass Bioenergy* 86, 11–20. <https://doi.org/10.1016/j.biombio.2016.01.002>.
- Kosińska, A., Karamač, M., Penkacik, K., Urbalewicz, A., Amarowicz, R., 2011. Interactions between tannins and proteins isolated from broad bean seeds (*Vicia faba* Major) yield soluble and non-soluble complexes. *Eur. Food Res. Technol.* 233, 213–222. <https://doi.org/10.1007/s00217-011-1506-9>.
- Kumari, S., Naresh Kumar, R., 2020. Electrocoagulation for COD, turbidity, ammonia and phosphate removal from municipal wastewater. *J. Indian Chem. Soc.* 97, 527–532.
- Maeng, S.K., Timmes, T.C., Kim, H.C., 2017. Characteristics of flocs formed by polymer-only coagulation in water treatment and their impacts on the performance of downstream membrane separation. *Environ. Technol.* 38, 2601–2610. <https://doi.org/10.1080/09593330.2016.1271460>.
- Maisuria, K.J., Shah, K.A., Rana, J.K., 2022. Removal of Tannic acid and COD from synthetic Tannery wastewater. *IOP Conf. Ser. Earth Environ. Sci.* 1086, 012035 <https://doi.org/10.1088/1755-1315/1086/1/012035>.
- Mansouri, K., Elsaid, K., Bedoui, A., Bensalah, N., Abdel-Wahab, A., 2011. Application of electrochemically dissolved iron in the removal of tannic acid from water. *Chem. Eng. J.* 172, 970–976. <https://doi.org/10.1016/j.cej.2011.07.009>.
- Mezzomo, R., Paulino, P.V.R., Detmann, E., Teixeira, C.R.V., Alves, L.C., Assunção, R.N., 2015. Tannin on non-degradable digestible protein from proteic sources in cattle rumen. *Acta Sci. Anim. Sci.* 37, 389–395. <https://doi.org/10.4025/actascianimsci.v37i4.28126>.
- Mohamad, Z., Razak, A.A., Krishnan, S., Singh, L., Zularisam, A.W., Nasrullah, M., 2022. Treatment of palm oil mill effluent using electrocoagulation powered by direct photovoltaic solar system. *Chem. Eng. Res. Des.* 177, 578–582. <https://doi.org/10.1016/j.cherd.2021.11.019>.
- Muruganathan, M., Raju, G.B., Prabhakar, S., 2005. Removal of tannins and polyhydroxy phenols by electrochemical techniques. *J. Chem. Technol. Biotechnol.* 80, 1188–1197. <https://doi.org/10.1002/jctb.1314>.
- Nasrullah, M., Ansar, S., Krishnan, S., Singh, L., Peera, S.G., Zularisam, A.W., 2022. Electrocoagulation treatment of raw palm oil mill effluent: optimization process using high current application. *Chemosphere* 299, 134387. <https://doi.org/10.1016/j.chemosphere.2022.134387>.
- Nkhili, E., Loonis, M., Mihai, S., El Hajji, H., Dangles, O., 2014. Reactivity of food phenols with iron and copper ions: binding, dioxygen activation and oxidation mechanisms. *Food Funct.* 5, 1186–1202. <https://doi.org/10.1039/c4fo00007b>.
- Nowacka, A., Włodarczyk-Makula, M., Macherzyński, B., 2014. Comparison of effectiveness of coagulation with aluminum sulfate and pre-hydrolyzed aluminum coagulants. *Desalination Water Treat.* 52, 3843–3851. <https://doi.org/10.1080/19443994.2014.888129>.
- Oh, H., Hoff, J.E., 1987. pH dependence of complex formation between condensed tannins and proteins. *J. Food Sci.* 52, 1267–1269. <https://doi.org/10.1111/j.1365-2621.1987.tb14059.x>.
- Oktiawan, W., Priyambada, I.B., Aji, S., Budi, F.S., 2021. Effect of current strength on electrocoagulation using Al-Fe electrodes in COD and TSS removal of domestic wastewater. *IOP Conf. Ser. Earth Environ. Sci.* 623 <https://doi.org/10.1088/1755-1315/623/1/012080>.
- Osawa, R., Walsh, T.P., 1993. Effects of acidic and alkaline treatments on tannic acid and its binding property to protein. *J. Agric. Food Chem.* 41, 704–707. <https://doi.org/10.1021/jf00029a004>.

- Özacar, M., Şengil, I.A., 2003. Evaluation of tannin biopolymer as a coagulant aid for coagulation of colloidal particles. *Colloids Surfaces A Physicochem. Eng. Asp.* 229, 85–96. <https://doi.org/10.1016/j.colsurfa.2003.07.006>.
- Phalakornkule, C., Karakat, B., Nuyut, T., Ruttithiwapanich, T., 2010a. Investigation of electrochemical variables and performance of a continuous upflow electrocoagulation process in the treatment of reactive blue 140. *Water Environ. Res.* 82, 2325–2332. <https://doi.org/10.2175/106143010x12681059116815>.
- Phalakornkule, C., Mangmeemak, J., Intrachod, K., Nuntakumjorn, B., 2010b. Pretreatment of palm oil mill effluent by electrocoagulation and coagulation. *Sci. Asia* 36, 142–149. <https://doi.org/10.2306/scienceasia1513-1874.2010.36.142>.
- Phalakornkule, C., Polgumhang, S., Tongdaung, W., Karakat, B., Nuyut, T., 2010c. Electrocoagulation of blue reactive, red disperse and mixed dyes, and application in treating textile effluent. *J. Environ. Manag.* 91, 918–926. <https://doi.org/10.1016/j.jenvman.2009.11.008>.
- Proença, C.S., Serrano, B., Correia, J., Araújo, M.E.M., 2022. Evaluation of Tannins as Potential Green Corrosion Inhibitors of Aluminium Alloy Used in Aeronautical Industry. *Metals (Basel)*, vol. 12. <https://doi.org/10.3390/met12030508>.
- Rakamthong, C., Prasertsan, P., 2011. Decolorization and phenol removal of anaerobic palm oil mill effluent by phanerochaete chrysosporium ATCC 24725. *TiChE Int. Conf.* 10–12.
- Rakhmania, Kamyab, H., Yuzir, M.A., Abdullah, N., Quan, L.M., Riyadi, F.A., Marzouki, R., 2022. Recent applications of the electrocoagulation process on agro-based industrial wastewater: a review. *Sustain. Times* 14, 1–19. <https://doi.org/10.3390/su14041985>.
- Rana, M., Saini, K., 2022. A study on waste water treatment of chemical industry using electro-coagulation. *J. Emerg. Technol. Innov. Res.* 9, 478–481.
- Reilly, M., Cooley, A.P., Tito, D., Tassou, S.A., Theodorou, M.K., 2019. Electrocoagulation treatment of dairy processing and slaughterhouse wastewaters. *Energy Proc.* 161, 343–351. <https://doi.org/10.1016/j.egypro.2019.02.106>.
- Seengenyong, J., Mamimin, C., Prasertsan, P., O-Thong, S., 2019. Pilot-scale of biohythane production from palm oil mill effluent by two-stage thermophilic anaerobic fermentation. *Int. J. Hydrogen Energy* 44, 3347–3355. <https://doi.org/10.1016/j.ijhydene.2018.08.021>.
- Shankar, R., Singh, L., Mondal, P., Chand, S., 2014. Removal of COD, TOC, and color from pulp and paper industry wastewater through electrocoagulation. *Desalination Water Treat.* 52, 7711–7722. <https://doi.org/10.1080/19443994.2013.831782>.
- Soares, Susana, Brandão, E., Guerreiro, C., Soares, Sónia, Mateus, N., De Freitas, V., 2020. Tannins in food: insights into the molecular perception of astringency and bitter taste. *Molecules* 25, 1–26. <https://doi.org/10.3390/molecules25112590>.
- Subramonian, W., Wu, T.Y., Chai, S.P., 2014. A comprehensive study on coagulant performance and floc characterization of natural Cassia obtusifolia seed gum in treatment of raw pulp and paper mill effluent. *Ind. Crop. Prod.* 61, 317–324. <https://doi.org/10.1016/j.indcrop.2014.06.055>.
- Tchamango, S.R., Wandji Ngayo, K., Belibi Belibi, P.D., Nkouam, F., Ngassoum, M.B., 2021. Treatment of a dairy effluent by classical electrocoagulation and indirect electrocoagulation with aluminum electrodes. *Separ. Sci. Technol.* 56, 1128–1139. <https://doi.org/10.1080/01496395.2020.1748889>.
- Tibebe, D., Kassa, Y., Bhaskarwar, A.N., 2019. Treatment and characterization of phosphorus from synthetic wastewater using aluminum plate electrodes in the electrocoagulation process. *BMC Chem* 13, 1–14. <https://doi.org/10.1186/s13065-019-0628-1>.
- Uğurlu, M., Gürses, A., Doğar, Ç., Yalçın, M., 2008. The removal of lignin and phenol from paper mill effluents by electrocoagulation. *J. Environ. Manag.* 87, 420–428. <https://doi.org/10.1016/j.jenvman.2007.01.007>.
- Ujang, F.A., Roslan, A.M., Osman, N.A., Norman, A., Idris, J., Farid, M.A.A., Halmi, M.I. E., Gozan, M., Hassan, M.A., 2021. Removal behaviour of residual pollutants from biologically treated palm oil mill effluent by Pennisetum purpureum in constructed wetland. *Sci. Rep.* 11, 1–12. <https://doi.org/10.1038/s41598-021-97789-0>.
- Wahyono, T., Astuti, D.A., Komang Gede Wiryawan, I., Sugoro, L., Jayanegara, A., 2019. Fourier transform mid-infrared (FTIR) spectroscopy to identify tannin compounds in the panicle of sorghum mutant lines. *IOP Conf. Ser. Mater. Sci. Eng.* 546 <https://doi.org/10.1088/1757-899X/546/4/042045>.
- Zahrim, A.Y., 2014. Palm oil mill biogas producing process effluent treatment: a short review. *J. Appl. Sci.* 14, 3149. <https://doi.org/10.3923/jas.2014.3149.3155>, 2155.



Efficiency enhancement of electrocoagulation, ion-exchange resin and reverse osmosis (RO) membrane filtration by prior organic precipitation for treatment of anaerobically-treated palm oil mill effluent

Peerawat Khongkliang^{a,b}, Sasikarn Nuchdang^c, Dussadee Rattanaphra^c, Wilasinee Kingkam^c, Sithipong Mahathanabodee^d, Jarungwit Boonnorat^e, Abudukeremu Kadier^{f,g}, Putu Teta Prihartini Aryanti^h, Chantaraporn Phalakornkule^{a,b,i,*}

^a The Joint Graduate School of Energy and Environment, King Mongkut's University of Technology Thonburi, Bangkok, 10140, Thailand

^b Research Center for Circular Products and Energy, KMUTNB, Bangkok, 10800, Thailand

^c Nuclear Technology Research and Development Center, Thailand Institute of Nuclear Technology, Nakorn Nayok, 26120, Thailand

^d Department of Production Engineering, Faculty of Engineering, King Mongkut's University of Technology North Bangkok, Bangkok, 10800, Thailand

^e Department of Environmental Engineering, Faculty of Engineering, Rajamangala University of Technology Thanyaburi (RMUTT), Pathum Thani, 12110, Thailand

^f Laboratory of Environmental Science and Technology, The Xinjiang Technical Institute of Physics and Chemistry, Key Laboratory of Functional Materials and Devices for Special Environments, Chinese Academy of Sciences (CAS), Urumqi, 830011, Xinjiang, China

^g Center of Materials Science and Optoelectronics Engineering, University of Chinese Academy of Sciences, Beijing, 100049, China

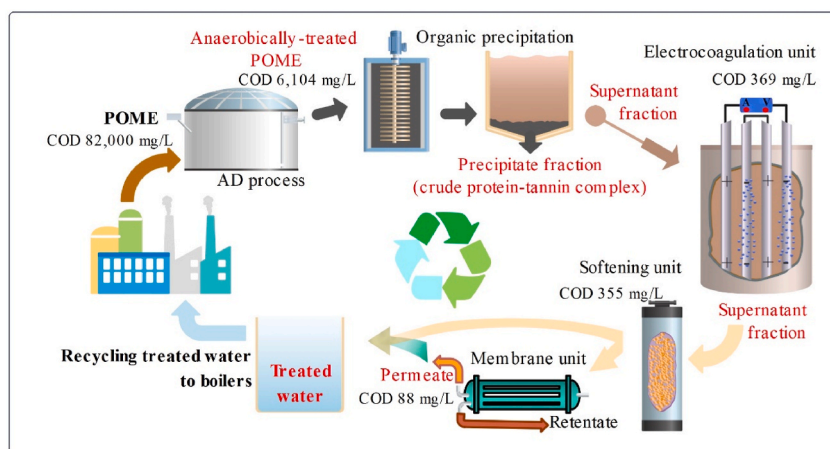
^h Chemical Engineering Department, Faculty of Engineering, Universitas Jenderal Achmad Yani, Cibeer Cimahi - West Java, Indonesia

ⁱ Department of Chemical Engineering, Faculty of Engineering, King Mongkut's University of Technology North Bangkok, Bangkok, 10800, Thailand

HIGHLIGHTS

- The integrated process comprised organic precipitation, EC, ion-exchange resin, RO.
- The organic precipitation of tannins in POME was performed using pig blood proteins.
- The efficiency of COD removal from anaerobically-treated POME was 98.5%.
- The integrated treatment process increased water hardness removal to 99%.
- The properties of treated POME met the criteria for industrial boiler use.

GRAPHICAL ABSTRACT



* Corresponding author. Department of Chemical Engineering, Faculty of Engineering, King Mongkut's University of Technology North Bangkok, Bangkok, 10800, Thailand

E-mail addresses: peerawatkhongkliang@gmail.com (P. Khongkliang), abudukeremu@ms.xjb.ac.cn (A. Kadier), p.teta@lecture.unjani.ac.id (P.T.P. Aryanti), chantaraporn.p@eng.kmutnb.ac.th (C. Phalakornkule).

<https://doi.org/10.1016/j.chemosphere.2024.142899>

Received 11 March 2024; Received in revised form 1 July 2024; Accepted 17 July 2024

Available online 17 July 2024

0045-6535/© 2024 Elsevier Ltd. All rights reserved, including those for text and data mining, AI training, and similar technologies.

ARTICLE INFO

Handling editor: A ADALBERTO NOYOLA

Keywords:

Anaerobic treatment
 Palm oil mill effluent
 Organic precipitation
 Electrocoagulation
 Ion exchange resin
 Reverse osmosis membrane

ABSTRACT

Anaerobically-treated palm oil mill effluent (POME) still has unacceptable properties for water recycling and reuse, with an unpleasant appearance due to the brownish color caused by tannins and phenolic compounds. This study proposes an approach for treating anaerobically-treated POME for water recycling by combining organic precipitation, electrocoagulation (EC), and ion-exchange resin, followed by reverse osmosis (RO) membrane filtration in series. The results indicated that the organic precipitation enhanced the efficiency of EC treatment in reducing the concentrations of tannins, color, and chemical oxygen demand (COD) of the anaerobically-treated POME effluent, with reductions of 95.73%, 96.31%, and 93.96% for tannin, color, and COD, respectively. Moreover, organic precipitation affected the effectiveness of Ca^{2+} and Mg^{2+} ion removal using ion exchange resin and RO membrane filtration. Without prior organic precipitation, the ion-exchange resin process required a longer contact time, and the RO membrane filtration treatment was hardly effective in removing total dissolved solids (TDS). The combined process gave a water quality that meets the criteria set by the Thailand Ministry of Industry for industrial boiler use (COD 88 mg/L, TDS <0.001 mg/L, water hardness <5 mg- CaCO_3 /L, and pH 6.9).

1. Introduction

The main products of the palm oil industry are palm oil and its derivatives, which are consumed and used as intermediates in thousands of consumer product chains of over a million metric tons annually (Murphy et al., 2021). However, palm oil mill effluent (POME), which is wastewater generated during palm oil processing, is particularly damaging to the environment because of its high chemical oxygen demand (COD) of over 82,000 mg/L and acidity (pH < 5) (Khongkliang et al., 2019; Khemkhao et al., 2022). A feasible approach for treating POME is anaerobic digestion (AD), which uses microbial processes to break down organic matter into methane, which can be used as an energy source. The AD process could remove COD from POME as high as 80%, leaving the residual COD content in the range of 16,500 mg/L (Kan et al., 2024). In addition, the anaerobically-treated POME is brown because of tannins and phenolic compounds, with a color intensity reaching up to 22,000 Pt-Co. These substances cause an unpleasant appearance in wastewater and increase the COD content to as high as 6146 mg/L (Khongkliang et al., 2023). Therefore, secondary and tertiary treatments are required to improve water quality to meet effluent discharge standards, reduce environmental impacts, and aid in the shift to a circular water economy.

Electrocoagulation (EC) is an alternative secondary treatment applied to POME (Hakizimana et al., 2017; Nasrullah et al., 2018). In the EC process, the electricity is supplied to the electrodes, causing a sacrificial anode (typically Fe or Al) to release electrons and cations at the anodes, and H_2 and OH^- ions at the cathodes. Under an electric field, hydroxide flocs (metal hydroxides, polyhydroxides, and polyhydroxy metallic compounds) that can adsorb both dissolved and suspended solids onto their surfaces are generated (Phalakornkule et al., 2010; Al-Zghoul et al., 2023). Previous studies have shown that the efficiency of EC in removing tannins and phenolic compounds reaches 75% using one pair of electrodes, current densities ranging from 3 to 30 mA/cm², and electrolysis times of 10–60 min. However, the extended electrolysis time and high current density result in a high energy consumption of 6–40 kW h/m³ (Fajardo et al., 2015; Maisuria et al., 2022; Khongkliang et al., 2023). In addition, inter-electrode distance is an important design parameter of EC to obtain efficient distribution of electric fields and high treatment efficiency. For example, an electrode gap of less than 10 mm may lead to a rise in current density and consequent increase in energy usage, whereas a large inter-electrode spacing (>15 mm) may decrease coagulation effectiveness and lower the rates at which contaminants are removed (Khongkliang et al., 2023).

The high energy consumption of EC demonstrates the importance of combining additional techniques, such as organic precipitation, to increase efficiency and lower the energy cost of the EC process when treating POME. Prior research has demonstrated that organic precipitation is a pretreatment technique that improves the effectiveness of the EC procedure for the anaerobic treatment of POME (Khongkliang et al.,

2023). Organic precipitation forms complexes with proteins, leading to the precipitation of tannin-protein complexes (Banch et al., 2019). Khongkliang et al. (2023) demonstrated that pig blood protein, containing aspartic acid as the main amino acid composition, could form strong interactions with tannins, resulting in 60% tannin removal from POME. Combining organic precipitation with EC may provide a more sustainable method of tannin harvesting without the requirement for inorganic coagulants. It can also extend electrode life and reduce sludge production by reducing aluminum release.

The quality of the treated water can be further refined using a tertiary water treatment. Ion exchange resins play a crucial role in the removal of Ca^{2+} and Mg^{2+} ions from water, which are known to cause limestone slag in boiler pipelines and heat-transfer equipment (Al-Asheh and Aidan, 2021). In addition, reverse osmosis (RO) membrane filtration is typically employed to remove dissolved solids, microorganisms, and any remaining impurities from treated wastewater. The RO membrane acts as a selective barrier, allowing only pure water molecules to permeate, while blocking contaminants (Faroon et al., 2023). This process yields high-quality treated wastewater that is well-suited for recycling in various industrial processes. However, the RO system did not work well when applied to POME because the present tannins and phenolic chemicals cause membrane fouling (Yunos et al., 2019; Saad et al., 2021). Therefore, applying organic precipitation before an RO system might help enhance its efficiency and the lifetime of the membrane.

This study proposes a new approach for treating anaerobically-treated POME for water recycling and tannin harvesting by integrating organic precipitation with EC as a secondary treatment and ion-exchange resin and RO membrane filtration as a tertiary treatment. The effects of prior organic precipitation (POP) on EC (removal efficiency, energy consumption, characteristic of pitting corrosion, and properties of floc formed through the EC), ion-exchange resin, and RO membrane filtration efficiencies were investigated. In addition, the electrode arrangement was studied to reduce the energy consumption in the EC process. The proposed approach holds promise for addressing the environmental challenges associated with POME, while promoting sustainable water management practices within the palm oil industry.

2. Materials and methods

2.1. Raw materials

Wastewater samples were collected from the effluent discharge point of the anaerobic cover lagoon at Suksomboon Vegetable Oil Co., Ltd., Chonburi, Thailand. These samples, known as “anaerobically-treated POME,” were stored at 4 °C before use. Additionally, pig blood was collected from a slaughterhouse to prepare a stock solution containing 11,000 ± 102 mg/L of stable protein, which was stored at 4 °C for

further use.

Soda ash (Na_2CO_3 , AR grade) and salt tablets (99.8% NaCl) were purchased from Ajax Finechem Pty., Ltd. (Taren Point, New South Wales, Australia) and Pen K Intertrading Co., Ltd. (Bangkok, Thailand), respectively. The cation-exchange resin (Resinex KW-8, food grade, Jacobi Carbons Ltd., Lancashire, UK) was made of crosslinked polystyrene divinylbenzene, with sizes ranging from 0.42 to 1.25 mm. The ion exchange resin was stirred three times with 0.1 M NaCl for 30 min and rinsed twice with deionized water before use. The RO membranes (Ultratek TW 1812-50 GPD) were purchased from Function International Co., Ltd. (Bangkok, Thailand). RO membranes are thin-film composites (TFC) with an ultrathin polyamide (PA) coating layer supported by a porous support membrane.

Gallotannin was purchased from HiMedia Laboratories Pvt., Ltd. (Mumbai, India). Standard solutions of gallotannin were prepared at five different concentrations (2.5, 5, 10, 20, and 30 $\mu\text{g}/\text{mL}$). Bovine serum albumin (BSA) was purchased from Sigma-Aldrich Co. (St. Louis, Missouri, USA). The BSA standard solutions were prepared with eleven different concentrations ranging from 0.5 to 10 g/L according to [Martina and Vojtech \(2015\)](#).

2.2. Organic precipitation

The anaerobically treated POME was poured into a 2000-mL beaker with a working capacity of 1500 mL. The 200-mL pig blood solution was poured into 1350 mL of the anaerobically treated POME at a protein-to-tannin ratio of 0.33 (w/w), and the pH of the mixture was adjusted to 5.0. The mixture was stirred for 3 min at 150 rpm and 5 min at 60 rpm, after which it was allowed to settle for 15 min. Supernatants were collected for subsequent treatment.

2.3. Secondary treatment with electrocoagulation process

Al electrodes were placed in a 700-mL reactor with a 540-mL working capacity. Each electrode had a total contact area of 100 cm^2 (5×10 cm). Each electrode was connected to a direct current (DC) electricity source with a maximum current capacity of 30 A and maximum output electrical power of 15 V. Before and following each experiment, all electrodes were cleaned with tap water, immersed in

2.5% HCl (v/v) for at least 5 min, and then rinsed once more with deionized water.

Two types of wastewater were treated with EC: (1) supernatant from organic precipitation and (2) anaerobically-treated POME. In every test run, the inter-electrode distance was set to 10 mm, and the current density was fixed at 30 mA/cm^2 , according to a previous study ([Khongkliang et al., 2023](#)). Four electrode arrangements were studied: (1) monopolar in parallel (MP), (2) monopolar in series (MS), (3) bipolar in series (BS), and (4) one pair (OPE) ([Fig. 1](#)). Data was collected at the electrolysis times 2, 4, 6, 8, 10, 12, 14, and 16 min. After the allotted EC period, the system was left to settle at ambient temperature for 15 min, and the supernatant was collected for chemical analysis.

2.4. Tertiary treatment with Na_2CO_3 and ion-exchange resin

The removal of hardness in the EC-treated wastewater, both with and without preceding organic precipitation, was performed using Na_2CO_3 and an ion-exchange resin in batch mode using a 300-mL Erlenmeyer flask and a 150-mL working capacity. Na_2CO_3 and ion-exchange resin were individually introduced into the aqueous test solution at 10–300 g/L concentrations. After 5 min of stirring at 150 rpm, 25 min at 60 rpm, and then left undisturbed for 1 min, the supernatant was collected to measure the remaining hardness.

Water hardness was removed in continuous mode in a plastic column with an internal diameter of 6.10 cm and height of 30.48 cm packed with ion-exchange resin. Before each experiment, the ion-exchange resin was washed with 0.1 M NaCl by pumping the saline solution through the column at a constant flow rate of 100 mL/min for 30 min and rinsed with deionized water for 30 min to remove any excess reagents. The experiments were conducted using 3, 5, 10, and 15-min contact times. The samples were collected every 4 min for 60 min to determine the residual hardness of the aqueous solution.

2.5. Tertiary wastewater treatment with reverse osmosis membrane

A flat sheet membrane apparatus with an effective surface area of 0.39 m^2 was used for the RO membrane filtration. Membrane filtration was performed cross-flow with a feed flow rate of 188 mL/min for 12 h. The efficiency of membrane filtration was evaluated regarding the

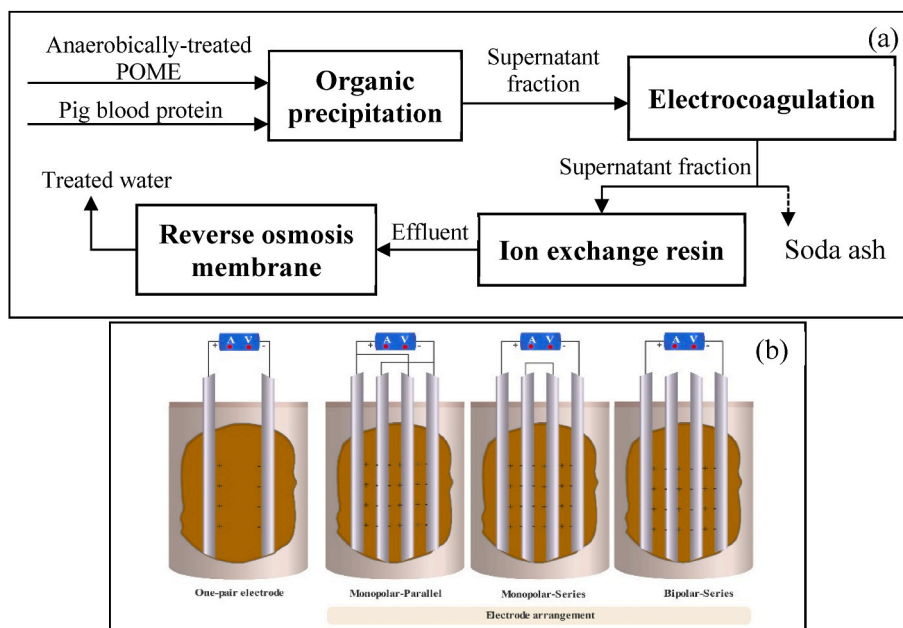


Fig. 1. Schematic of the experimental setup: (a) the combined process consisting of organic precipitation, EC, ion exchange resin, and RO in series; (b) the electrocoagulation system with different electrode arrangements.

permeate and rejection flow rates, transmembrane pressures (TMP), percentage removal of tannins, COD, hardness, and color.

2.6. Analytical methods

2.6.1. Chemical and physical analysis

Aqueous pH was measured using a pH meter (Model LAQUA-PH2000, Horiba Advanced Techno Co., Ltd., Kyoto, Japan). Total dissolved solids (TDS) and conductivity were measured using a portable pH and TDS meter (Yieryi, C-600, Shen Zhen Yage Technology Co., Ltd., Longgang, China). The total hardness was measured using the titrimetric method with EDTA, tannin content was measured using the colorimetric method, total suspended solids (TSS) were measured using the gravimetric method, and chemical oxygen demand (COD) was measured using the closed reflux titrimetric method. All measurements were conducted according to standard methods (APHA, AWWA, WEF, 2012).

Calibration curves of the light absorbance as a function of the concentrations of standard tannin and BSA were obtained using a visible spectrophotometer (Model V-1100D, Shanghai Mapada Instruments Co., Ltd., Shanghai, China) at wavelengths of 700 and 540 nm, respectively. The concentrations of tannins (expressed as tannin equivalents) and proteins (expressed as protein equivalents) in the liquid samples were determined from calibration curves using linear interpolation of the light absorbance readings. According to the manufacturer's instructions, the colors of the wastewater and treated water samples were assessed in American Dye Manufacturers Institute (ADMI) units using a colorimeter (MERCCK Spectroquant Unk Prove 100, Merck Ltd., Darmstadt, Germany). The turbidity of the water samples was assessed using a turbidimeter manufactured by Hach Co. (Model 2100AN, Loveland, Colorado, USA).

The concentrations of Al^{3+} in the supernatant and precipitate fractions were analyzed using inductively coupled plasma optical emission spectrometry (ICP-OES; PerkinElmer Optima 5300 DV, PerkinElmer Inc., Shelton, Connecticut, USA). Before analysis, the precipitate fractions were digested according to Baraud et al. (2020). The digested liquid and supernatant fractions were filtered through a 0.45 μm syringe filter to remove solid residues.

The chemical functional groups on the surfaces of the tannin standard, protein standard, and sludge after EC were determined using attenuated total reflectance Fourier transform infrared spectroscopy (FTIR) (Nicolet iS50, Thermo Fisher Scientific Inc., Waltham, Massachusetts, USA) with a scan number of 64 over a wavenumber range of 400–4000 cm^{-1} and a resolution of 4 cm^{-1} . Scanning electron microscopy (SEM) with energy-dispersive X-ray spectrometry (EDS) (Model JEOL JSM-IT300, Oxford Instruments Plc, Oxfordshire, UK) was used to examine the characteristics and compositions of the dried flocs.

The electrodes' surfaces were examined using a light microscope (Olympus DSX1000 digital microscope; Tokyo, Japan). The electrodes' mass was analyzed before and after the EC tests using microscope image analysis software (PRECiV DSX, Olympus). Before analysis, the electrodes were washed and dried to remove any impurities attached to the surface.

2.7. Calculations

The electrical energy consumption was calculated as follows:

$$SEC = \frac{E \times I \times t}{V} \quad (1)$$

where SEC is the specific energy consumption (kWh/m^3), E is the cell voltage (V), I is the current (A), t is the electrolysis time (h), and V is the volume of the solution (m^3).

The mass of pit electrode loss during the EC process was calculated as follows:

$$MEP = \frac{V_p}{A_p} \times \rho \quad (2)$$

where MEP is the mass of aluminum loss (kg/m^2), V_p is the volume of the electrode pit (m^3), A_p is the area of the electrode pit (m^2), and ρ is the density of aluminum ($2700 kg/m^3$).

The removal efficiency was determined by calculating the percentage (%) removal for each parameter using the formula $(D_0 - D_t)/D_0$, where D_0 and D_t represent the initial and residual concentrations of tannins and the hardness of the wastewater, respectively.

3. Results and discussions

3.1. Effect of organic precipitation treatment and electrode arrangement on the electrocoagulation process for removing soluble protein-tannin complexes

Fig. 2a shows the efficiency of tannin removal using EC with different electrode arrangements with and without POP. In all the setups, the EC with POP required a significantly shorter electrolysis time than those without POP to achieve the same tannin removal efficiency. For example, with an MS arrangement and electrolysis time of 8 min, the tannin removal efficiencies of EC with and without POP were 90% and 72%, respectively. The role of blood proteins in the EC of tannins has been described previously (Khongkliang et al., 2023). The remaining blood proteins helped form protein-tannin complexes during EC treatment, resulting in decreased solubility of tannins and an increased ability of Al^{3+} ions to coagulate tannins. It was also noted that the organic precipitation treatment had a greater effect on tannin removal efficiency than the electrode arrangement.

When comparing different electrode arrangements, the MS arrangement provided higher tannin removal efficiencies than the OPE, MP, and BS. For example, the tannin removal efficiencies of EC with

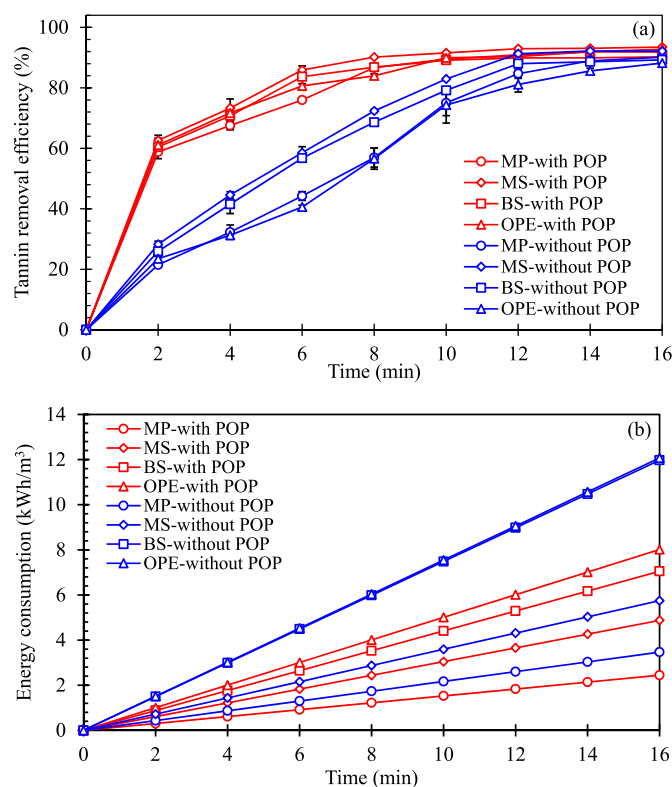


Fig. 2. Effects of electrode arrangement and electrolysis time on the tannin removal: (a) tannin removal efficiency and (b) energy consumption.

added blood protein and an electrolysis time of 8 min were approximately 90, 83, 86, and 86% with MS, OPE, MP, and BS, respectively. The higher removal efficiency of EC with MS compared to that with OPE can be explained by the fact that the effective area of the electrode in the MS arrangement is larger than that of the OPE, resulting in increased amounts of Al^{3+} , OH^- , and $\text{Al}(\text{OH})_3$ (Solak et al., 2009; Nugroho et al., 2021; Al-Zghoul et al., 2023). Compared with MP, the higher removal efficiency of EC with MS can be explained by the fact that the current is divided between all the electrodes in the MP arrangement. In contrast, in the MS configuration, the current passing through the electrodes is kept constant at the expense of a higher potential difference (Bazrafshan et al., 2015). In addition, the higher removal efficiency of the EC with the MS than that with BS can be explained by the fact that current bypass (or parasitic electrical currents) is likely to occur in bipolar electrode stacks (Muthukumar et al., 2004). Similar to the results of this study, Nasrullah et al. (2018) reported that EC with an MS arrangement was more efficient at removing COD from POME (65%) than those with MP (61%) and BS (56%) arrangements.

3.2. Effect of organic precipitation treatment and electrode arrangement on energy consumption

Fig. 2b shows the energy consumption of the EC system with different electrode arrangements with and without POP. The energy consumption varied between 0.31 and 12.07 kW h/m³, depending on the application of organic precipitation, electrode arrangements, and electrolysis time. The POP not only improved the efficiency of tannin removal but also decreased the energy consumption for the same electrode arrangement and electrolysis time. With MS arrangement and 8 min electrolysis time, the tannin removal was 90 and 72%, and the energy consumption was 2.43 and 2.87 kW h/m³ for the EC with and without POP, respectively. The POP helped reduce the energy consumption because the conductivity of the system with added blood protein ($23,500 \pm 1200 \mu\text{m}/\text{cm}$) was almost double that without added blood protein ($12,180 \pm 531 \mu\text{m}/\text{cm}$), resulting in decreased ohmic resistance and decreased applied voltage for the same applied current (Hakizimana et al., 2017; Kadier et al., 2022).

The electrode arrangement was found to have a greater effect on energy consumption than organic precipitation. With POP and 8 min electrolysis time, the energy consumption of different electrode arrangements can be ranked as follows: OPE (4.01 kW h/m³) > BS (3.53 kW h/m³) > MS (2.43 kW h/m³) > MP (1.22 kW h/m³). Without POP and 8 min electrolysis time, the energy consumption of different electrode arrangements can be ranked as follows: OPE (6.04 kW h/m³) > BS (5.99 kW h/m³) > MS (2.87 kW h/m³) > MP (1.73 kW h/m³). Reducing energy consumption is associated with a decrease in the applied voltage for the same electrical current. For the system with POP, the applied voltages for OPE, BS, MS, and MP were 5.41, 4.76, 3.29, and 1.65 V, respectively. Without POP, the applied voltage was 8.15, 8.08, 3.88, and 2.34 V for OPE, BS, MS, and MP, respectively. Similarly, Demirci et al. (2015) reported that applied voltages of 73, 53, and 22 V were required for EC with BS, MS, and MP arrangements to treat textile wastewater at the same electrolysis time of 60 min and a current density of 10.4 mA/cm². The total voltage of the MP arrangement was the lowest because the current was divided between all the electrodes in the MP arrangement, resulting in a lower voltage for each individual cell compared with the other electrode arrangements (Hakizimana et al., 2017; Ghernaout et al., 2019).

3.3. Characteristics of flocs formed during EC with and without POP treatment

Fig. S1 shows the SEM images and EDS spectra of the flocs formed during EC with and without POP for the same electrode configuration (MS arrangement), fixed electrolysis time of 8 min, inter-electrode distance of 10 mm, and current density of 30 mA/cm². Flocs from the EC

with POP appeared relatively smooth (Fig. S1a), whereas those from EC without POP had rough surfaces and irregular shapes (Fig. S1b). A possible explanation is that the added blood proteins that remained in the aqueous phase helped bridge the small particles, resulting in dense flocs. The EDS analysis revealed that the primary elements present in the flocs were Al, Mg, O, C, Cl, K, and Na. In addition, flocs from EC with POP had higher C and O contents because of the presence of blood proteins (Fig. S1c). In contrast, the percentages of Al and Cl in the flocs from EC without POP were significantly higher (4.26% and 21.34%, respectively) than those from EC with POP (1.96% and 10.52%, respectively). These results suggest that, without blood proteins, a higher dose of Al is required to form flocs of approximately the same size. In addition, the presence of Cl in the flocs suggests the formation of cationic monomeric and polymeric aluminum hydroxides, that is, $\text{Al}(\text{OH})^+$, $\text{Al}(\text{OH})_2^+$, and $\text{Al}_6(\text{OH})_{15}^{3+}$, which are favorably formed over a relatively large pH range of 5–7.5 (Trompette and Lahitte, 2021).

Fig. S2 compares the FTIR spectra of commercial tannins, proteins, and flocs from 400 to 4000 cm⁻¹. The FTIR spectra of the flocs were similar to those of the commercial proteins and tannins. The vibrations of the hydroxyl groups (–OH) were responsible for the broad and strong peaks at 3351 and 3241 cm⁻¹. (Pantoja-Castro and Gonzalez-Rodriguez, 2011; Omwene and Kobya, 2018), whereas the peaks between 1631 and 1606 cm⁻¹ indicate the presence of aromatic C=C, the characteristics of the phenolic group in tannins (Cefarin et al., 2021). The FTIR peaks between 1585 cm⁻¹ and 1514 cm⁻¹ were due to the stretching vibration of the C=C bonds of the phenolic aromatic ring. The peaks at 1444 cm⁻¹ were ascribed to the C–H bending transition of the aromatic ring, C–O stretching, and C–OH deformation (Konai et al., 2017). The peak at 1405 cm⁻¹ is associated with the stretching of the C–C bonds. (Espina et al., 2022). The FTIR spectra suggest the presence of blood proteins in the flocs from the EC with POP. The peaks between 1647 and 1620 cm⁻¹ are attributed to the strong N–H bending vibration of aspartic acid (Liu et al., 2019). Similarly, Khongkliang et al. (2023) reported that aspartic acid is the major amino acid with the highest concentration in pig blood protein and plays an important role in binding with tannin to form protein-tannin complexes. Furthermore, the peaks observed at 1647 cm⁻¹ in the FTIR spectrum are attributed to the stretching vibration of the C=O bond in aspartic acid, which is crucial to forming interconnected nanoparticles (Răuciu et al., 2022).

3.4. Pitting corrosion of aluminum electrodes subjected to EC with and without POP

Table 1 lists the mass losses of the electrodes due to the EC process with an electrolysis time of 8 min, an inter-electrode distance of 10 mm, and a current density of 30 mA/cm². The metal loss during the process with and without POP was not significantly different ($P > 0.05$) but was significantly higher than the theoretical value based on Faraday's law. This can be explained by the pitting corrosion, which causes additional metal dissolution. The degree of pitting corrosion depends not only on the applied current but also on other design and operating parameters,

Table 1
Effect of prior organic precipitation on the pitting corrosion of Al electrodes.

Al electrode erosion	With prior organic precipitation	Without prior organic precipitation	Theoretical electrode dissolution
Pitting mass (kg/m ²)	0.042 ± 0.003	0.048 ± 0.005	0.013
Pitting depth (μm)	73.94 ± 12.70	38.98 ± 4.72	–
Pitting width (μm)	176.94 ± 15.92	138.95 ± 13.06	–
Pitting corrosion shape	Elliptical	Elliptical	–

such as the inter-electrode distance, aqueous pH, and chloride concentration (Garcia-Segura et al., 2017; Changmai et al., 2019; Cruz et al., 2019).

Fig. 3 shows a comparison of the surfaces of the spent electrodes. Despite the comparable mass loss, the depth, width, and number of pits (black areas in Fig. 3a and b) on the surfaces of the two electrodes were remarkably different. The pits were lower for the spent electrode subjected to EC with POP. However, an optical micrograph at $140\times$ magnification showed that the depth and width of the pits on the spent electrode subjected to EC with POP were significantly greater than those without organic precipitation (Table 1). This might be because the aqueous pH of the EC system with POP was weakly acid with a pH of 5.30 ± 0.01 (Table 2). Acids can disrupt the passive film that protects metal surfaces, accelerating metal dissolution, and pit formation (Chen et al., 2016). The increase in chloride concentration in the EC system with POP may be another factor that promotes the degree of pitting corrosion (Wellner et al., 2018). This is because the chloride concentration in the pig blood protein was as high as 18,180 mg/L, causing increased water conductivity from $12,180 \pm 531$ to $23,500 \pm 1200$ $\mu\text{S}/\text{cm}$ along with increased pitting corrosion.

The assumption for the effect of chloride concentration on pit formation was tested by performing two EC experiments on the wastewater: one with added NaCl to obtain a water conductivity of $23,517 \pm 25$ and the other $12,173 \pm 15$ $\mu\text{S}/\text{cm}$ to represent the EC with and without POP, respectively. Fig. S3 shows the pattern and size of the corrosion pits on the electrode surface. The distribution and size of the pits on the surface of the electrodes subjected to EC with higher NaCl concentrations were the same as those subjected to EC with POP. The distribution and size of the pits on the surface of the electrode subjected to EC with lower NaCl concentration were similar to those subjected to EC without POP. Similar to this study, Wint et al. (2019) investigated the effect of NaCl concentrations in the 10–1000 mg/L range on the size and distribution of pits on Al electrodes. They found that when the NaCl concentration increased from 10 to 100 and 1000 mg/L, the pit size increased, whereas the pits decreased. In contrast, the pit size decreased, whereas the number of pits increased with decreasing NaCl

concentration. An increase in pits caused the electrode surface to become rougher, potentially decreasing the efficiency of the EC process. Chen et al. (2000) suggested that the rough surface of an electrode associated with a high number of pits makes it more difficult to generate small bubbles, resulting in decreased efficiency in removing both suspended and dissolved solids. Therefore, the lower number of pits associated with the EC with POP could benefit the sustainability of the combined process.

3.5. Effect of prior organic precipitation on aluminum distribution

Fig. 4 shows the concentrations of Al in the precipitate and supernatant fractions from the EC process with an inter-electrode distance of 10 mm, current density of $30 \text{ mA}/\text{cm}^2$, electrolysis time between 0 and 16 min, and with and without POP. Compared with the EC without POP, both the precipitate and supernatant fractions from the EC process with POP had lower Al contents. Table 2 lists the mass balance of Al and its distribution in precipitate and supernatant fractions. The Al input was 42.02 ± 3.01 g and 47.95 ± 5.22 g for the EC with and without POP, respectively. With POP, more than 99% of the Al input (41.68 ± 4.50 g) of Al ended up in the precipitate fraction, whereas less than 1% (0.39 ± 0.03 g) was accumulated in the supernatant fraction. Without POP, about 95% of the Al input (45.56 ± 0.13 g) was accumulated in the precipitate fraction and 3% (1.16 ± 0.05 g) in the supernatant fraction. These results suggest that the added protein helped increase the interaction between the protein-tannin complex and aluminum ions, resulting in higher aluminum accumulation in the precipitate fraction. In addition, the aqueous concentration of Al was lower for the EC with POP because the aqueous pH ($\text{pH } 5.30 \pm 0.07$ for the EC with POP and $\text{pH } 6.50 \pm 0.01$ for the EC without POP) was closer to the pH range in which aluminum has a minimum solubility ($\text{pH } 5.5\text{--}6.0$) (World Health Organisation, 1998). However, the aluminum concentration in the supernatant was higher than the standard value for drinking water, 0.20 mg/L (Aly et al., 2014), and should be reduced before discharge to the environment.

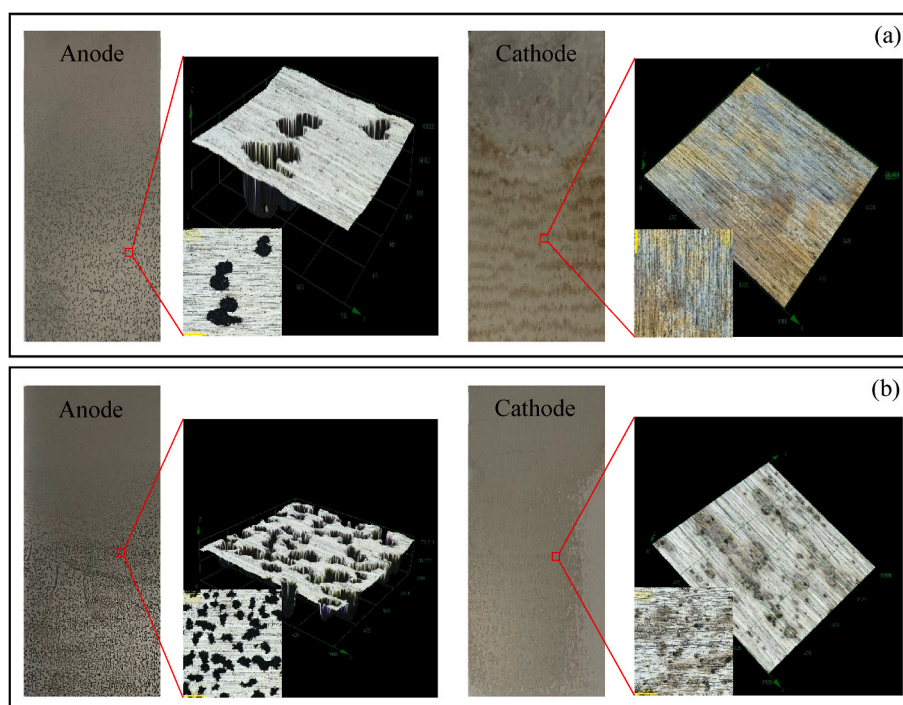


Fig. 3. Light microscope images of electrode surface after electrocoagulation with a fixed current density of $30 \text{ mA}/\text{cm}^2$, inter-electrode distance of 10 mm, and electrolysis time of 8 min: (a) with and (b) without prior organic precipitation.

Table 2
Mass balance of aluminum.

Conditions	Mass loss of Al electrode (g) ^a	Distribution of Al ^b		Balance of Al	% Error
		Amount of Al in precipitate fraction (g)	Amount of Al in supernatant fraction (g)		
With prior organic precipitation	42.02 ± 3.01	41.68 ± 4.50	0.39 ± 0.03	0.05	0.12
Without prior organic precipitation	47.95 ± 5.22	45.56 ± 0.13	1.16 ± 0.05	-1.26	2.64

Note: ^{a,b} Data were obtained from an image analysis and ICP-OES as described in Section 2.6.1.

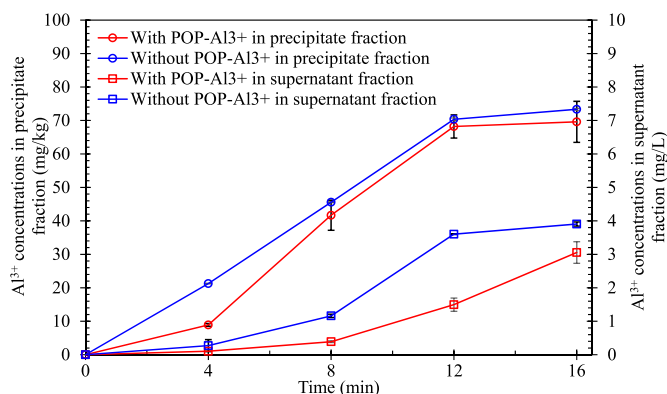


Fig. 4. Al³⁺ concentrations in the supernatant and precipitate fractions after electrocoagulation with and without prior organic precipitation with a fixed current density of 30 mA/cm², an inter-electrode distance of 10 mm, and electrolysis time of 4–16 min.

3.6. Comparative hardness removal of wastewater with and without prior organic precipitation

Fig. S4 shows the hardness removal as a function of the Na₂CO₃ dose from EC-treated wastewater with and without POP treatment. With POP treatment, the hardness removal rates were 41.1% and 66.5% at Na₂CO₃ doses of 10 and 300 g/L, respectively. Without POP treatment, the hardness removal was only 19.5–56.3%. In both cases, an increase in the Na₂CO₃ dose from 50 to >100 mg/L only slightly increased hardness removal. This was because the high Na₂CO₃ dose caused the pH to rise above 10, which hindered the precipitation of Mg and Ca (O'Connor et al., 2009).

Fig. S5 shows the hardness removal as a function of ion-exchange resin dosage from EC-treated wastewater with and without POP treatment. For an ion-exchange resin dosage of 10–100 g/L, the hardness removal was in the range of 27.3–89.3% and 24.6–91.2% with and without POP treatment, respectively. Increasing the ion-exchange resin dosage from 100 to 150, 200, 250, and 300 g/L further increased the hardness removal to >90% in both cases. Fig. 5 shows the effect of the contact time on the hardness removal performance of the ion-exchange resin. With POP treatment, an increase in the contact time from 3 to 5 min increased the hardness removal efficiency from 62.2 to 96.7% and decreased the residual hardness from 432.5 ± 17.7 to 38.8 ± 1.8 mg-CaCO₃/L. With an extended contact time of 10–15 min, the hardness removal efficiency increased to 99.7% with a residual hardness of 3.8 ± 1.8 mg-CaCO₃/L. Without the POP treatment, the hardness removal efficiency at a contact time of less than 5 min was significantly lower than that of the POP treatment. When the contact time was extended from 3 to 5 min, the hardness removal increased from 25.1% to 86.3%. When the contact time was increased to 15 min, the hardness removal efficiency increased to 99.6% with a residual hardness of 6.3 ± 1.8 mg-CaCO₃/L (Fig. 5b).

The removal of hardness from EC-treated wastewater, both with and without POP treatment, was more successful than that from groundwater. Apell and Boyer (2010) reported removing 54% of hardness from

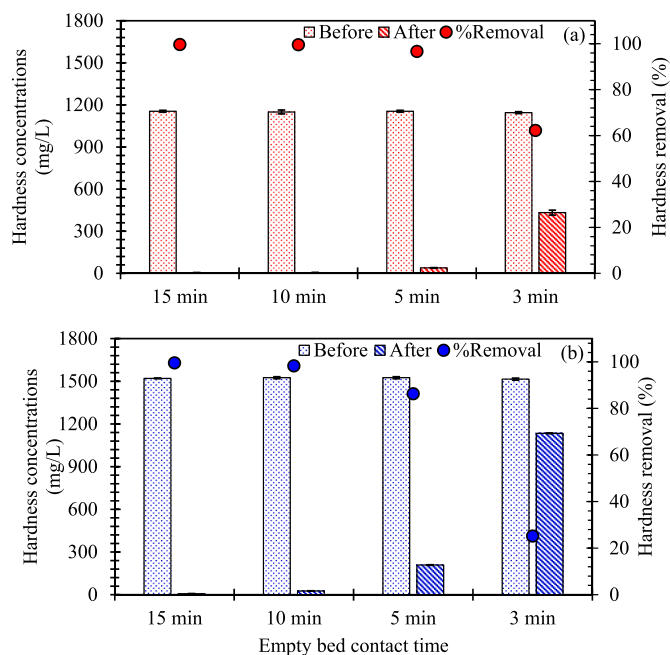


Fig. 5. Effects of empty bed contact time on the hardness removal with the ion exchange resin: (a) with and (b) without prior organic precipitation.

groundwater using the MIEX-Na cation exchange resins with a contact time of 50 min. They achieved a reduction in hardness from 275 to 127 mg-CaCO₃/L. Compared to the hardness removal by CaCO₃ and MgCO₃ precipitation, there was a small difference in the hardness removal from EC-treated wastewater with and without POP treatment when using the ion-exchange resin. This is because the binding preference of the styrene-divinylbenzene resins for calcium and magnesium ions over sodium and potassium ions was due to the charges of the ions (Moran, 2018; Al-Asheh and Aidan, 2021; Dzyazko, 2023).

3.7. Comparative reverse osmosis treatment of secondary effluent with and without POP

This section referred to the wastewater treated with EC and an ion-exchange resin as the secondary effluent. Fig. 6 shows the residual concentrations of tannins, COD, hardness, and color of the secondary effluent as a function of the RO membrane filtration treatment time. With POP, the permeate flux was 5.07 ± 0.41 L/m² h, the permeate flow rate was 1.98 L/h, and the concentrate was rejected at a rate of 3.49 L/h (Fig. S6), corresponding to an overall water recovery rate of 36.1%. Compared with the secondary effluent treated with organic precipitation, the concentrate flow of the secondary effluent without POP was higher at 4.56 L/h. In contrast, the permeate flow and overall water recovery were significantly reduced to 0.97 L/h and 17.6% (Fig. S6). In addition, the TMP in the cross-flow mode of the RO membrane module without POP (2.89–2.93 bar) was higher than that with POP (2.48–2.52 bar) (Fig. S7). An explanation for this is that the secondary effluent

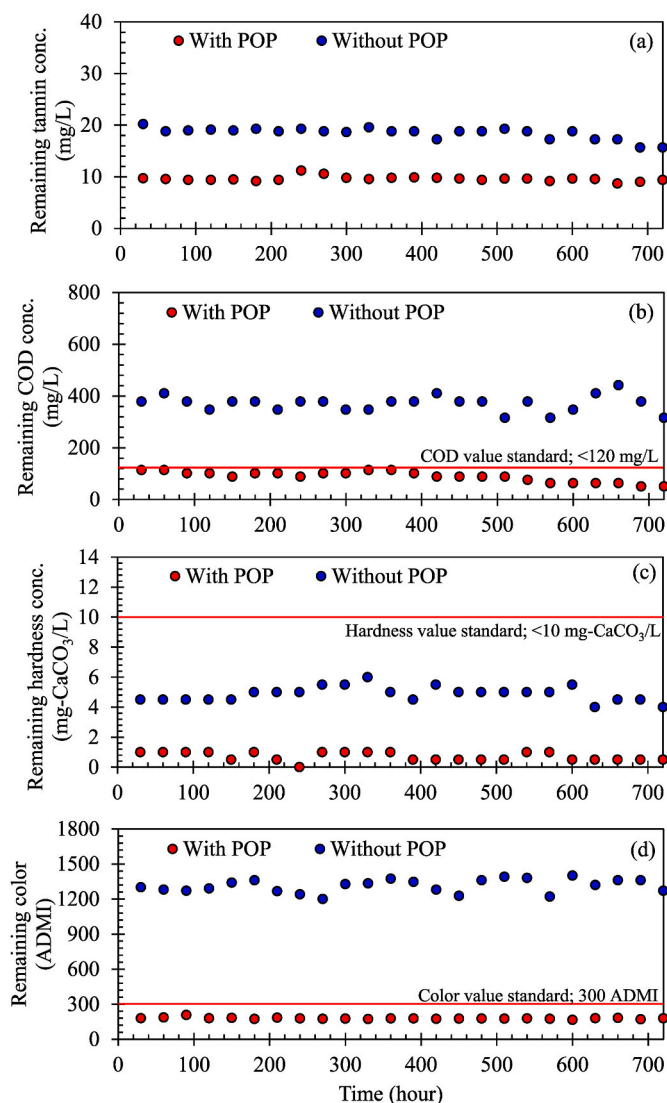


Fig. 6. Properties of wastewater after RO treatment: (a) tannin concentration, (b) COD concentration, (c) hardness concentration, and (d) color. (For interpretation of the references to color in this figure legend, the reader is referred to the Web version of this article.)

without POP contained a higher concentration of soluble tannins, which could have led to a higher rate of fouling layer accumulation and higher mass transfer resistance to water permeation. Yang et al. (2021) reported that cake formation is the main pore-blocking mechanism during ultrafiltration of tannin wastewater. In addition to the higher permeate flow, RO treatment of the secondary effluent with POP could remove more tannins, COD, and color with removal efficiencies of 84.5, 75.1, and 45.9%, respectively. These results imply that the efficiency of the RO system depends on the degree of membrane fouling, which is likely to be higher for secondary effluents without POP.

Table 3 compares the properties of the permeate flow with and without POP. The color and COD of the treated wastewater with POP followed the criteria specified by the Thailand Ministry of Industry that regulated the color of water for industrial boilers to be < 300 ADMI, COD < 120 mg/L, water hardness < 10 mg-CaCO₃/L and pH in the range of 5.5–9.0 (Ministry of Industry, 2006, 2017). In contrast, the color and COD of the treated wastewater without POP (1312.25 ± 57.42 ADMI and 370.74 ± 31.21 mg/L) were higher than the control values. The water hardness of the treated wastewater with POP was substantially reduced from 1150.25 ± 7.32 to 4.58 ± 0.77 mg-CaCO₃/L by the ion-exchange resin with 10 min contact time and further to 0.71 ± 0.29

mg-CaCO₃/L by RO membrane filtration treatment. Without POP, the water hardness of the treated wastewater was reduced from 1528.94 ± 4.53 to 6.50 ± 0.97 mg-CaCO₃/L by the ion-exchange resin with 15 min contact time. Furthermore, the subsequent RO membrane filtration treatment only marginally decreased the water hardness.

The optimal operating parameters for each unit in the combined process were as follows: a protein-to-tannin ratio of 0.33 (w/w) and pH 5.0 for the organic precipitation, an MS arrangement, an electrolysis time of 8 min, pH 5, an inter-electrode distance of 10 mm, and a current density of 30 mA/cm² for the EC operation, 10 min contact time for the operation of ion-exchange resin, and a feed flux of 5.1 L/m² h and a driving pressure of 252 kPa for the RO membrane filtration. The COD removal of the combined process was higher than the removal efficiency obtained from a series of treatments consisting of a membrane bioreactor, ultrafiltration, and an RO membrane, as reported by Loh et al. (2013). In their study, the initial and final COD values and the COD removal were 2523 and 701 mg/L and 72%, respectively, whereas, in this study, the initial and final COD values and the COD removal were 6104 and 88 mg/L and 98.6%, respectively.

3.8. Cost analysis

Table S1 estimates the operating costs for the combined process, including power consumption and chemical costs. For the first stage of organic precipitation, the estimated cost was 25.57 USD/m³ for pig blood protein, 3 M HCl, and electricity costs. For the EC unit, the main expense was the electricity cost of 21.54 USD/m³. The main expense for the ion exchange resin process was the NaCl reagent and electricity costs of 17.99 USD/m³. For the final stage of RO membrane filtration, the electricity cost was 8.49 USD/m³. The total operational cost of the combined treatment process amounted to 73.59 USD/m³.

The organic precipitation cost was relatively high compared to the existing advanced oxidation treatment, e.g., ozonation. The operating cost of ozonation was estimated to be 0.0031 USD/m³ based on the value of 0.2 g O₃/m³ POME (Krishnan et al., 2023) and the value of 250 g O₃/1.9 kW h (Watcharasuwanseree and Phalakornkule, 2020). Nevertheless, tannins were not valued because the ozone treatment caused the deterioration of tannins. The revenue from the harvested crude tannin-protein complexes, a valuable by-product of the treatment process, can be as high as 260.32 USD/m³, resulting in a substantial net profit of 186.73 USD/m³. This preliminary economic study demonstrated the combined treatment process's sustainability by highlighting its resource efficiency and offsetting its operational expenses with a sizable revenue generated.

4. Conclusion

This study investigated the effectiveness of the combined process of organic precipitation with blood proteins, EC, ion exchange resin, and RO in series in treating anaerobically-treated POME for water recycling and tannin harvesting. In the context of wastewater treatment, placing the organic precipitation in front of the conventional secondary treatment increased the efficiency of each treatment. With POP, the efficiency of the EC treatment in reducing the concentrations of tannin, COD, and color was higher. That is, using EC with an optimal configuration (an MS arrangement, an electrolysis time of 8 min, pH 5, an inter-electrode distance of 10 mm, and a current density of 30 mA/cm²), the concentration of tannin, COD, and color in the anaerobically-treated POME effluent decreased from 545.25 ± 13.10 mg/L, 6104.53 ± 89.60 mg/L, and 9630.01 ± 253.57 ADMI to 23.26 ± 2.18 mg/L, 368.65 ± 12.09 mg/L, and 355.33 ± 4.62 ADMI (with POP) and to 55.37 ± 1.36 mg/L, 671.50 ± 8.06 mg/L, and 1563.33 ± 5.77 ADMI (without POP). The water hardness of the treated wastewater with POP was substantially reduced from 1150.25 ± 7.32 to 4.58 ± 0.77 mg-CaCO₃/L by the ion-exchange resin with 10 min contact time. In contrast, without POP, it was necessary to use an ion-exchange resin treatment in series

Table 3
Characteristics of anaerobically-treated palm oil mill effluent before and after treatment.

Parameter	Unit	Anaerobically-treated POME	After precipitation and electrocoagulation		After ion exchange resin	
			With prior organic precipitation	Without prior organic precipitation	With prior organic precipitation	Without prior organic precipitation
pH	–	6.74 ± 0.02	5.30 ± 0.07	6.50 ± 0.01	7.49 ± 0.08	6.77 ± 0.04
TDS	mg/L	6523.33 ± 5.77	<0.01	7850.33 ± 32.15	<0.01	7371.43 ± 99.24
TSS	mg/L	2.30 ± 0.20	0.29 ± 0.15	0.20 ± 0.05	0.83 ± 0.04	0.89 ± 0.08
Conductivity	µS/cm	13,053 ± 11	23,233 ± 305	15,556 ± 28	23,277 ± 237	14,723 ± 211
COD	mg/L	6104.53 ± 89.60	368.65 ± 12.09	671.50 ± 8.06	355.19 ± 18.47	554.41 ± 57.91
Tannin	mg/L	545.25 ± 13.10	23.26 ± 2.18	55.37 ± 1.36	15.73 ± 0.43	25.26 ± 0.78
Turbidity	NTU	267.30 ± 1.08	15.78 ± 2.74	147.40 ± 11.87	10.87 ± 0.92	21.44 ± 0.68
Total hardness	CaCO ₃ /L	2200.21 ± 178.37	1150.25 ± 7.32	1528.94 ± 4.53	4.58 ± 0.77	6.50 ± 0.97
Color	ADMI	9630.01 ± 253.57	355.33 ± 4.62	1563.33 ± 5.77	330.01 ± 17.32	1386.67 ± 25.17
Parameter	Unit	After membrane With prior organic precipitation	Without prior organic precipitation	Factory Wastewater Drainage Control Standards 2017 CE	Properties of water for feeding the boiler 2006 CE	
pH	–	6.86 ± 0.03	6.43 ± 0.03	5.5–9.0	5.8–9.5	
TDS	mg/L	<0.001	7271 ± 103	<3000	<3500 ^a	
TSS	mg/L	0.2 ± 0.04	0.83 ± 0.06	<50		
Conductivity	µS/cm	22,516 ± 96	15,107 ± 172			
COD	mg/L	88.34 ± 20.04	370.74 ± 31.21	<120		
Tannin	mg/L	9.98 ± 0.49	18.44 ± 1.14			
Turbidity	NTU	5.31 ± 0.18	7.69 ± 0.76			
Total hardness	CaCO ₃ /L	0.71 ± 0.29	4.88 ± 0.49		<10	
Color	ADMI	178.27 ± 7.62	1312.25 ± 57.42	300 ADMI		

^a Boiler water.

with RO membrane filtration to reduce the water hardness to <10 mg-CaCO₃/L. With POP, the properties of the treated wastewater followed the criteria specified by the Thailand Ministry of Industry for industrial boilers. In the context of waste valorization, the harvested tannin in the form of tannin-protein complexes is a potential value by-product. Further research should evaluate the integrated treatment technique on a pilot scale, and a more thorough investigation of electrode passivation-a significant issue in EC- is warranted.

CRedit authorship contribution statement

Peerawat Khongkliang: Writing – original draft, Visualization, Methodology, Investigation, Conceptualization. **Sasikarn Nuchdang:** Resources, Investigation. **Dussadee Rattanaphra:** Resources. **Wilasinee Kingkam:** Resources. **Sithipong Mahathanabodee:** Resources, Investigation. **Jarungwit Boonnorat:** Resources, Investigation. **Abudukeremu Kadier:** Writing – review & editing. **Putu Teta Prihartini Aryanti:** Writing – review & editing. **Chantaraporn Phalakornkule:** Writing – review & editing, Visualization, Supervision, Resources, Methodology, Conceptualization.

Declaration of competing interest

The authors declare that they have no known competing financial interests or personal relationships that could have appeared to influence the work reported in this paper.

Data availability

Data will be made available on request.

Acknowledgments

The authors gratefully acknowledge the financial support provided by King Mongkut's University of Technology North Bangkok (Grant No. KMUTNB–FF–B-19), and the Thailand Science Research and Innovation (TSRI). The authors gratefully acknowledge the postdoctoral grant to Peerawat Khongkliang from the Science and Technology Postgraduate

Education and Research Development Office (PERDO) and the Joint Graduate School of Energy and Environment (JGSEE), King Mongkut's University of Technology Thonburi (Grant No. JGSEE/THESIS/343, and Bioeconomy_PI_2563_04).

Appendix A. Supplementary data

Supplementary data to this article can be found online at <https://doi.org/10.1016/j.chemosphere.2024.142899>.

References

- Al-Asheh, S., Aidan, A., 2021. A comprehensive method of ion exchange resins regeneration and its optimization for water treatment. Promising Techniques for Wastewater Treatment and Water Quality Assessment. IntechOpen. <https://doi.org/10.5772/intechopen.93429>.
- Aly, Z., Graulet, A., Scales, N., Hanley, T., 2014. Removal of aluminium from aqueous solutions using PAN-based adsorbents: Characterisation, kinetics, equilibrium and thermodynamic studies. Environ. Sci. Pollut. Res. 21, 3972–3986. <https://doi.org/10.1007/s11356-013-2305-6>.
- Al-Zghoul, T.M., Al-Qodah, Z., Al-Jamrah, A., 2023. Performance, modeling, and cost analysis of chemical coagulation-assisted solar powered electrocoagulation treatment system for pharmaceutical wastewater. Water (Switzerland) 15. <https://doi.org/10.3390/w15050980>.
- Apell, J.N., Boyer, T.H., 2010. Combined ion exchange treatment for removal of dissolved organic matter and hardness. Water Res. 44, 2419–2430. <https://doi.org/10.1016/j.watres.2010.01.004>.
- APHA, AWWA, WEF, 2012. Standard Methods for the Examination of Water and Wastewater, twenty-second ed.
- Banch, T.J.H., Hanafiah, M.M., Alkarkhi, A.F.M., Abu Amr, S.S., 2019. Factorial design and optimization of landfill leachate treatment using tannin-based natural coagulant. Polymers 11, 1349. <https://doi.org/10.3390/polym11081349>.
- Baraud, F., Zaiter, A., Porée, S., Leleyter, L., 2020. New approach for determination of Cd, Cu, Cr, Ni, Pb, and Zn in sewage sludges, fired brick, and sediments using two analytical methods by microwave-induced plasma optical spectrometry and induced coupled plasma optical spectrometry. SN Appl. Sci. 2, 1–10. <https://doi.org/10.1007/s42452-020-03220-0>.
- Bazrafshan, E., Mohammadi, L., Ansari-Moghaddam, A., Mahvi, A.H., 2015. Heavy metals removal from aqueous environments by electrocoagulation process - a systematic review. J. Environ. Heal. Sci. Eng. 13 <https://doi.org/10.1186/s40201-015-0233-8>.
- Cefarin, N., Bedolla, D.E., Surowka, A., Donato, S., Sepperer, T., Tondi, G., Drossi, D., Sodini, N., Birarda, G., Vaccari, L., 2021. Study of the spatio-chemical heterogeneity of tannin-furanic foams: from 1D FTIR spectroscopy to 3D FTIR micro-computed tomography. Int. J. Mol. Sci. 22 <https://doi.org/10.3390/ijms222312869>.

- Changmai, M., Pasawan, M., Purkait, M.K., 2019. Treatment of oily wastewater from drilling site using electrocoagulation followed by microfiltration. *Sep. Purif. Technol.* 210, 463–472. <https://doi.org/10.1016/j.seppur.2018.08.007>.
- Chen, G., Chen, X., Yue, P.L., 2000. Electrocoagulation and electroflotation of restaurant wastewater. *J. Environ. Eng.* 126, 858–863. [https://doi.org/10.1061/\(ASCE\)0733-9372\(2000\)126:9\(858\)](https://doi.org/10.1061/(ASCE)0733-9372(2000)126:9(858)).
- Chen, Z., Zhang, G., Bobaru, F., 2016. The influence of passive film damage on pitting corrosion. *J. Electrochem. Soc.* 163, C19–C24. <https://doi.org/10.1149/2.0521602jes>.
- Cruz, K.D., Mateo, N.M., Tangara, N.P., Almendrala, M.C., 2019. Reactor design optimization on the electrocoagulation treatment of sugarcane molasses-based distillery wastewater. *IOP Conf. Ser. Earth Environ. Sci.* 344 <https://doi.org/10.1088/1755-1315/344/1/012023>.
- Demirci, Y., Pekel, L.C., Albaz, M., 2015. Investigation of different electrode connections in electrocoagulation of textile wastewater treatment. *Int. J. Electrochem. Sci.* 10, 2685–2693.
- Dzyazko, Y., 2023. Applications of ion exchange resins in water softening. In: *Materials Research Foundations*, pp. 142–165. <https://doi.org/10.21741/9781644902219-8>.
- Espina, A., Sanchez-Cortes, S., Jurašeková, Z., 2022. Vibrational study (Raman, SERS, and IR) of plant gallnut polyphenols related to the fabrication of iron gall inks. *Molecules* 27, 1–17. <https://doi.org/10.3390/molecules27010279>.
- Fajardo, A.S., Rodrigues, R.F., Martins, R.C., Castro, L.M., Quinta-Ferreira, R.M., 2015. Phenolic wastewaters treatment by electrocoagulation process using Zn anode. *Chem. Eng. J.* 275, 331–341. <https://doi.org/10.1016/j.cej.2015.03.116>.
- Faroon, M., Alsaad, Z., Albadran, F., Ahmed, L., 2023. Review on technology-based on reverse osmosis. *Anbar J. Eng. Sci.* 14, 89–97. <https://doi.org/10.37649/aengs.2023.139414.1047>.
- Garcia-Segura, S., Eiband, M.M.S.G., de Melo, J.V., Martínez-Huitle, C.A., 2017. Electrocoagulation and advanced electrocoagulation processes: a general review about the fundamentals, emerging applications and its association with other technologies. *J. Electroanal. Chem.* 801, 267–299. <https://doi.org/10.1016/j.jelechem.2017.07.047>.
- Gheraout, D., Alghamdi, A., Ghernaout, B., 2019. Electrocoagulation process: a mechanistic review at the dawn of its modeling. *J. Environ. Sci. Allied Res.* 2, 22–38. <https://doi.org/10.29199/2637-7063/esar-201019>.
- Hakizimana, J.N., Gourich, B., Chafi, M., Stiriba, Y., Vial, C., Drogui, P., Naja, J., 2017. Electrocoagulation process in water treatment: a review of electrocoagulation modeling approaches. *Desalination* 404, 1–21. <https://doi.org/10.1016/j.desal.2016.10.011>.
- Kadier, A., Al-Qodah, Z., Akkaya, G.K., Song, D., Peralta-Hernández, J.M., Wang, J.Y., Phalakornkule, C., Bajpai, M., Niza, N.M., Gilhotra, V., Bote, M.E., Ma, Q., Obi, C.C., Igwegbe, C.A., 2022. A state-of-the-art review on electrocoagulation (EC): an efficient, emerging, and green technology for oil elimination from oil and gas industrial wastewater streams. *Case Stud. Chem. Environ. Eng.* 6 <https://doi.org/10.1016/j.csee.2022.100274>.
- Kan, K.W., Chan, Y.J., Tiong, T.J., Lim, J.W., 2024. Maximizing biogas yield from palm oil mill effluent (POME) through advanced simulation and optimisation techniques on an industrial scale. *Chem. Eng. Sci.* 285, 119644 <https://doi.org/10.1016/j.ces.2023.119644>.
- Khemkhao, M., Domrongpakkaphan, V., Phalakornkule, C., 2022. Process performance and microbial community variation in high-rate anaerobic continuous stirred tank reactor treating palm oil mill effluent at temperatures between 55 and 70 °C. *Waste and Biomass Valorization* 13, 431–442. <https://doi.org/10.1007/s12649-021-01539-2>.
- Khongkhiang, P., Jehlee, A., Kongjan, P., Reungsang, A., O-Thong, S., 2019. High efficient biohydrogen production from palm oil mill effluent by two-stage dark fermentation and microbial electrolysis under thermophilic condition. *Int. J. Hydrogen Energy* 44, 31841–31852. <https://doi.org/10.1016/j.ijhydene.2019.10.022>.
- Khongkhiang, P., Khemkhao, M., Mahathanabodee, S., O-Thong, S., Kadier, A., Phalakornkule, C., 2023. Efficient removal of tannins from anaerobically-treated palm oil mill effluent using protein-tannin complexation in conjunction with electrocoagulation. *Chemosphere* 321, 138086. <https://doi.org/10.1016/j.chemosphere.2023.138086>.
- Konai, N., Raidandi, D., Pizzi, A., Meva'a, L., 2017. Characterization of Ficus sycomorus tannin using ATR-FT MIR, MALDI-TOF MS and ¹³C NMR methods. *Eur. J. Wood Wood Prod.* 75, 807–815. <https://doi.org/10.1007/s00107-017-1177-8>.
- Krishnan, S., Homroskla, P., Saritpongteeraka, K., Suttinun, O., Nasrullah, M., Tirawanichakul, Y., Chairapat, S., 2023. Specific degradation of phenolic compounds from palm oil mill effluent using ozonation and its impact on methane fermentation. *Chem. Eng. J.* 451, 138487 <https://doi.org/10.1016/j.cej.2022.138487>.
- Liu, F., Csetenyi, L., Gadd, G.M., 2019. Amino acid secretion influences the size and composition of copper carbonate nanoparticles synthesized by ureolytic fungi. *Appl. Microbiol. Biotechnol.* 103, 7217–7230. <https://doi.org/10.1007/s00253-019-09961-2>.
- Loh, S.K., Lai, M.E., Ngatiman, M., Lim, W.S., Choo, Y.M., Zhang, Z., Salimon, J., 2013. Zero discharge treatment technology of palm oil mill effluent. *J. Oil Palm Res.* 25, 273–281.
- Maisuria, K.J., Shah, K.A., Rana, J.K., 2022. Removal of Tannic acid and COD from synthetic Tannery wastewater. *IOP Conf. Ser. Earth Environ. Sci.*, 012035 <https://doi.org/10.1088/1755-1315/1086/1/012035>.
- Martina, V., Vojtech, K., 2015. A Comparison of Biuret, Lowry and Bradford Methods for Measuring the Egg'S Proteins, 1. *Mendelnet*, pp. 394–398.
- Ministry of Industry, T., 2017. 2017. Notification of Ministry of industry: industrial effluent standards B.E.2560 [WWW Document]. 2017. URL <https://www.fao.org/faolex/results/details/en/c/LEX-FAOC211105/>.
- Ministry of Industry, T., 2006. 2006. Notification of Ministry of industry: the water properties for A boiler, B.E.2549, 2006. URL <https://www.mhm.co.th/GAdatabas e/Program IEAT/pages/en/Keyword/27.html>.
- Moran, S., 2018. Clean water unit operation design. In: *An Applied Guide to Water and Effluent Treatment Plant Design*. Elsevier, pp. 69–100. <https://doi.org/10.1016/b978-0-12-811309-7.00007-2>.
- Murphy, D.J., Goggin, K., Paterson, R.R.M., 2021. Oil palm in the 2020s and beyond: challenges and solutions. *CABI Agric. Biosci.* 2, 1–22. <https://doi.org/10.1186/s43170-021-00058-3>.
- Muthukumar, K., Sundaram, P.S., Anantharaman, N., Basha, C.A., 2004. Treatment of textile dye wastewater by using an electrochemical bipolar disc stack reactor. *J. Chem. Technol. Biotechnol.* 79, 1135–1141. <https://doi.org/10.1002/jctb.1104>.
- Nasrullah, M., Singh, L., Krishnan, S., Sakinah, M., Zularisam, A.W., 2018. Electrode design for electrochemical cell to treat palm oil mill effluent by electrocoagulation process. *Environ. Technol. Innov.* 9, 323–341. <https://doi.org/10.1016/j.eti.2017.10.001>.
- Nugroho, F.A., Arif, A.Z., Sabila, G.Z.M., Ariyanti, P.T.P., 2021. Slaughterhouse wastewater treatment by electrocoagulation process. *IOP Conf. Ser. Mater. Sci. Eng.* 1115, 012037 <https://doi.org/10.1088/1757-899x/1115/1/012037>.
- O'Connor, J.T., O'Connor, T., Twait, R., 2009. Lime softening. *Water treat. Plant perform. Eval. Oper.* 33–40 <https://doi.org/10.1002/9780470431474.ch3>.
- Omwene, P.I., Koby, M., 2018. Treatment of domestic wastewater phosphate by electrocoagulation using Fe and Al electrodes: a comparative study. *Process Saf. Environ. Protect.* 116, 34–51. <https://doi.org/10.1016/j.psep.2018.01.005>.
- Pantoja-Castro, M.A., Gonzalez-Rodriguez, H., 2011. Study by infrared spectroscopy and thermogravimetric analysis of Tannins and Tannic acid. *Rev. Latinoam. Quim.* 39, 107–112.
- Phalakornkule, C., Polgumhang, S., Tongdaung, W., Karakat, B., Nuyut, T., 2010. Electrocoagulation of blue reactive, red disperse and mixed dyes, and application in treating textile effluent. *J. Environ. Manag.* 91, 918–926. <https://doi.org/10.1016/j.jenvman.2009.11.008>.
- Răcuciu, M., Barbu-Tudoran, L., Oancea, S., Drăghici, O., Morosanu, C., Grigoras, M., Brînză, F., Creangă, D.E., 2022. Aspartic acid stabilized iron oxide nanoparticles for biomedical applications. *Nanomaterials* 12. <https://doi.org/10.3390/nano12071151>.
- Saad, M.S., Wirzal, M.D.H., Putra, Z.A., 2021. Review on current approach for treatment of palm oil mill effluent: integrated system. *J. Environ. Manag.* 286, 112209 <https://doi.org/10.1016/j.jenvman.2021.112209>.
- Solak, M., Kiliç, M., Hüseyin, Y., Şencan, A., 2009. Removal of suspended solids and turbidity from marble processing wastewaters by electrocoagulation: comparison of electrode materials and electrode connection systems. *J. Hazard Mater.* 172, 345–352. <https://doi.org/10.1016/j.jhazmat.2009.07.018>.
- Trompette, J.L., Lahitte, J.F., 2021. Effects of some ion-specific properties in the electrocoagulation process with aluminum electrodes. *Colloids Surfaces A Physicochem. Eng. Asp.* 629 <https://doi.org/10.1016/j.colsurfa.2021.127507>.
- Watcharasuwanseree, S., Phalakornkule, C., 2020. Field analysis of PSA O₂-ozone production process for water recycling. *Water Environ. J.* 34, 223–231. <https://doi.org/10.1111/wej.12455>.
- Wellner, D.B., Couperthwaite, S.J., Millar, G.J., 2018. Influence of operating parameters during electrocoagulation of sodium chloride and sodium bicarbonate solutions using aluminum electrodes. *J. Water Process Eng.* 22, 13–26. <https://doi.org/10.1016/j.jwpe.2017.12.014>.
- Wint, N., Khan, K., Sullivan, J.H., McMurray, H.N., 2019. Concentration effects on the spatial interaction of corrosion pits occurring on zinc in dilute aqueous sodium chloride. *J. Electrochem. Soc.* 166, C3028–C3038. <https://doi.org/10.1149/2.0051911jes>.
- World Health Organisation, 1998. Aluminium in drinking-water background. *Guidel. Drink. Qual.* 2, 29.
- Yang, F., Huang, Z., Huang, J., Wu, C., Zhou, R., Jin, Y., 2021. Tanning wastewater treatment by ultrafiltration: process efficiency and fouling behavior. *Membranes* 11, 1–17. <https://doi.org/10.3390/membranes11070461>.
- Yunos, K.F.M., Mazlan, N.A., Naim, M.N.M., Baharuddin, A.S., Hassan, A.R., 2019. Ultrafiltration of palm oil mill effluent: effects of operational pressure and stirring speed on performance and membranes fouling. *Environ. Eng. Res.* 24, 263–270. <https://doi.org/10.4491/EER.2018.175>.



Performance of combined organic precipitation, electrocoagulation, and electrooxidation in treating anaerobically treated palm oil mill effluents

Peerawat Khongkliang^{1,2} · Kaewmada Chalearmkul³ · Kettawan Boonloh³ · Nunthakan Kanjanasombun³ · Tipaporn Darnsawat³ · Jarungwit Boonnorat⁴ · Abudukeremu Kadier^{5,6} · Putu Teta Prihartini Aryanti⁷ · Chantaraporn Phalakornkule^{1,2,3}

Received: 14 May 2024 / Accepted: 1 September 2024
© The Author(s) 2024

Abstract

Palm oil mill effluent (POME), wastewater generated from palm oil production, is known for its extremely high chemical oxygen demand and brownish color. Anaerobic digestion is the primary treatment method for POME in the palm oil industry; however, anaerobically treated POME has high concentrations of residual contaminants and color intensity. This study proposes an approach to treat anaerobically-treated POME in recycled water for industrial applications by integrating preliminary organic precipitation, electrocoagulation, and electrooxidation (EO). The EO process was optimized in terms of the current density, electrolysis time, electrode arrangement, and feed flow rate. At a current density of 60 mA/cm² and an electrolysis time of 9 min, the EO process with a graphite anode and stainless-steel cathode in the monopolar electrode configuration reduced the phenolic concentration and color in the preliminary-treated POME from 8.95 mg/L and 317.19 ADMI to 0.25 mg/L and 26.10 ADMI, respectively. Additionally, the EO process exhibited a 92.26% efficiency in lowering the ammonium-nitrogen content.

Keywords Palm oil mill effluent · Anaerobically-treated POME · Organic precipitation · Electrocoagulation · Electrooxidation · Electrode configurations

✉ Chantaraporn Phalakornkule
chantaraporn.p@eng.kmutb.ac.th; cphalak21@gmail.com

Peerawat Khongkliang
peerawatkhongkliang@gmail.com

Jarungwit Boonnorat
jarungwit_b@rmutt.ac.th

Abudukeremu Kadier
abudukeremu@ms.xjb.ac.cn

Putu Teta Prihartini Aryanti
p.teta@lecture.unjani.ac.id

¹ The Joint Graduate School of Energy and Environment, King Mongkut's University of Technology Thonburi, Bangkok 10140, Thailand

² Research Center for Circular Products and Energy, KMUTNB, Bangkok 10800, Thailand

³ Department of Chemical Engineering, Faculty of Engineering, King Mongkut's University of Technology North Bangkok, Bangkok 10800, Thailand

⁴ Department of Environmental Engineering, Faculty of Engineering, Rajamangala University of Technology Thanyaburi (RMUTT), Khlong Luang 12110, Pathum Thani, Thailand

⁵ Laboratory of Environmental Science and Technology, The Xinjiang Technical Institute of Physics and Chemistry, Key Laboratory of Functional Materials and Devices for Special Environments, Chinese Academy of Sciences (CAS), Ürümqi 830011, Xinjiang, China

⁶ Center of Materials Science and Optoelectronics Engineering, University of Chinese Academy of Sciences, Beijing 100049, China

⁷ Chemical Engineering Department, Faculty of Engineering, Universitas Jenderal Achmad Yani, Cibeber Cimahi, West Java, Indonesia

Abbreviations

POME	Palm oil mill effluent
EC	Electrocoagulation
EO	Electrooxidation
POP	Prior organic precipitation
POP-EC-EO-treated POME	Prior organic precipitation–electrocoagulation–electrooxidation-treated POME
EC-EO- treated POME	Electrocoagulation–electrooxidation-treated POME
ADMI	American dye manufacturers institute
COD	Chemical oxygen demand
AD	Anaerobic digestion
BSA	Bovine serum albumin
MP	Monopolar-parallel
MS	Monopolar-series
BS	Bipolar-series

Introduction

Over a million metric tons of palm oil and its products are consumed and utilized annually in thousands of corporate supply chains (Murphy et al. 2021). However, the palm oil production process generates a substantial volume of wastewater known as palm oil mill effluent (POME), characterized by high chemical oxygen demand (COD), brownish color, and acidic pH. (Khongkliang et al. 2019; Khemkhao et al. 2022). Most palm oil mills employ anaerobic digestion (AD) as the primary treatment to convert POME's biodegradable portions to methane for energy generation and COD reduction. However, ammonium, tannins, and phenolic chemicals are barely removed by AD, resulting in residual COD in anaerobically-treated POME of approximately 5000–6000 mg/L (Khongkliang et al. 2023) and ammonia–nitrogen of approximately 200–350 mg/L (Zahrim et al. 2014; Khongkliang et al. 2023). Furthermore, anaerobically-treated POME has a brownish color due to the presence of plant constituents such as lignin, tannin, humic and fulvic acid, and phenolic compounds (caffeic, ferulic, gallic, protocatechuic, p-coumaric, syringic, 4-hydroxybenzoic, and 4-hydroxyl phenylacetic acids) (Edem 2002; Zahrim et al. 2009; Kongnoo et al. 2012).

Secondary treatments for removing plant constituents in POME have been proposed using various techniques such as coagulation/flocculation (Zahrim et al. 2014; Khongkliang et al. 2023; Aryanti et al. 2024), flotation (Poh et al. 2014), membrane processes (Tan et al. 2017; Aryanti et al. 2024), Fenton processes (Taha and Ibrahim 2014), and photocatalysis (Alhaji et al. 2016). Various coagulants

have been studied for the coagulation/flocculation process, including calcium lactate (Zahrim et al. 2014), blood protein (Khongkliang et al. 2023), *Moringa Oleifera* extract (Yap et al. 2021), and polyhydroxide and polyhydroxy metallic compounds produced in situ from iron and aluminum anodes by electrocoagulation (EC) (Saad et al. 2022). However, additional operating costs often hinder secondary treatment of anaerobically-treated POME. This has prompted increased attention to waste valorization when dealing with anaerobically-treated POME. In a recent study, Khongkliang et al. (2023) proposed an economically feasible approach that integrates protein-tannin complexation and EC at pH 5 to harvest plant constituents from anaerobically-treated POME effluents and improve the quality of the treated wastewater. One advantage of an operating pH of 5 is that it helps postpone the onset of electrode passivation, which is a significant obstacle to the implementation of EC (Al-Qodah et al. 2024). This is because the low pH environment effectively inhibits the formation of surface layers (Ingelsson et al. 2020). In addition, the proteins in pig blood can form complexes with condensed tannins via hydrogen bonds, hydrophobic interactions, and covalent bonds between the amino acids in the protein and the hydroxyl and phenolic groups in the tannins (Girard et al. 2018; Pizzi 2021), resulting in the simultaneous harvesting of tannins and > 90% removal of COD and color. The tannins harvested by the protein–tannin complexation method could be further utilized as animal food additives and nutraceuticals for pets. In addition, the quality of the treated POME can be further improved using subsequent EC, which precipitates highly soluble plant constituents. As a result, the secondary-treated POME has a remaining ammonia–nitrogen of approximately 23–27 mg/L, a color of approximately 700–800 Pt–Co, and a yellowish color owing to the presence of a residual tannin concentration of approximately 30–40 mg/L. The properties did not meet the criteria specified by the Thailand Ministry of Industry that regulated the color of water for industrial effluent to be < 300 ADMI, COD < 120 mg/L, phenolic compound < 1 mg/L, and pH in the range of 5.5–9.0 (Ministry of Industry 2017).

Due to the presence of residual ammonia–nitrogen ($\text{NH}_3\text{-N}$) in the secondary-treated POME, discharge of the secondary-treated POME to the environment can cause nitrogen deposits, which have a direct effect on soil acidification and vegetation (Bashir et al. 2016; Jefferson et al. 2016). Furthermore, the color of the secondary-treated POME might cause public resistance to recycled water for industrial applications. Thus, removing ammonia–nitrogen and decolorizing secondary-treated POME is an essential step toward water recycling in the palm oil industry. The application of electrooxidation (EO) in the decolorization of various types of wastewater is well documented: tannery wastewater (Rao et al. 2001), ammonium-containing

wastewater (Zöllig et al. 2015), textile wastewater (Kaur et al. 2018; Gilpavas et al. 2020), and phenolic wastewater (Kiss et al. 2023; Pu et al. 2023; Đuričić et al. 2023). In addition, the EO of ammonium-containing water generates strong oxidizing agents in situ (hypochlorite, nitrogen oxide radicals, and ozone), causing color reduction and the oxidation of ammonium ions into N_2 and large phenolic compounds into small molecules (Rao et al. 2001). However, to our knowledge, no studies have reported the application of EO in refining the quality of treated POME.

This study investigated the simultaneous reduction of ammonia–nitrogen and decolorization of secondary-treated POME using EO. Specifically, the effects of secondary treatment (EC alone and organic precipitation followed by EC), electrode configuration of an EO reactor with a graphite anode (monopolar in series, monopolar in parallel, and bipolar), and feed flow rates on the efficiency of EO in removing residual tannins and ammonia–nitrogen, decolorization efficiency, and energy consumption were examined.

Materials and methods

Raw materials

Wastewater samples were collected from the effluent discharge point of an anaerobic cover lagoon at Suksomboon Vegetable Oil Co., Ltd., Chonburi, Thailand. These samples, labeled "anaerobically-treated POME," were kept at 4 °C before usage. The anaerobically-treated POME had a concentration of phenolic compounds of 224.46 ± 13.17 mg/L, total chemical oxygen demand (tCOD) of 5440.80 ± 78.40 mg/L, pH of 8.32 ± 0.06 , NH_3 -N concentration of 37.98 mg/L, and color of $13,337.5 \pm 1178.60$ ADML. Additionally, pig blood was collected from a slaughterhouse to prepare a stock solution containing $11,297 \pm 79$ mg/L of stable protein, which was kept at 4 °C.

Gallotannin was purchased from HiMedia Laboratories Pvt. Ltd. (Mumbai, India). Standard solutions of gallotannin (phenolic compounds) were prepared at five different concentrations (2.5, 5, 10, 20, and 30 μ g/mL). Bovine serum albumin (BSA) was purchased from Sigma–Aldrich (St. Louis, Missouri, USA). The BSA standard solutions were prepared with eleven different concentrations ranging from 0.5 to 10 g/L according to Martina and Vojtech (2015). Ammonium chloride (NH_4Cl , AR grade) was purchased from Elago Enterprises Pty. Ltd. (New South Wales, Australia). The NH_3 -N standard solutions were prepared at five different concentrations ranging from 0.25 to 2 mg/L according to Le and Boyd (2012).

Preliminary treatment using organic precipitation in series with electrocoagulation

The anaerobically treated POME was transferred to a 2000-mL beaker with a working capacity of 1660 mL. The pig blood solution was added to the anaerobically treated POME at a tannin-to-protein ratio of 0.33 (w/w), and the pH of the mixture was adjusted to 5.0 ± 0.2 . The mixture was stirred for 3 min at 150 rpm and 5 min at 60 rpm, then allowed to settle for 15 min. The supernatants were collected for subsequent treatment and referred to as POP-treated POME.

Two types of wastewater were treated with EC: (1) POP-treated POME, and (2) anaerobically-treated POME without organic precipitation. The EC process was conducted in a 700 mL acrylic reactor, assembled with four Al electrodes in the monopolar parallel electrode connection mode. Each electrode had a surface area of 100 cm^2 ($10\text{ cm} \times 5\text{ cm} \times 0.2\text{ cm}$) and was placed 10 mm apart. Each electrode was linked to a direct current (DC) electricity source with a maximum current capacity of 30 A and an output electrical power of 15 V. The EC reactor was filled with 620 mL of wastewater, and the reaction was initiated by supplying an electrical current to the electrodes at a fixed current density of 30 mA/cm^2 for 10 min. After the allotted EC period, the system was left to settle at ambient room temperature (298–303 K) for 15 min, and the supernatant was collected for subsequent treatment and chemical analysis. The supernatants from the EC treatment of POP-treated POME and anaerobically-treated POME are referred to as POP-EC-treated POME and EC-treated POME, respectively. Before and after each experiment, all the electrodes were cleaned with piped water, immersed in 2.5% HCl (v/v) for at least 5 min, and rinsed with DI water.

Electrooxidation reactor setup with different electrode arrangements

POP-EC-treated POME and EC-treated POME wastewater samples were further treated with EO. The EO process was conducted in a 910 mL acrylic reactor with a graphite anode and a stainless-steel cathode. Figure 1 shows the reactor configuration with the water inlet, outlet, and electrodes. Each electrode had a total surface area of 260 cm^2 ($10\text{ cm} \times 13\text{ cm} \times 0.1\text{ cm}$) and was placed 10 mm apart. Three electrode configurations were investigated: monopolar in parallel (MP), monopolar in series (MS), and bipolar in series (BS). The electrodes were connected to a DC electricity source with a maximum current capacity of 30 A and a maximum output electrical voltage of 15 V.

The EO reactor was filled with 750 mL of each wastewater sample. The reaction was initiated by supplying an electrical current to the electrodes at specified current densities (20, 30, 40, 50, 60, or 70 mA/cm^2) and electrolysis times (3,

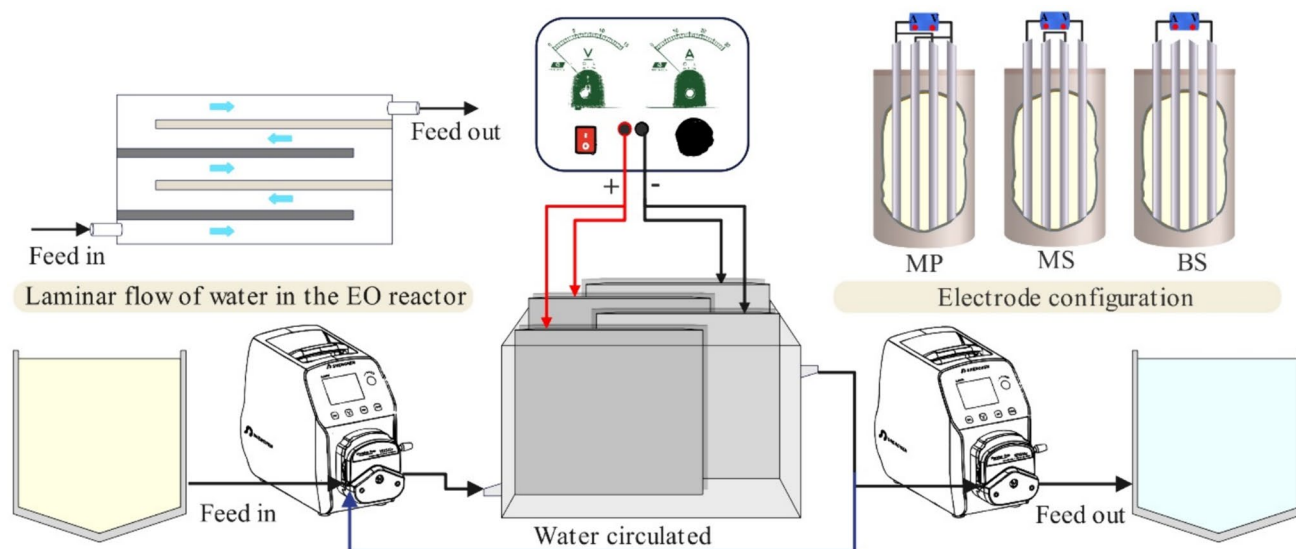


Fig. 1 Schematic configuration of the electrooxidation reactor

6, 9, 12, 15, 18, or 21 min). Wastewater was circulated in the reactor at a specified flow rate (80, 100, 120, 140, or 160 mL/min) until the total hydraulic retention time reached the specified electrolysis time. After the allotted EO period, the system was left to settle at ambient room temperature (298–303 K) for 15 min, and the supernatant was collected for chemical analysis. The supernatants from the EO treatment of POP-EC-treated POME and EC-treated POME are referred to as POP-EC-EO-treated POME and EC-EO-treated POME, respectively.

Analytical method

Aqueous pH was measured using a pH meter (Model LAQUA-PH2000, Horiba Advanced Techno Co. Ltd., Kyoto, Japan). The phenolic compound content was measured using a standard colorimetric method (APHA et al. 2012). The $\text{NH}_3\text{-N}$ content was measured using the salicylate method described by Le and Boyd (2012).

Calibration curves of light absorbance as a function of the concentrations of the standard phenolic compounds, BSA, and $\text{NH}_3\text{-N}$ were obtained using a visible spectrophotometer (Model V-1100D, Shanghai Mapada Instruments Co. Ltd., Shanghai, China) at wavelengths of 700, 540, and 640 nm, respectively. The concentrations of phenolic compounds (expressed as phenolic compound equivalents), proteins (expressed as protein equivalents), and $\text{NH}_3\text{-N}$ (expressed as $\text{NH}_3\text{-N}$ equivalents) in the liquid samples were determined from the calibration curves using linear interpolation of light absorbance readings. The colors of the wastewater and treated water samples were assessed in American Dye Manufacturers Institute (ADMI) units using a colorimeter

according to the manufacturer's instructions (MERCK Spectroquant Unk Prove 100, Merck Ltd., Darmstadt, Germany).

The output voltages and currents were monitored using a digital multimeter (Model XL830L, Shenzhen Ruizhi Industrial Co. Ltd., Guangdong, China).

The chemicals in POP-EC-treated and POP-EC-EO-treated POME were analyzed using a gas chromatography-mass spectrometer (GC-MS, QP2020 NX series, Shimadzu Co., Kyoto, Japan) equipped with an Rxi-5Sil MS capillary column (30 m \times 0.25 mm ID \times 0.25 μm df). The splitless injection was performed at a ratio of 1:10, and the injection temperature was maintained at 280 $^\circ\text{C}$. The column temperature was increased from 50 to 300 $^\circ\text{C}$ at a rate of 10 $^\circ\text{C}/\text{min}$. Helium was the carrier gas at a constant flow rate of 3 mL/min. The mass spectrometer was operated in the electronic-impact mode with an ionization energy of 70 eV. The detection was performed in the full scan mode from 35 to 500 m/z.

Calculations

The electrical energy consumption was calculated as follows:

$$SEC = \frac{E \times I \times t}{V} \quad (1)$$

where *SEC* is the specific energy consumption (kWh/m^3), *E* is the cell voltage (V), *V* is the volume of treated water (m^3), *t* is the electrolysis time (s), and *I* is the current (A).

The boundary layer thickness, which represents the film layer on a smooth plate under laminar flow conditions, was calculated using the Blasius equation:

$$\delta = \frac{5x}{\sqrt{Re_x}} \quad (2)$$

$$Re_x = \frac{U_\infty x}{\nu} \quad (3)$$

where δ is the boundary layer thickness (cm), Re_x is Reynolds number, ν is the kinematic viscosity (m^2/s), U_∞ is the liquid upstream velocity (m/s), and x is the distance from the edge of the electrode (cm) along the horizontal axis.

The removal efficiency was determined by calculating the percentage (%) removal for each parameter using the formula $(D_0 - D_t)/D_0$, where D_0 and D_t represent the initial and residual concentrations of phenolic compounds, color, and $\text{NH}_3\text{-N}$ in the wastewater, respectively.

Results and discussion

Effect of preliminary treatment with organic precipitation on the removal of color and phenolic compounds by electrooxidation

Figure 2 shows the removal efficiency of color and (poly) phenolic compounds from two wastewater samples (POP-EC-treated POME and EC-treated POME) using EO with an MP configuration at an electrolysis time of 12 min and current density between 20 and 70 mA/cm^2 . The POP-EC-treated POME wastewater samples had lower initial phenolic compound concentrations in the range 7.64–11.12 mg/L , and the removal efficiency of phenolic compounds by EO in this wastewater was almost 100% at a current density of 60 mA/cm^2 (Fig. 2a). In contrast, the EC-treated POME wastewater samples had higher initial phenolic compound concentrations in the range 30.14–36.46 mg/L . They required a higher current density of 70 mA/cm^2 to reach 96.99% removal of phenolic compounds and a residual phenolic compound concentration of 1.09 mg/L (Fig. 2b). EO oxidizes phenolic compounds to simpler compounds through both direct and indirect oxidation mechanisms (Saputera et al. 2021). In the direct oxidation mechanism, phenolic compounds diffuse through the mass-transfer boundary layer and are oxidized at the anodic surface by radicals such as $\cdot\text{O}$, $\cdot\text{OH}$, and $\cdot\text{Cl}$. In the indirect oxidation mechanism, relatively stable oxidants such as active chlorine species are generated at the electrodes and diffuse across the boundary layer to the bulk liquid, where they are transferred by mass convection to react with complex phenolic compounds (Rao et al. 2001; Serrano 2018). These results suggest that preliminary organic precipitation substantially boosts the removal efficiency of phenolic compounds by EO, possibly by eliminating condensed tannins, thus lowering the

interference of large tannin molecules on the mass transfer of active species and interactions between active species and phenolic compounds.

The effect of preliminary organic precipitation on color removal was similar to that on phenolic compound removal. Figure 2c shows the efficiency of color removal using EO in POP-EC-treated POME wastewater with initial color concentrations in the 347.12–393.04 ADMI range. The EO treatment of the wastewater caused a significant reduction in the color concentrations from above 300 ADMI to 104.10 ADMI (70% color reduction) using a current density of 20 mA/cm^2 and to 4.85 ADMI (98.61% color reduction) using a current density of 70 mA/cm^2 (Fig. 2c). In contrast, the wastewater samples without preliminary organic precipitation had higher initial color concentrations in the range of 546.50–569.50 ADMI and required a higher current density of 70 mA/cm^2 to reach a color removal of 70.57% and a residual color concentration of 160.82 ADMI (Fig. 2d). The results showed that EO was effective in removing color caused by phenolic plant constituents, particularly when current densities $> 60 \text{ mA}/\text{cm}^2$ were applied to the wastewater samples with preliminary organic precipitation.

Effect of electrode configurations and current density on the removal of color and phenolic compounds by electrooxidation

As established in section "Effect of preliminary treatment with organic precipitation on the removal of color and phenolic compounds by electrooxidation", preliminary organic precipitation improves the efficiency of the EO process; therefore, further investigations in this study will be performed on POP-EC-treated POME wastewater samples. Figures 3 and 4 show the removal efficiencies of phenolic compounds and color from POP-EC-treated POME using EO with different electrode configurations (MP, MS, and BS), current densities (20–70 mA/cm^2), and electrolysis times (0–21 min). For all electrode configurations, increasing the current density increased the phenolic compound removal efficiency and color. Zhang et al. (2011) reported that using higher current densities during the EO process led to increased chlorine generation, which increased the reaction rates and extent of indirect oxidation. Moreover, the increased current density accelerates the electron transfer rate, thereby facilitating the direct oxidation of organic pollutants (Zhou et al. 2016).

Regarding the total elimination of phenolic compounds at lower electrolysis times and current densities, the EO process with the MP configuration performed better than those with the MS and BS configurations. The removal efficiency of phenolic compounds by the EO process with the MP configuration was 98.01% at a current density of

Fig. 2 Removal of phenolic compounds and color by EO: **a** removal of phenolic compounds from POP-EC-treated POME; **b** removal of phenolic compounds from EC-treated POME; **c** removal of color from POP-EC-treated POME; **d** removal of color from EC-treated POME

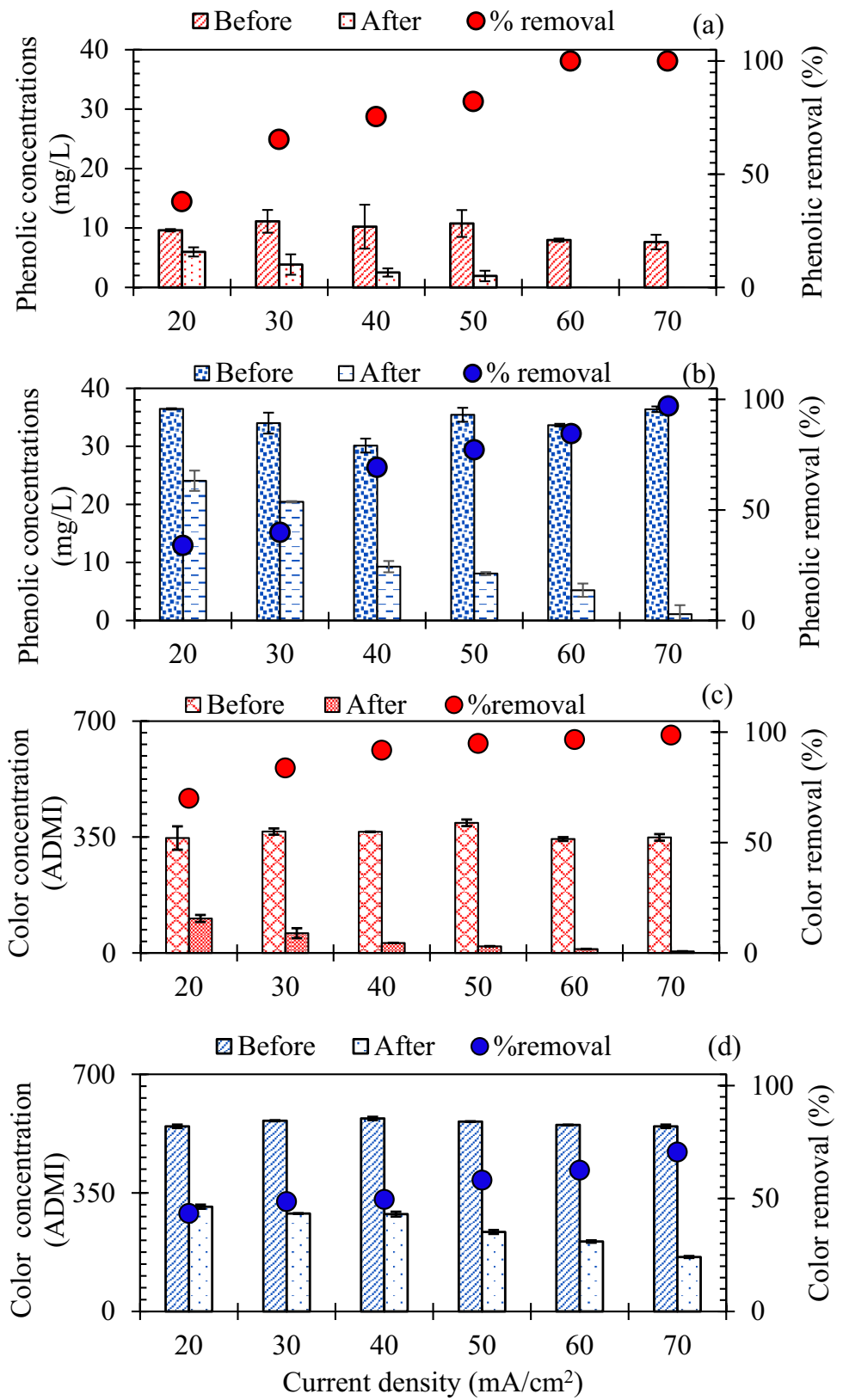
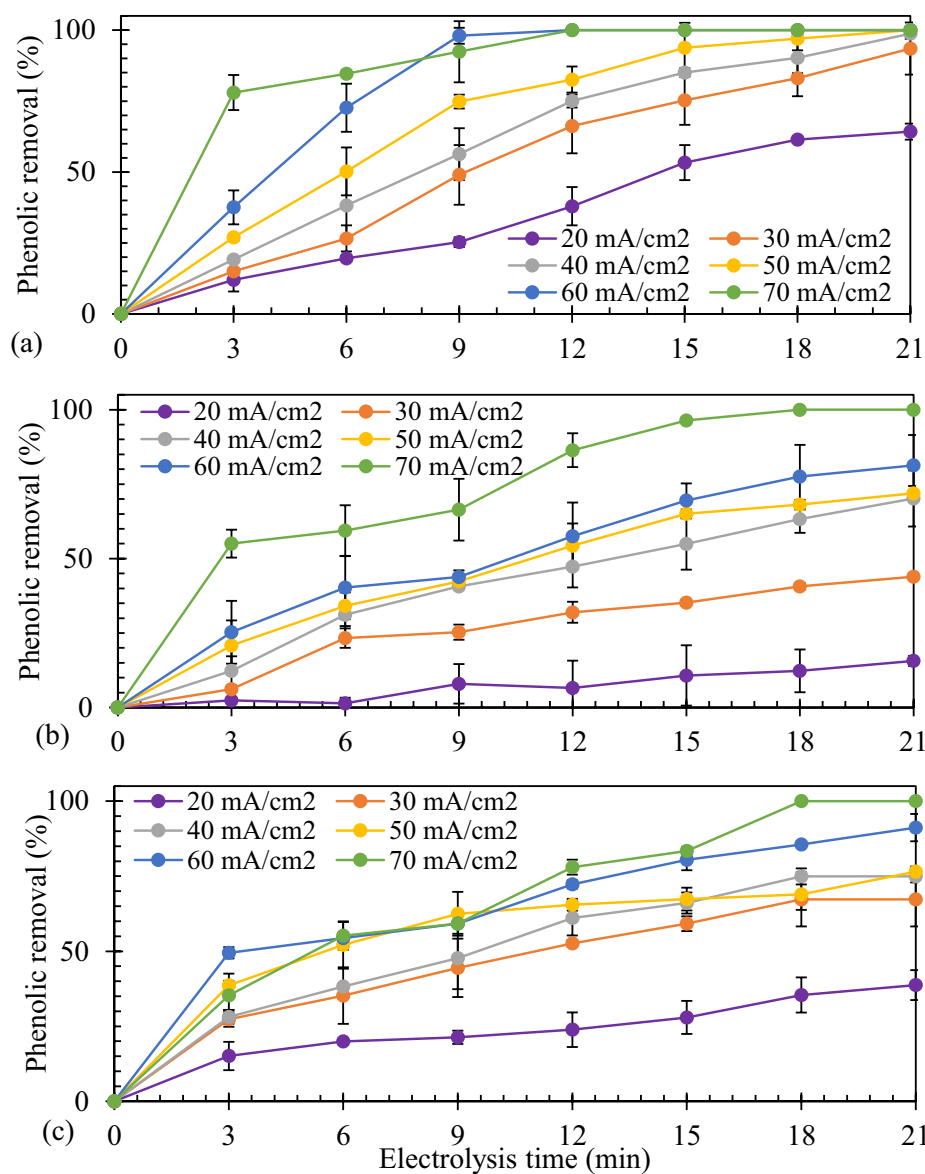


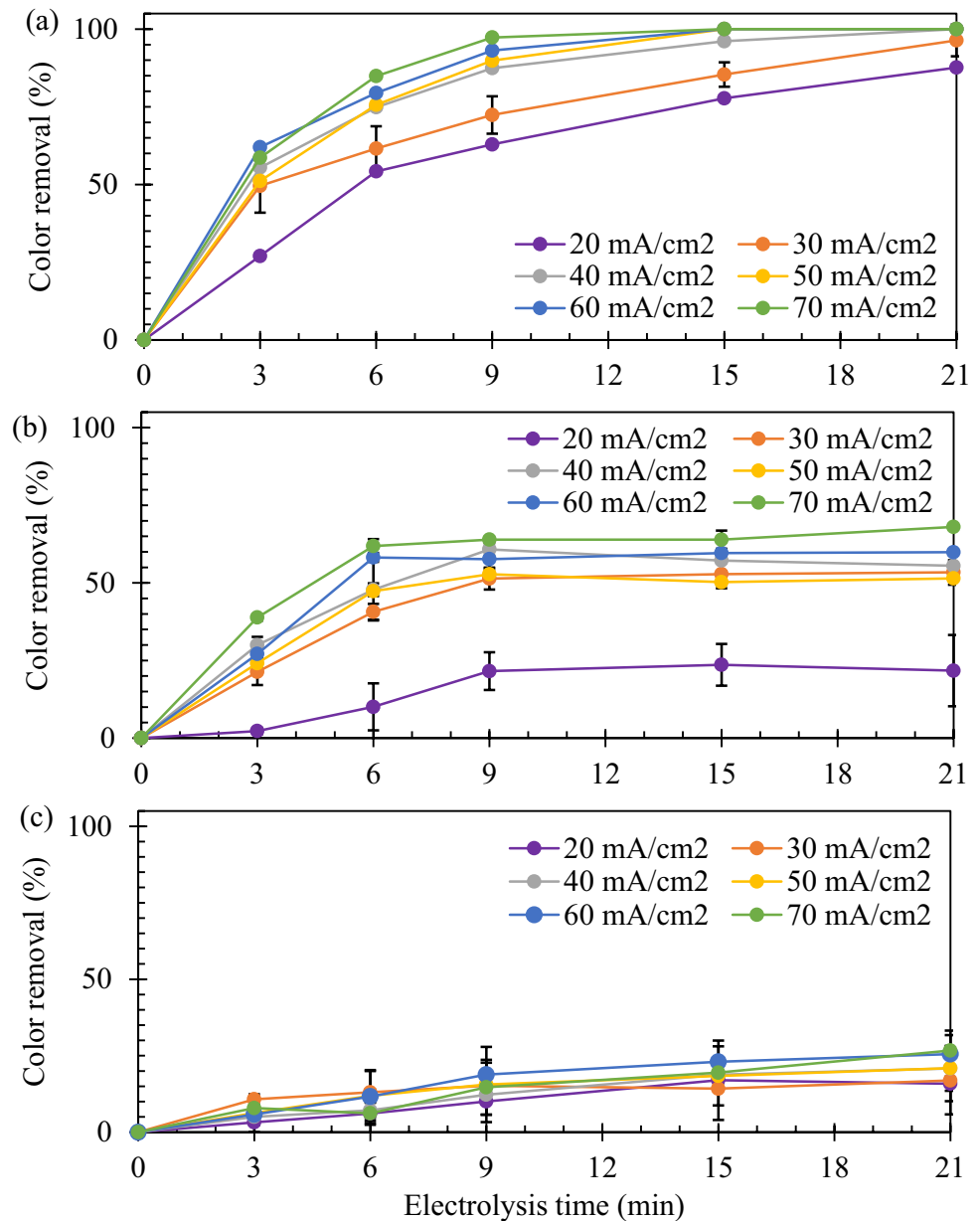
Fig. 3 Removal of phenolic compounds from POP-EC-treated POME by EO with different electrode arrangements: **a** MP; **b** MS, and **c** BS



60 mA/cm² and an electrolysis time of 9 min (Fig. 3a). In contrast, under these operating conditions, the removal efficiencies of phenolic compounds were only 40.24% and 59.19% in the MS and BS configurations, respectively. A current density of 70 mA/cm² and an electrolysis time of 15 min was required for the EO process with the MS and BS configurations to achieve removal efficiencies of 96.34% and 83.45%, respectively (Fig. 3b, c). The superior removal efficiency of phenolic compounds in the MP configuration might be attributed to its relatively uniform electric field compared with those associated with the MS and BS configurations. The more uniform the electric field, the more stable the generation of radicals and oxidizing agents and, therefore, the higher the reaction efficiency (Nava and de León 2018; Reza and Chen 2022).

The EO process with the MP configuration also performed better for color removal than those with the MS and BS configurations. For example, at an electrolysis time of 9 min and a current density of 60 mA/cm², the efficiencies of color removal were 93.10%, 57.64%, and 18.83% for the MP, MS, and BS configurations, respectively (Fig. 4a–c). In addition, with the MP configuration, a current density above 50 mA/cm², and an electrolysis time ≥ 15 min, the color was completely removed (100% removal efficiency). The treated POME wastewater samples became transparent, revealing very low concentrations of light-absorbing substances (Fig. 5).

Fig. 4 Removal of color from POP-EC-treated POME by EO with different electrode arrangements: **a** MP; **b** MS, and **c** BS



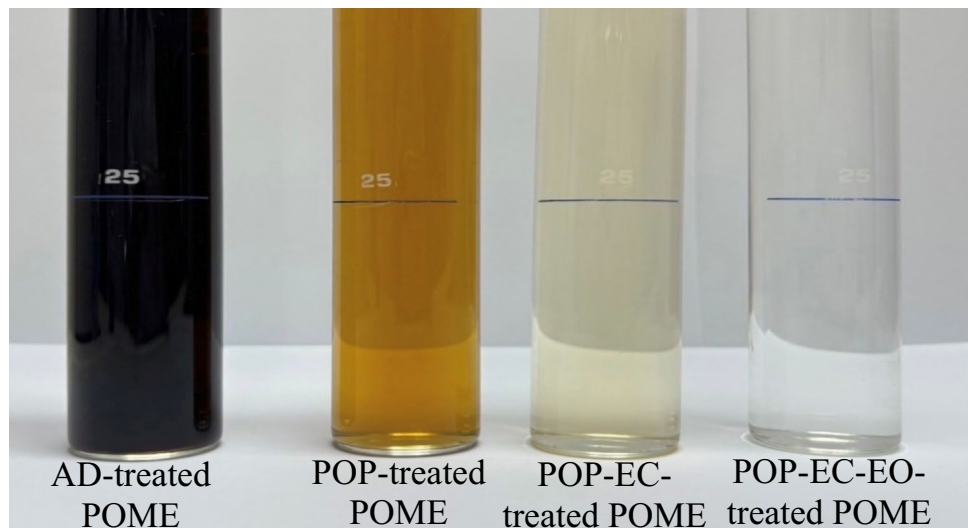
Effect of electrode configurations on energy consumption in the electrooxidation process

Figure 6 shows the energy consumption of the EO process with the MP, MS, and BS configurations. The energy consumption by the EO process varied greatly from 0.39 to 21.80 kWh/m³, depending on the current density (20–70 mA/cm²), electrolysis time (3–21 min), and electrode configuration (MP, MS, and BS configurations). In the MP configuration, the current is divided between the electrodes, whereas in the MS and BS configurations, the current passing through each electrode pair is kept constant. In this study, we kept the current passing each electrode pair in all configurations at 2.4 A, and the total current in the MP

configuration was 7.2 A. For the same electrolysis time and current density, the energy consumption of the EO with the MP configuration was slightly higher than those with BS and MS configurations. For example, with a current density of 60 mA/cm² and an electrolysis time of 9 min, the ranking order of energy consumptions was: MP (4.81 kWh/m³) > BS (4.78 kWh/m³) > MS (3.89 kWh/m³). Energy consumption was directly proportional to the applied voltage: 4.81 V for the MP, 4.78 V for BS, and 3.89 V for MS.

The electrode configuration had a greater effect on the removal of phenolic compounds and color than on the reduction in energy consumption. Considering the removal efficiency of the phenolic compounds, the EO process with the MP configuration resulted in a removal efficiency

Fig. 5 Visual appearance of the treated POME wastewater samples



of 98.01% at the lowest current density (60 mA/cm²), electrolysis time (9 min), and energy consumption (6.93 kWh/m³). With the MS and BS configurations, the removal efficiencies of the phenolic compounds were 96.34% and 83.45%, respectively, with a current density of 70 mA/cm², electrolysis time of 15 min, and energy consumption of 14.00 and 11.70 kWh/m³, respectively.

Effect of feed flow rates on the removal of phenolic compounds, ammonium-nitrogen, and color by electrooxidation

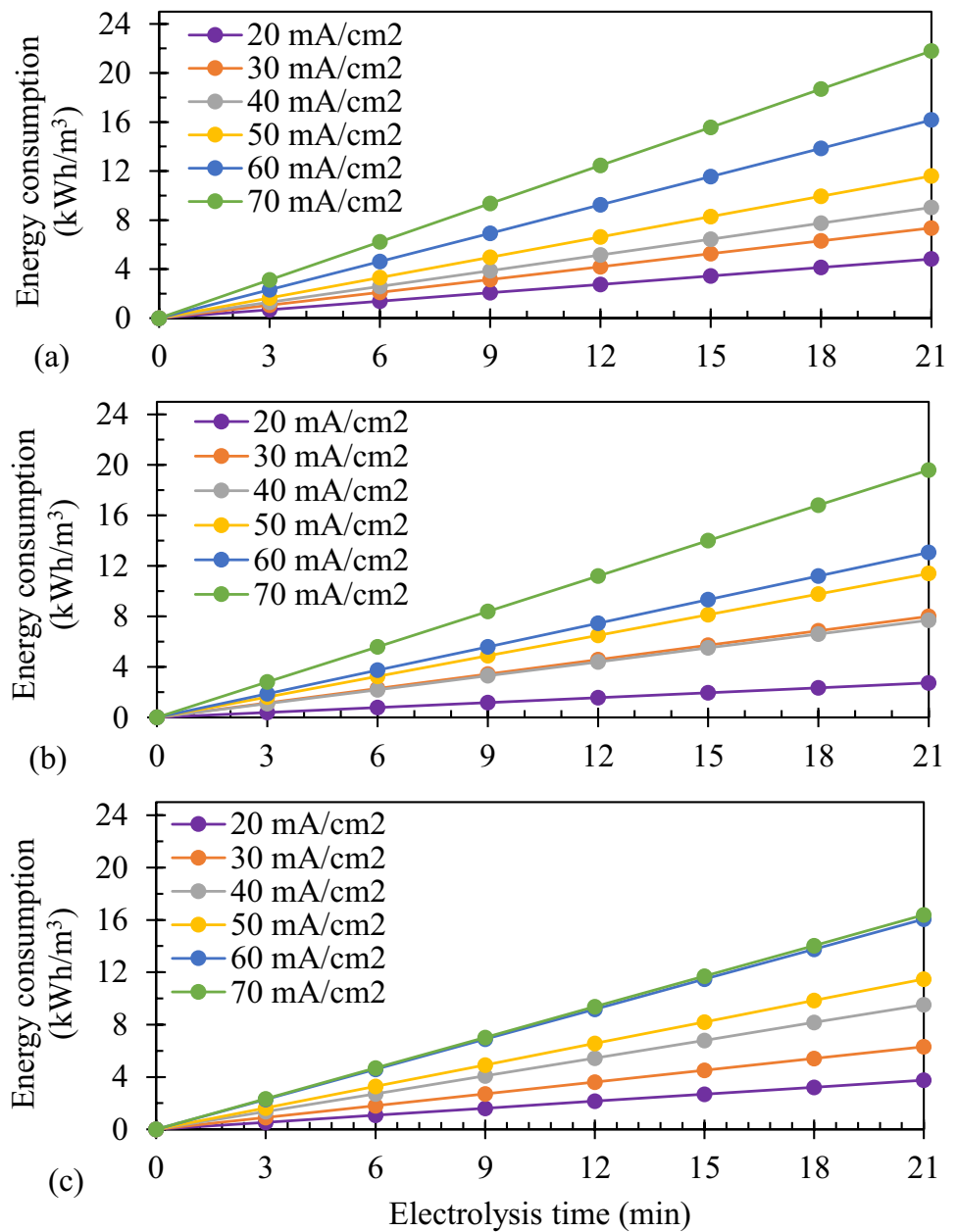
To examine the effects of feed flow rate on the removal of phenolic compounds, ammonium, and color, the feed flow was adjusted to rates between 80 mL/min (equivalent to a fluid velocity of 0.0017 m/s) and 160 mL/min (0.0033 m/s), the current density was fixed at 60 mA/cm², and the hydraulic retention time was maintained at an optimal electrolysis time of 9 min. Figure 7a shows the energy consumption and color removal in the EO process at feed flow rates of 80, 100, 120, 140, and 160 mL/min. The results show that varying the feed flow rates between 80 and 160 mL/min caused only small changes in the color removal efficiencies (in the range 98.02–100%). However, the feed flow rates had a profound effect on energy consumption, showing the lowest energy consumption of 3.12 kWh/m³ at the lowest flow rate of 80 mL/min and the highest energy consumption of 9.22 kWh/m³ at 160 mL/min. It should be noted that the direction of water flow was normal to the transport of charged species across the electrodes. Therefore, as the water flowed faster, the charged species traveled along longer paths across the electrodes due to the transverse liquid motion, thus increasing the electrical resistance.

Figure 7b shows the relationship between the removal efficiency of phenolic compounds, the thickness of the

boundary layer developed in the vicinity of the electrodes as calculated by the Blasius equation with $x=0.25$ cm, and the water velocity. There was a relatively large variation in the removal efficiency of phenolic compounds in the range 75.89–97.22% at different water velocities. The flow regime in this study was considered laminar, with a Reynolds number in the range 166–333. As expected, the increase in the feed flow rate and thus the water velocity led to a decrease in the boundary layer thickness from 0.61 to 0.44 cm for water velocities of 0.0017 m/s and 0.0033 m/s, respectively. The decreased boundary layer thickness, in turn, increased the mass transport rate of the oxidizing agents and phenolic compounds between the electrode surface and bulk liquid. Yavuz and Shahbazi (2012) suggested that an increase in the liquid flow rate could reduce heat accumulation in an EO system because the liquid flow helps dissipate heat by promoting convective heat transfer. In addition, Angulo et al. (2020) suggested that an increase in the liquid flow rate could reduce the accumulation of gas bubbles near the electrode surface, impeding mass and electron transfer and leading to localized heating. However, the removal efficiency of phenolic compounds in this study was highest at a median velocity of 0.0025 m/s (corresponding to a feed flow rate of 120 mL/min). An explanation for this is that as the water velocity increased, the contact time for both the oxidizing agents and phenolic compounds in the bulk decreased, causing the reaction efficiency to decrease. Therefore, the results revealed that the interplay among the water flow rate, boundary layer thickness, and reaction contact time is important for optimizing the removal efficiency of phenolic compounds in the EO process.

EO, with its proven ability to effectively remove NH₃-N, offers promising solutions. For instance, Zhou et al. (2016) reported the removal of NH₃-N from landfill leachate using an EO system with boron-doped diamond electrodes at a

Fig. 6 Energy consumption of the EO process with different electrode arrangements: **a** MP; **b** MS, and **c** BS



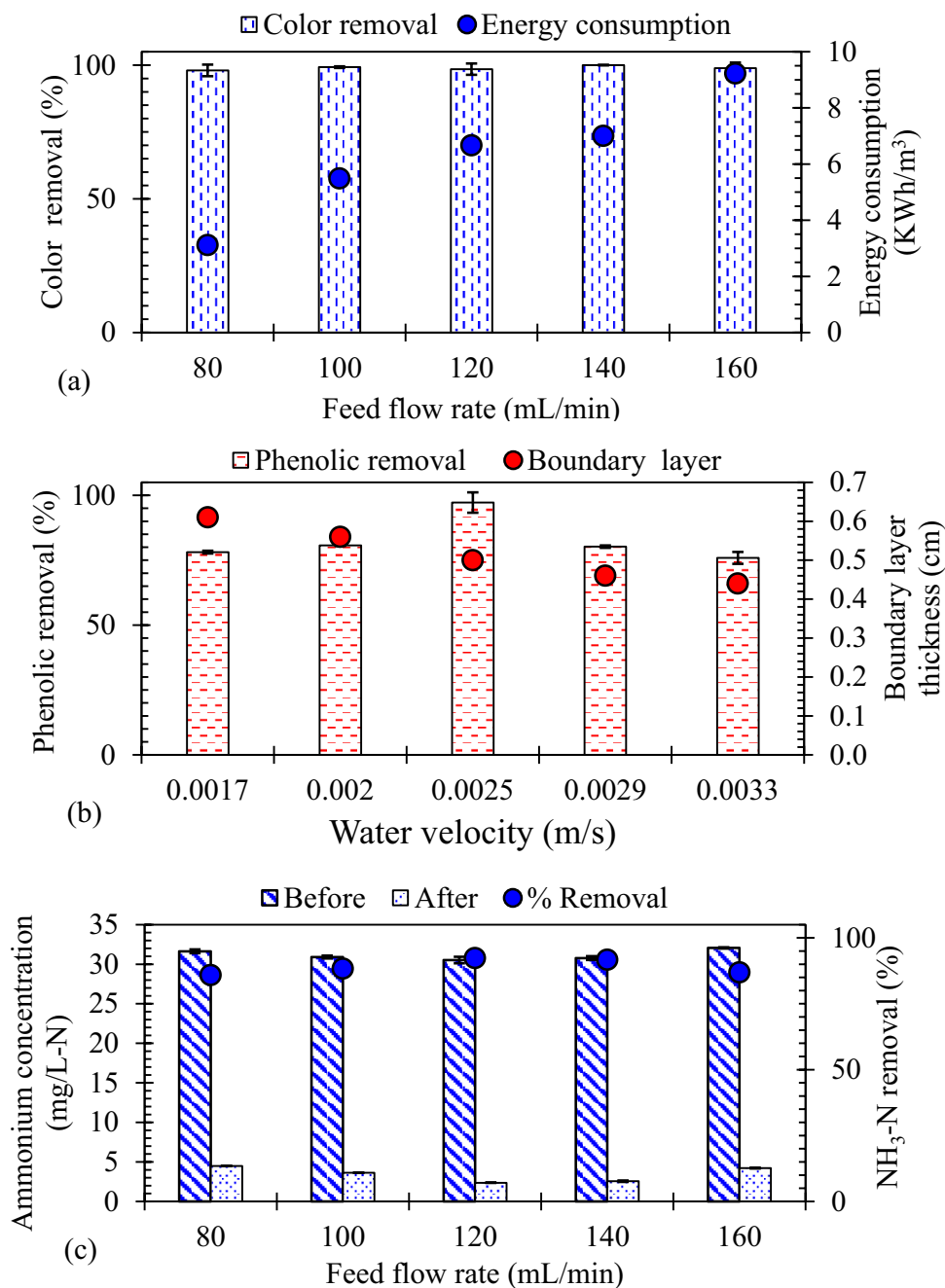
current density of 50 mA/cm², electrolysis time of 6 h, and feed flow rate of 100 mL/min. They achieved a removal efficiency of NH₃-N of 74.06%, with an energy consumption of 223.2 kWh/m³, demonstrating the energy efficiency of the EO system. The removal of NH₃-N is suggested to occur via an indirect oxidation reaction, as follows (Rao et al. 2001):



In this study, the effect of the feed flow rate on NH₃-N removal was investigated and found to be similar to that on the removal of phenolic compounds. Figure 7c shows the removal efficiency of NH₃-N at various feed flow rates in the range of

80–160 mL/min. The highest removal efficiency of NH₃-N (92.26%) was achieved at a feed flow rate of 120 mL/min and the residual NH₃-N concentration was 2.36 mg/L. In contrast, when the feed flow rate was increased or decreased from the optimal value, the removal efficiency of NH₃-N decreased. For example, at feed flow rates of 80 and 160 mL/min, the removal efficiency of NH₃-N was reduced to 85.82% and 86.85%, respectively.

Fig. 7 Effect of feed flow rates and water velocity on EO efficiency: **a** color removal and energy consumption; **b** phenolic compound removal and boundary layer thickness, and **c** ammonium removal

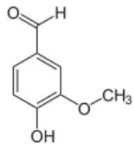
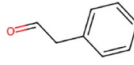
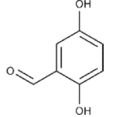
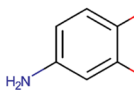
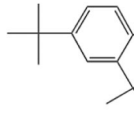
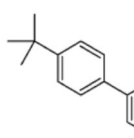
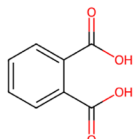
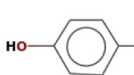


GC–MS analysis of profiles of phenolic compounds before and after electrooxidation

Table 1 presents the major phenolic compounds in the POP-EC-treated POME based on GC–MS analysis (Table 1). The major phenolic compounds, presented in order of their relative chromatographic peak areas, were vanillin, 2,5-dihydroxybenzaldehyde, 2,4-di-tert-butylphenol, benzeneacetaldehyde, 4-amino-1,2-benzenediol, 4-(4-tert-butylphenyl)-1,3-thiazol-2-ylamine, 1,2-benzenedicarboxylic acid, phenol, 4,4'-(1-methylethylidene)bis-, and phenol,

4-(1,1-dimethyl propyl)-. The relative peak areas of the first and second compounds were more than double that of the third compound (Table 1). Vanillin, the phenolic compound with the highest concentration in POP-EC-treated POME, belongs to the benzaldehyde family and contains hydroxy and methoxy substituents at positions 3 and 4, respectively (Jenkins et al. 2024). When dissolved in water, vanillin causes the water to appear orange-yellow. 2,5-dihydroxybenzaldehyde, the phenolic compound with the second-highest concentration in POP-EC-treated POME, belongs to the benzaldehyde family and has hydroxyl

Table 1 Major phenolic compounds in the POP-EC-treated POME based on GC–MS analysis

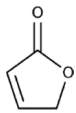
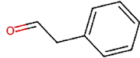
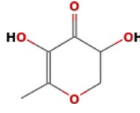
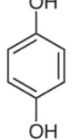
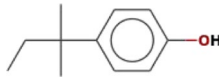
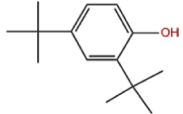
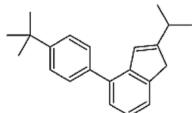
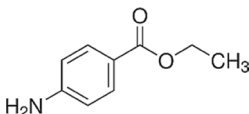
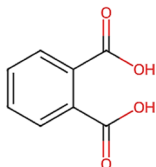
No.	Retention time (min)	Name	Area (%)	Chemical formula	Chemical structure
1	6.0	Vanillin	23.87	C ₈ H ₈ O ₃	
2	7.8	Benzeneacetaldehyde	9.25	C ₈ H ₈ O	
3	8.5	2,5-Dihydroxybenzaldehyde	22.68	C ₇ H ₆ O ₃	
4	10.6	4-Amino-1,2-benzenediol	10.62	C ₆ H ₇ NO ₂	
5	13.0	Phenol 4-(1,1-dimethyl propyl)-	3.09	C ₁₁ H ₁₆ O	
6	14.4	2,4-Di-tert-butylphenol	10.73	C ₁₄ H ₂₂ O	
7	15.8	4-(4-tert-butylphenyl)-1,3-thiazol-2-ylamine	8.75	C ₁₃ H ₁₆ N ₂ S	
8	18.4	1,2-Benzenedicarboxylic acid	6.15	C ₈ H ₆ O ₄	
9	21.5	Phenol 4,4'-(1-methylethylidene)bis-	4.85	C ₁₅ H ₁₆ O	

substituents at positions 2 and 5 (Brito et al. 2017). When dissolved in water, 2,5-dihydroxybenzaldehyde causes water to appear yellow, green, and brown. Based on their concentrations in the wastewater samples and their color properties, it is likely that the color of the EC-treated POME was mainly caused by the presence of vanillin and 2,5-dihydroxybenzaldehyde.

Table 2 presents the major phenolic and heterocyclic organic compounds in the POP-EC-EO-treated POME wastewater samples based on GC–MS analysis. The major phenolic and heterocyclic organic compounds, presented in order of their relative chromatographic peak areas, were 2,3-dihydro-3,5-dihydroxy-6-methyl-(4H)-pyran-4-one (DDMP), a phenylmethyl-related compound (*m/z* 91 and a retention time of 21.4 min), benzeneacetaldehyde,

ethyl *p*-acetamidobenzoate, 2,4-di-tert-butylphenol, hydroquinone, 1,2-benzenedicarboxylic acid, phenol 4-(1,1-dimethyl propyl)-, 2(5H)-furanone, and 4-(4-tert-butylphenyl)-1,3-thiazol-2-ylamine. The relative peak area of the first, second, and third compounds were more than double that of the fourth compound (Table 2). Vanillin and 2,5-dihydroxybenzaldehyde were not detected in the POP-EC-EO-treated POME samples, indicating that the colored compounds were degraded, whereas hydroquinone and furanone, which are common end products of oxidized aromatics and ring-opening products (Đuričić et al. 2023), were detected. In addition, DDMP was suggested to be a ring-opening product of the oxidation reactions because it was present in relatively large quantities but was not detected in the wastewater samples before the EO process.

Table 2 Major end products of the electrooxidation of the POP-EC-treated POME with graphite electrodes based on GC–MS analysis

No.	Retention time (min)	Name	Area (%)	Chemical formula	Chemical structure
1	6.0	2(5H)-Furanone	1.67	C ₄ H ₄ O ₂	
2	7.8	Benzeneacetaldehyde	19.15	C ₈ H ₈ O	
3	9.5	2,3-dihydro-3,5-dihydroxy-6-methyl-(4H)-pyran-4-one (DDMP)	30.87	C ₆ H ₈ O ₄	
4	11.2	Hydroquinone (1,4-Dihydroxybenzene)	2.43	C ₆ H ₆ O ₂	
5	13.0	Phenol 4-(1,1-dimethyl propyl)-	1.99	C ₁₁ H ₁₆ O	
6	14.4	2,4-Di-tert-butylphenol	4.54	C ₁₄ H ₂₂ O	
7	15.8	4-(4-tert-butylphenyl)-1,3-thiazol-2-ylamine	1.33	C ₁₃ H ₁₆ N ₂ S	
8	17.0	Ethyl p-acetamidobenzoate	10.67	C ₉ H ₁₁ NO ₂	
9	18.4	1,2-Benzenedicarboxylic acid	2.02	C ₈ H ₆ O ₄	
10	21.4	Phenylmethyl-related compound	25.33	–	–

Cost analysis

Table 3 estimates the operating costs of the combined process, including power consumption and chemical costs. The estimated cost for the organic precipitation unit was 25.6 USD/m³ for pig blood protein, 3 M HCl, and electricity costs. The main expense for the EC unit was the electricity cost of 21.5 USD/m³. For the EO unit, the electricity cost was 123.2 USD/m³. The total operational cost of the combined treatment process amounted to 170 USD/m³, which was notably higher than the cost of fresh water in normal situations. However, the revenue from

the harvested crude tannin-protein complexes, a valuable by-product of the treatment process, can be as high as 260 USD/m³, resulting in a substantial net profit of 90 USD/m³. Similar to a previous report on olive oil wastewater treatment (Al-Qodah et al. 2022), olive mill wastewater has been identified as a source of various bioactive materials, mainly phenolic compounds. These phenolic compounds can be valorized as by-products because they are notable for their antioxidant properties and can be used as additives for different consumable products and cosmetic applications.

Table 3 Analysis of the operating costs of the combined wastewater treatment process with organic precipitation, electrocoagulation, and electrooxidation in series

Items	Unit	Value
Operating cost		
Organic precipitation	USD/m ³	25.57
Pig blood protein		
3M HCl		
Electricity		
Electrocoagulation	USD/m ³	21.54
Electricity		
Electrooxidation	USD/m ³	123.15
Electricity		
Total operation cost	USD/m ³	170.26
Revenue from crude tannin-protein complex	USD/m ³	260.32
Net profit	USD/m ³	90.06

Cost and revenue calculation based on 1 THB = 0.027 USD, a market price of pig blood at 10.26 USD/m³ (price at a local market), a market price of crude tannin-protein complex at 24,840 USD/ton (<https://longleafbio.en.made-in-china.com/product/qwEifFoVbQBkC/China-Supply-90-Galla-Chinensis-Extract-Powder-Tannin-90-.html>), an electricity cost of 0.09 USD/kWh (<https://www.mea.or.th/our-services/tariff-calculation/other/D5xEaEwgU>), a market price of HCl at 5778 USD/m³ (Qrec, New Zealand), a market price of NaCl at 974 USD/ton (Ajax, Australia)

Conclusions

This study demonstrated the efficiency of EO in removing residual phenolic compounds, color, and NH₃-N from POME treated in series with anaerobic digestion, organic precipitation, and EC. Preliminary organic precipitation significantly enhanced the efficiency of EO, particularly in phenolic compound removal, possibly by eliminating condensed tannins that could interfere with EO reactions. Decreases in phenolic compound concentration (97.22%), color (98.49%), and NH₃-N concentration (92.26%) in the treated POME were obtained using the EO process with an MP configuration at a current density of 60 mA/cm², feed flow rate of 120 mL/min, and electrolysis duration of 9 min. Furthermore, GC-MS analysis confirmed the degradation of colored compounds and the generation of end products such as hydroquinone and furanone, demonstrating the efficiency of EO in refining the quality of treated POME. Future studies should examine EC prior to biological treatment to evaluate its efficacy and cost-effectiveness compared to the existing procedure for treating wastewater.

Acknowledgements The authors gratefully acknowledge the financial support provided by the Thailand Science Research and Innovation (TSRI) and King Mongkut's University of Technology North Bangkok (Grant No. KMUTNB-FF-67-B-21).

Author contributions PK: Conceptualization, Methodology, Investigation, Visualization, Writing-original draft. KC: Investigation. KB: Investigation. NK: Investigation. TD: Investigation. JB: Investigation, Resources. AK: Review and Editing. PTPA: Review and Editing. CP: Conceptualization, Methodology, Resources, Visualization, Writing-Review and Editing, Supervision.

Funding The authors thank Thailand Science Research and Innovation (TSRI) and King Mongkut's University of Technology North Bangkok (Grant No. KMUTNB-FF-67-B-21) for financial support.

Declarations

Conflict of interest The authors declare that they have no known competing financial interests or personal relationships that could have appeared to influence the work reported in this paper.

Ethical approval The authors affirm their full participation in this research and adherence to ethical research practices. We all agree to the final form of the manuscript and declare that this research did not involve human participants or animals.

Open Access This article is licensed under a Creative Commons Attribution-NonCommercial-NoDerivatives 4.0 International License, which permits any non-commercial use, sharing, distribution and reproduction in any medium or format, as long as you give appropriate credit to the original author(s) and the source, provide a link to the Creative Commons licence, and indicate if you modified the licensed material. You do not have permission under this licence to share adapted material derived from this article or parts of it. The images or other third party material in this article are included in the article's Creative Commons licence, unless indicated otherwise in a credit line to the material. If material is not included in the article's Creative Commons licence and your intended use is not permitted by statutory regulation or exceeds the permitted use, you will need to obtain permission directly from the copyright holder. To view a copy of this licence, visit <http://creativecommons.org/licenses/by-nc-nd/4.0/>.

References

- Al-Qodah Z, Al-Zghoul TM, Jamrah A (2024) The performance of pharmaceutical wastewater treatment system of electrocoagulation assisted adsorption using perforated electrodes to reduce passivation. *Environ Sci Pollut Res* 31:20434–20448. <https://doi.org/10.1007/s11356-024-32458-z>
- Al-Qodah Z, Al-Zoubi H, Hudaib B et al (2022) Sustainable vs. conventional approach for olive oil wastewater management: a review of the state of the art. *Water* (Switzerland). <https://doi.org/10.3390/w14111695>
- Alhaji MH, Sanaullah K, Lim SF et al (2016) Photocatalytic treatment technology for palm oil mill effluent (POME)—a review. *Process Saf Environ Protect* 102:673–686. <https://doi.org/10.1016/j.psep.2016.05.020>
- Angulo A, van der Linde P, Gardeniers H et al (2020) Influence of bubbles on the energy conversion efficiency of electrochemical reactors. *Joule* 4:555–579. <https://doi.org/10.1016/j.joule.2020.01.005>
- APHA, AWWA, WEF (2012) *Standard Methods for the Examination of Water and Wastewater*, 22nd edn
- Aryanti PTP, Nugroho FA, Anwar N et al (2024) Integrated bipolar electrocoagulation and PVC-based ultrafiltration membrane process for palm oil mill effluent (POME) treatment. *Chemosphere*

- 347:140637. <https://doi.org/10.1016/J.CHEMOSPHERE.2023.140637>
- Bashir MJK, Mau Han T, Jun Wei L et al (2016) Polishing of treated palm oil mill effluent (POME) from ponding system by electrocoagulation process. *Water Sci Technol* 73:2704–2712. <https://doi.org/10.2166/wst.2016.123>
- Brito RE, Mellado JMR, Montoya MR et al (2017) Spectroscopic determination of the dissociation constants of 2,4- and 2,5-dihydroxybenzaldehydes and relationships to their antioxidant activities. *C R Chim* 20:365–369. <https://doi.org/10.1016/j.crci.2016.05.004>
- Đuričić T, Prosen H, Kravos A et al (2023) Electrooxidation of phenol on boron-doped diamond and mixed-metal oxide anodes: process evaluation, transformation by-products, and ecotoxicity. *J Electrochem Soc* 170:023503. <https://doi.org/10.1149/1945-7111/acb84b>
- Edem DO (2002) Palm oil: biochemical, physiological, nutritional, hematological, and toxicological aspects: a review. *Plant Foods Hum Nutr* 57:319–341. <https://doi.org/10.1023/A:1021828132707>
- Gilpavas E, Dobrosz-Gómez I, Gómez-García MÁ (2020) Efficient treatment for textile wastewater through sequential electrocoagulation, electrochemical oxidation and adsorption processes: optimization and toxicity assessment. *J Electroanal Chem* 878:114578. <https://doi.org/10.1016/j.jelechem.2020.114578>
- Girard AL, Bean SR, Tilley M et al (2018) Interaction mechanisms of condensed tannins (proanthocyanidins) with wheat gluten proteins. *Food Chem* 245:1154–1162. <https://doi.org/10.1016/j.foodchem.2017.11.054>
- Ingelsson M, Yasri N, Roberts EPL (2020) Electrode passivation, faradaic efficiency, and performance enhancement strategies in electrocoagulation—a review. *Water Res* 187:116433. <https://doi.org/10.1016/j.watres.2020.116433>
- Jefferson EE, Kanakaraju D, Tay MG (2016) Removal efficiency of ammoniacal nitrogen from palm oil mill effluent (Pome) by varying soil properties. *J Environ Sci Technol* 9:111–120. <https://doi.org/10.3923/jest.2016.111.120>
- Jenkins AF, Niederhaus BR, Gonzalez JA (2024) Vanillin. *Encycl Toxicol*. <https://doi.org/10.1016/b978-0-12-824315-2.00150-0>
- Kaur P, Kushwaha JP, Sangal VK (2018) Electrocatalytic oxidative treatment of real textile wastewater in continuous reactor: degradation pathway and disposability study. *J Hazard Mater* 346:242–252. <https://doi.org/10.1016/j.jhazmat.2017.12.044>
- Khemkhao M, Domrongpakkaphan V, Phalakornkule C (2022) Process performance and microbial community variation in high-rate anaerobic continuous stirred tank reactor treating palm oil mill effluent at temperatures between 55 and 70 °C. *Waste Biomass Valoriz* 13:431–442. <https://doi.org/10.1007/s12649-021-01539-2>
- Khongkliang P, Jehlee A, Kongjan P et al (2019) High efficient biohydrogen production from palm oil mill effluent by two-stage dark fermentation and microbial electrolysis under thermophilic condition. *Int J Hydrogen Energy*. <https://doi.org/10.1016/j.ijhydene.2019.10.022>
- Khongkliang P, Khemkhao M, Mahathanabodee S et al (2023) Efficient removal of tannins from anaerobically-treated palm oil mill effluent using protein-tannin complexation in conjunction with electrocoagulation. *Chemosphere* 321:138086. <https://doi.org/10.1016/j.chemosphere.2023.138086>
- Kiss L, Kunsági-Máté S, Szabó P (2023) Studies of phenol electrooxidation performed on platinum electrode in dimethyl sulphoxide medium. Determination of unreacted phenol by the effect of 4-vinylbenzenesulphonate on the electrooxidation process. *Electroanalysis* 35:1–9. <https://doi.org/10.1002/elan.202200268>
- Kongnoo A, Suksaroj T, Intharapat P et al (2012) Decolorization and organic removal from palm oil mill effluent by fenton's process. *Environ Eng Sci* 29:855–859. <https://doi.org/10.1089/ees.2011.0181>
- Le PTT, Boyd CE (2012) Comparison of phenate and salicylate methods for determination of total ammonia nitrogen in freshwater and saline water. *J World Aquac Soc* 43:885–889. <https://doi.org/10.1111/j.1749-7345.2012.00616.x>
- Martina V, Vojtech K (2015) A comparison of biuret, lowry and Bradford methods for measuring the egg's proteins. *Mendelnet* 1:394–398
- Ministry of Industry T (2017) Notification of Ministry of Industry: Industrial Effluent Standards B.E.2560 (2017). In: 2017. <https://www.fao.org/faolex/results/details/en/c/LEX-FAOC211105/>
- Murphy DJ, Goggin K, Paterson RRM (2021) Oil palm in the 2020s and beyond: challenges and solutions. *CABI Agric Biosci* 2:1–22. <https://doi.org/10.1186/s43170-021-00058-3>
- Nava JL, de León CP (2018) Reactor design for advanced oxidation processes. *Handb Environ Chem* 61:263–286. https://doi.org/10.1007/698_2017_54
- Pizzi A (2021) Covalent and ionic bonding between tannin and collagen in leather making and shrinking: a maldi-tof study. *J Renew Mater* 9:1345–1353. <https://doi.org/10.32604/jrm.2021.015663>
- Poh PE, Ong WYJ, Lau EV, Chong MN (2014) Investigation on micro-bubble flotation and coagulation for the treatment of anaerobically treated palm oil mill effluent (POME). *J Environ Chem Eng* 2:1174–1181. <https://doi.org/10.1016/j.jece.2014.04.018>
- Pu Y, Zhao F, Chen Y et al (2023) Enhanced electrocatalytic oxidation of phenol by SnO₂-Sb₂O₃/GAC particle electrodes in a three-dimensional electrochemical oxidation system. *Water (Switzerland)*. <https://doi.org/10.3390/w15101844>
- Rao NN, Somasekhar KM, Kaul SN, Szyrkowicz L (2001) Electrochemical oxidation of tannery wastewater. *J Chem Technol Biotechnol* 76:1124–1131. <https://doi.org/10.1002/jctb.493>
- Reza A, Chen L (2022) Electrochemical treatment of livestock waste streams: a review. Springer, Berlin
- Saad MS, Joe NC, Shuib HA et al (2022) Techno-economic analysis of an integrated electrocoagulation-membrane system in treatment of palm oil mill effluent. *J King Saud Univ Sci* 34:102015. <https://doi.org/10.1016/j.jksus.2022.102015>
- Saputera WH, Putrie AS, Esmailpour AA et al (2021) Technology advances in phenol removals: current progress and future perspectives. *Catalysts*. <https://doi.org/10.3390/catal11080998>
- Serrano KG (2018) Indirect electrochemical oxidation using hydroxyl radical, active chlorine, and peroxydisulfate. Elsevier Inc, Hoboken
- Taha MR, Ibrahim AH (2014) COD removal from anaerobically treated palm oil mill effluent (AT-POME) via aerated heterogeneous Fenton process: optimization study. *J Water Process Eng* 1:8–16. <https://doi.org/10.1016/j.jwpe.2014.02.002>
- Tan YH, Goh PS, Ismail AF et al (2017) Decolourization of aerobically treated palm oil mill effluent (AT-POME) using polyvinylidene fluoride (PVDF) ultrafiltration membrane incorporated with coupled zinc-iron oxide nanoparticles. *Chem Eng J* 308:359–369. <https://doi.org/10.1016/j.cej.2016.09.092>
- Yap CC, Loh SK, Chan YJ et al (2021) Synergistic effect of anaerobic co-digestion of palm oil mill effluent (POME) with Moringa oleifera extract. *Biomass Bioenergy* 144:105885. <https://doi.org/10.1016/j.biombioe.2020.105885>
- Yavuz Y, Shahbazi R (2012) Anodic oxidation of Reactive Black 5 dye using boron doped diamond anodes in a bipolar trickle tower reactor. *Sep Purif Technol* 85:130–136. <https://doi.org/10.1016/j.seppur.2011.10.001>
- Zahrim AY, Rachel FM, Menaka S et al (2009) Decolourisation of anaerobic palm oil mill effluent via activated sludge-granular activated carbon. *World Appl Sci J* 5:126–129
- Zahrim AY, Nasimah A, Hilal N (2014) Pollutants analysis during conventional palm oil mill effluent (POME) ponding system

- and decolourisation of anaerobically treated POME via calcium lactate-polyacrylamide. *J Water Process Eng* 4:159–165. <https://doi.org/10.1016/j.jwpe.2014.09.005>
- Zhang H, Ran X, Wu X, Zhang D (2011) Evaluation of electro-oxidation of biologically treated landfill leachate using response surface methodology. *J Hazard Mater* 188:261–268. <https://doi.org/10.1016/j.jhazmat.2011.01.097>
- Zhou B, Yu Z, Wei Q et al (2016) Electrochemical oxidation of biological pretreated and membrane separated landfill leachate concentrates on boron doped diamond anode. *Appl Surf Sci* 377:406–415. <https://doi.org/10.1016/j.apsusc.2016.03.045>
- Zöllig H, Morgenroth E, Udert KM (2015) Inhibition of direct electrolytic ammonia oxidation due to a change in local pH. *Electrochim Acta* 165:348–355. <https://doi.org/10.1016/j.electacta.2015.02.162>

Publisher's Note Springer Nature remains neutral with regard to jurisdictional claims in published maps and institutional affiliations.